Hydrological Characterisation of a Live Pole Drain

Eefje Benschop

Hydrological Characterisation of a Live Pole Drain

Eefje Benschop

16 September 2022

In partial fulfilment of the requirements to obtain the degree of Master of Science in Civil Engineering at Delft University of Technology

To be defended publicly on 23 September 2022

Faculty of Civil Engineering and Geosciences
Department of Water Management

Student number: 4367375
Project duration: December 2021 – September 2022

Thesis committee:

Dr. T.A. Bogaard	TU Delft, Chair
Dr. A. González-Ollauri	Glasgow Caledonian University
Prof. Dr. S.B. Mickovski	Glasgow Caledonian University
Prof. Dr. M. Menenti	TU Delft

Drawings by Cato Benschop: catobenschop.nl

An electronic version of this thesis is available at repository.tudelft.nl

TU Delft Delft University of Technology

GCU Glasgow Caledonian University

Acknowledgements

During this project I was lucky enough to receive help and advice from many people. First of all, I would like to express my gratitude towards my supervisors. When I went to Thom 10 months ago in the middle of the millionth lockdown, I didn't dare hope that I would be allowed to go abroad for my thesis. Not only did you help make that happen, but you were also available for a meeting anytime. You helped shape my research by giving great suggestions and asking many critical questions. Thank you, Alex and Bobby, for welcoming me to GCU and providing me with the opportunities to do very interesting fieldwork at a beautiful location and to build a lab experiment from scratch. Your open-office policy and regular visits to the lab encouraged me to discuss my work and learn from your different perspectives. I would also like to thank Massimo Menenti, for reading my thesis and asking interesting questions during the green light meeting.

My time in Glasgow would't have been the same without Fernanda, Lucie and Camille. Thank you for the fun times at the lab and at the pub. Together, we raised an abundant family of willow babies. Also many, many thanks to everyone who came to explore Glasgow with me: Cato, Loek, Laura and Yardèn, Karlijn, Nina and Madelief, Simone, Amber and Anneroos and my parents. I think I can safely say that we exhausted the city's tourist attractions. Cato, you set me up in my temporary home, planned long hikes to discover the city and, most importantly, called with me every day. On top of that, you made the amazing drawings for my report and presentation, thank you! Loek, LaTeX and overall programming expert, without you, both my model and this thesis would be much less organised. Most of all, I am very grateful to you for reading my entire report and talking away my doubts (towards the end of the project, every day). I would like to thank Renske for being my other editor and Eva for being my parter in crime. Lastly, I would like to like my family and flatmates for just being there, distracting me and cooking for me during the stressful lasts steps.

I enjoyed writing this thesis and I learned a lot about hillslope hydrology, modelling, fieldwork and lab experiments and, of course, Live Pole Drains. Enjoy reading.

Eefje Benschop

Abstract

Climate change causes an increase of precipitation intensity and frequency, which leads to an increased amount of landslide occurrences. Therefore, there is an urgent need for prevention measures. The risk of landslide occurrence can be mitigated by decreasing the pore water pressure in a hillslope, e.g. by drainage from the subsurface. The implementation of Nature Based Solutions (NBS) is advantageous, as these are not disruptive for the hillslope ecosystem. A Live Pole Drain (LPD) is a type of NBS which is inexpensive and can be installed at remote locations. However, its effect on hillslope hydrology has not been studied before.

In this study, fieldwork at an Open Air Lab, a laboratory experiment with miniature LPDs and the development of a conceptual model were used to characterise the hydrological behaviour of a slope in which a LPD is installed. After comparison of this hydrological behaviour to that of a slope with bare soil, it was found that a LPD facilitates rapid infiltration and drainage of precipitation and subsurface water. Furthermore, runoff volumes decrease after installation of a LPD and this effect is enhanced through plant development. Vegetation also contributes to the decrease of the stored volume of water in the subsurface through evapotranspiration. An increase of the design aspects diameter and macropore fraction of the LPD increases its drainage capacity. This study resulted in a first version of a numerical model to quantify the hydrological processes in a hillslope with LPD and the confirmation of the expected effect of drainage through preferential flow by a LPD.

Keywords: landslide, Nature Based Solution, Live Pole Drain, conceptual model, rainfall, Open Air Lab

List of Tables

List of Figures

Contents

Chapter 1
Introduction

1.1 The Live Pole Drain: a Nature Based Solution for Shallow Landslides

Due to climate change, both precipitation frequency and intensity are expected to increase in the coming years. As a result, natural hazards such as rainfall induced landslides will occur more often, causing damage to property, traffic disruptions and injury or even fatalities. A landslide was defined by Varnes (1978) as a "downward and outward movement of slope forming material under the influence of gravity". Hillslope hydrology plays an important role in a landslide area, as landslides occur when the pore pressure in the soil skeleton results in a reduction of shear strength. Landslides are separated into shallow and deep-seated types. This study focuses on a prevention method for shallow landslides, which are less than 2 m deep (Sidle and Bogaard, 2016). The trigger of many shallow landslides is a single rainfall event, but the cause may be a combination of several hydrological processes. These include filling, storing and draining of water (Bogaard and Greco, 2016). Rainfall intensity-duration thresholds have been established (Silvia et al., 2008) and with the expected increase in rainfall intensity, these are will be exceeded more often in the future. Therefore, there is a growing need for not only landslide early warning systems, but also prevention methods.

The risk of landslide occurrences can be mitigated by installing measures which decrease pore water pressure. Examples of such facilities on slopes are french drains, gravel drainpiles (Moayedi et al., 2011) and drainage tunnels (Yan et al., 2019). These grey solutions are disruptive for the hillslope environment. Nature-based solutions (NBS) on the other hand, are implemented for ecosystem protection. They are defined as "actions to protect, sustainably manage and restore natural or modified ecosystems, which address societal challenges [...] effectively and adaptively, while simultaneously providing human well-being and biodiversity benefits" (Cohen-Shacham et al., 2016). One of the approaches is issue-specific ecosystem-based adaptation, including ecosystem-based Disaster Risk Reduction (Eco-DRR). Eco-DDR is also used for landslide mitigation; Norwegian Geotechnical Institute (2016) divided approximately 70 NBS for landslides into 11 categories, varying from "NBS for erosion control" to "modifying the surface water regime" to "retaining structures to improve the slope stability". Gonzalez-Ollauri and Mickovski (2017c) also made an inventory of a plethora of NBS for slope stability. These cover ground bio- and eco-engineering techniques, both using biological materials as essential tools. Examples of these NBS are gravel drains, mulching, wattle fences and planting and reforestation techniques. The applications of these different solutions vary widely and are dependent on factors such as climate, landslide size and velocity and on-site vegetation. Most of these solutions have in common that their effects on hillslope hydrology have not been quantified.

Downsides of many NBS are that their effect is only significant after some time and that they require machinery to be installed, resulting in high costs. Live Pole Drains (LPDs) can be used without these disadvantages. Their installation can be executed with manual equipment, making the measure feasible in remote locations as well as economical. LPDs are bundles of live twigs, placed in trenches and covered with on-site materials (Figure 1.1). The working of LPDs has not been quantified and is scarcely documented. However, something can be said about their expected effect on hillslope hydrology. This effect is threefold:

- Drainage through preferential flow: immediately after installation, the LPD acts as a drain, transporting seeped and/or infiltrated water laterally through preferential flow.
- Plant water uptake: after the twigs have sprouted, water is transported out from the soil into the plants and to the atmosphere through evaporation.
- Stabilisation through root reinforcement: after the root system has developed, it can contribute to slope stability.

The first two effects are analysed in this study. LPDs are applied at slopes where soil instabilities are the result of excess of water in loose materials or debris scar areas (Polster and Bio, 1997). They are suitable for shallow landslides and are especially useful for revegetation of previously landslide-affected areas (Norwegian Geotechnical Institute, 2016). Landslides also occur in Scotland, where a LPD is applied in an Open Air Lab. It consists of willow (*Salix Viminalis*) fascines. Quantifying the effects of LPDs on hydrological processes on a hillslope will contribute to a better insight into their performance and applications. This will make design and implementation of this low-cost measure against shallow, rainfall-induced landslides on a wider scale possible.

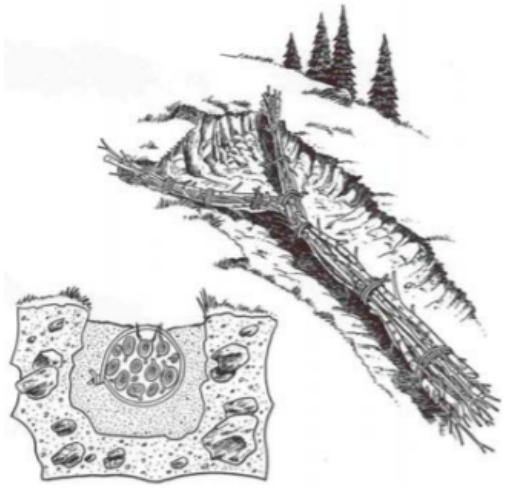

Figure 1.1: *Layout of a LPD without cover for clarity. The cross-section shows a typical soil cover (Polster and Bio, 1997).*

1.2 Research Questions

The main objective of this research is to gain an understanding of the hydrological behaviour of a slope in a temperate climate in which a LPD is installed. The focus is on the identification of the most relevant hydrological processes of a hillslope with LPD compared to a slope without LPD. The main research question is formulated as follows.

What is the hydrological behaviour of a Live Pole Drain?

Two subquestions were formulated to support the answer to the main question:

1. Can the hydrological behaviour of a Live Pole Drain be represented by a numerical model?
2. What is the hydrological response to a rain event of a hillslope with a Live Pole Drain compared to that of a bare slope?

This study provides a baseline and a first insight into the hydrological trends in a slope with LPD, after which findings can be tested with more data in future studies. This will ultimately contribute to making the LPD more widely applicable.

1.3 Thesis Outline

This thesis is divided into three parts. Part I comprises the fieldwork and lab experiment which were executed to gain insight into the behaviour of the LPD, gather input parameter values and collect testing data for the model. The methodologies for the fieldwork and lab experiment are described in Chapter 2. The results of the measurements and experiments are presented in Chapter 3 and these are discussed in Chapter 4. Part II concerns the numerical modelling of a LPD. Chapter 5 starts with a description of the theoretical background on which the model was based. Then, the model and the scenarios which used for simulations, are described. Lastly, the methodology of the sensitivity analysis is explained. The results of the model runs and the sensitivity analysis are presented in Chapter 6. The limitations of the methodology are given and the results are discussed in Chapter 7. The third and last part of this thesis consists of the synthesis of Part I and Part II, the conclusions that were drawn to answer the research questions and the recommendations for future research.

Part I

Fieldwork and Lab Experiment

Chapter 2
Methodology

The fieldwork and lab experiment were executed in order to gain insight in 1) the orders of magnitude of hydrological processes involving the LPD, 2) the partitioning of water which leaves the slope during and after a rain event and 3) the hydrological behaviour of a LPD in practice. These findings were used for the conceptualisation of the study site and as input or testing data for the model. Measurements and experiments which did not directly influence the model and their results are described in Appendices A (fieldwork), B (lab protocol) and C (results lab experiments). On-site, several soil characteristics were measured and dimensions of and flow through the LPD were studied. The lab experiment comprised three setups of three miniature LPDs each. These setups were built with materials from the study site. Five rainfall experiments of varying duration and intensity were conducted for the assessment of behaviour of the LPD during a precipitation event. Sections 2.1 and 2.2 deal with the methods used in the field and the laboratory, respectively. Section 2.1 contains a description of the study site (2.1.1) and the measurements and tests which were executed (2.1.2). In Section 2.2, the setup of the lab experiment (2.2.1) and the precipitation experiments (2.2.2) are described.

2.1 Fieldwork

2.1.1 Study Site

The LPD is located in an Open Air Lab (OAL) at Catterline Bay, Aberdeenshire, UK (WGS84 Long: -2.2152 Lat: 56.8955). It was constructed with cuttings from the basket willow (*Salix Viminalis*) and installed in a 25° to 30° slope with silty-sandy soil overlying conglomerate rock. It lies within the bottom 12 m of the slope and consists of one main drain and two branches at the most upslope part, creating a Y-shape (Figure 2.1b). The mean annual temperature is 8.9 °C and the mean annual rainfall is 565.13 mm. Precipitation occurs frequently and with a low intensity (Gonzalez-Ollauri and Mickovski, 2017a).

2.1.2 Measurements and Tests

Various tests and measurements were executed and conducted in April and June 2022, including soil tests and dimensions of and flow through the LPD. The soil tests were done in accordance with the protocols by Head (1994), Epps and Head (2006) and Head and Epps (2014). Tests were performed and soil samples were collected at three locations along the length of the LPD: Top (T), Middle (M) and Bottom (B), as depicted in Figure 2.1c. At each location, three samples at different horizons were taken: 0 – 15 cm depth (I), 15 – 30 cm depth (II) and 30 – 60 cm depth (III). The average porosity of all nine samples was used as input parameter for the model. A complete overview of the measurements and tests performed at the study site is given in Table A.1. Close to the LPD, eight falling head tests were executed to find the percolation rate. In addition to soil characteristics, the dimensions of the LPD were measured. The diameters of the bundle as a whole and of its cuttings were measured after digging around the bundle at the top of the left branch (Figure 2.1). The drain was inspected to gain an understanding of its structure and the presence of soil inside. Flow through the LPD was measured using two methods. The first is shown in Figure 2.2; on three measuring days, the discharge from the LPD was collected at its toe and measured. The second method was to install water pressure devices in the centre of the LPD at the top, middle, and toe (Figure 2.1c). These devices

(a) *(b)* *(c)*

Figure 2.1: *Layout and location of the LPD.* ***(a)*** *The slope in which the LPD was installed. The LPD is located within the box.* ***(b)*** *View from the bottom of the slope with LPD. The black lines indicate the centre of the LPD.* ***(c)*** *Locations of testing and sampling along the LPD. T: top, M: middle, B: bottom. The values are the distances between the locations measured along the slope.*

recorded the water pressure every 15 min from 18 April till 6 June 2022. Their specifications can be found in Table A.1. Meteorological time series recorded between April and June 2022 (Figure A.1) were used to interpret the LPD discharge measurements (Voor de Poorte, 2022).

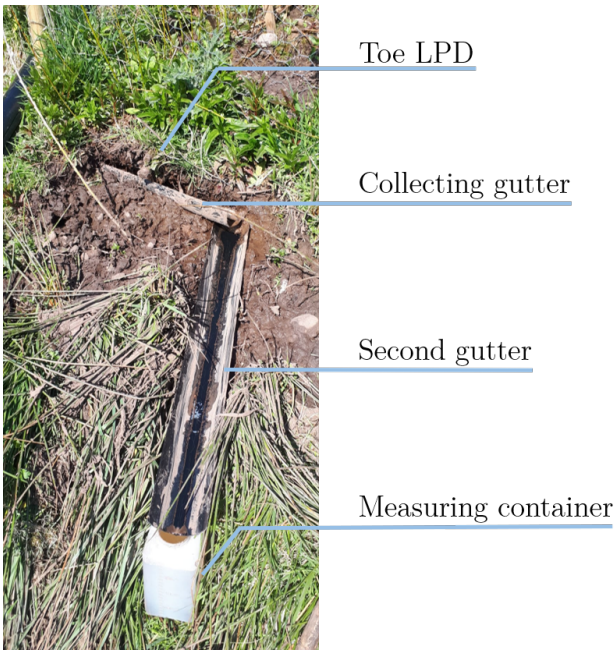

Figure 2.2: *Setup of the discharge measurements.*

2.2 Lab Experiment

2.2.1 Setup

One experiment setup consisted of three gutters: one filled with soil (Bare), one filled with soil and a LPD bundle (LPD) and one filled with soil, a LPD bundle and alfalfa seeds (LPD+). The setup was repeated three times, resulting in a total of nine gutters (Figure 2.3). Before the building of the experiment setup, soil and

Salix Viminalis cuttings were collected at the study site. The soil was air- and oven-dried and sieved under 2 mm. An overview of the tests performed on the soil is given in Table B.1. Cuttings with diameters 2 mm to 12 mm were used to create bundles with a diameter of approximately 38 mm.

Figure 2.3: *Front view of the lab experiment setup.* ***(a)*** *Photo of the setup.* ***(b)*** *Position of the LPD bundle in a gutter before it is covered with soil.* ***(c)*** *Schematic drawing of the setup. LPD: gutter with soil and a LPD bundle; LPA+A: gutter with soil, a LPD bundle and alfalfa seeds; Bare: gutter with only soil.*

The setup is shown in Figure 2.4. All gutters were watered continuously by means of a drip irrigation system. Plastic containers were placed underneath the setups to collect water from runoff, lateral flow, percolation at the top half and at the bottom half of the gutter. The gutters were placed in an environmental chamber in which a temperature of 20 °C to 22 °C and a humidity of 80% were maintained. A growing lamp was installed above the setup and turned on for 14 h per day between 6 AM and 10 PM to stimulate vegetation development. The gutters were placed at an angle of 30° to mimic the field conditions. Moisture sensors (SEN0193 and SEN0308), tensiometers (T5) and temperature probes (107 Campbell Scientific Temperature Sensor) were inserted into the soil next to the bundles. After the installation, several aspects of the setup were measured at regular intervals (Table B.2).

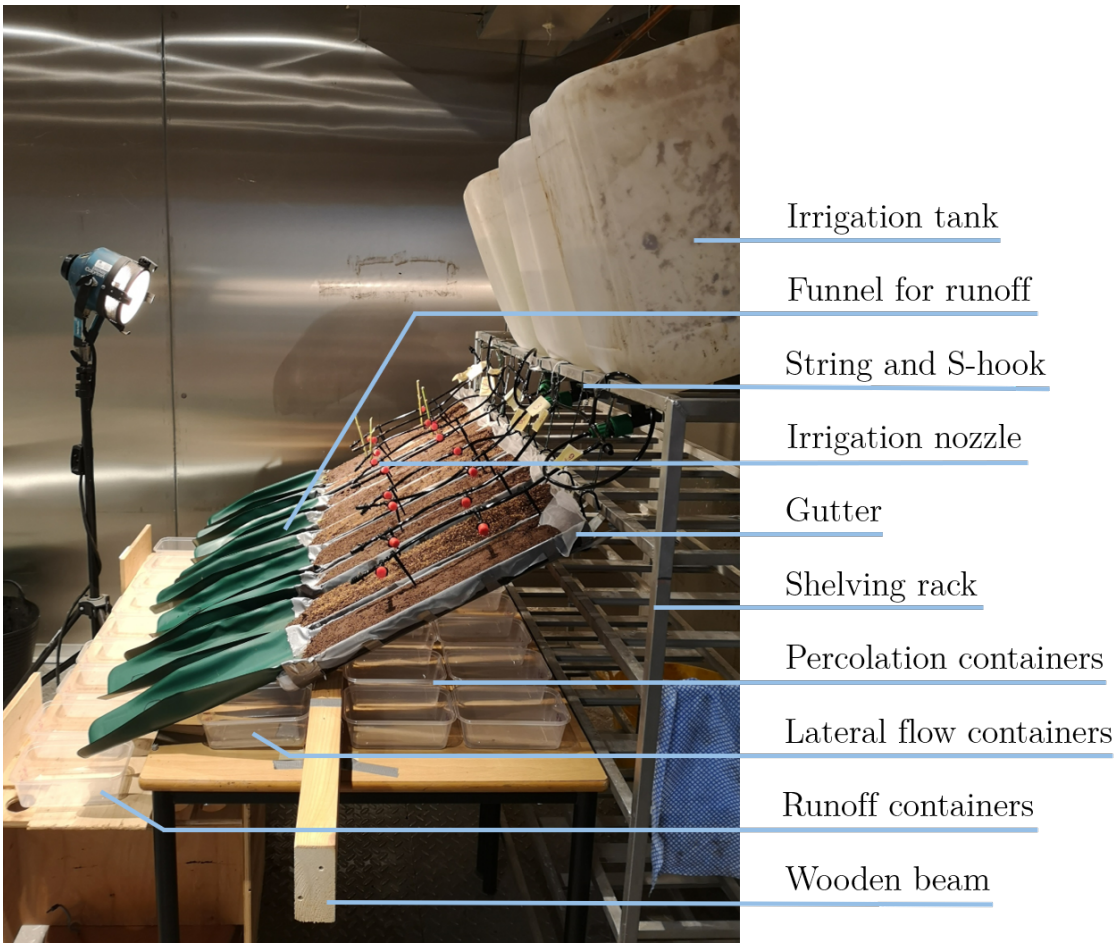

Figure 2.4: *Side view of the lab experiment setup with annotations indicating the different elements.*

2.2.2 Precipitation Experiments

Five different precipitation simulation experiments were conducted. Each experiment was conducted at least twice. The first run always occurred 4 h after closing the irrigation tanks. The second run occurred 24 h later, without irrigation in between the runs. Before and after each experiment, several soil and ambient variables were recorded.

Precipitation was simulated by one nozzle at the top of the gutter, mimicking the collection and drainage of upslope water by the LPD in the field (Figure 2.5). By varying rainfall duration and intervals, different intensities were obtained (Table 2.1). Using the entire gutter area for the calculation, it was found that an intensity of 6.21 mm/min was simulated by the nozzles, of which 80% was assumed to reach the gutter surface (Table C.3).

During each event the lateral flow was recorded every 30 s by means of 100 mL indicator stripes on the containers. During the 30 min after the final rainfall interval, lateral flow was recorded every 2 min. After 30 min, all containers were removed from the setup. The water volume inside all containers was measured and recorded. The partitioning consists of five components: runoff, lateral flow, percolation at the top, percolation at the toe and storage. The magnitude of the storage component was determined for each gutter by subtracting the measured volumes of water inside the containers from the total water input (Table 2.1). If the summed volume inside all containers of one gutter exceeded the assumed total water input, this summed volume was taken as assumed total water input, resulting in a storage component of zero.

Table 2.1: *Descriptions of the laboratory precipitation experiments.*

Exp.	**Duration and intervals**	**Simulated intensity** (mm/min)	**Total input volume per gutter** (mL)	**Times repeated and initial conditions**
1	1 interval of 1 min.	4.97	251	Once 4 h after turning off irrigation tanks, once 24 h later and a third time after 4 d.
2	7 intervals of 1 min; pauses of 1 min.	2.67	1758	Once 4 h after turning off irrigation tanks and a second time 24 h later.
3	10 intervals of 30 s; pauses of 30 s.	2.62	1256	Once 4 h after turning off irrigation tanks and a second time 24 h later.
4	3 intervals of 1 min; pauses of 4 min.	1.35	754	Once 4 h after turning off irrigation tanks and a second time 24 h later.
5	2 intervals of 2 min; pauses of 5 min.	2.21	1005	Once 24 h after the previous experiment and a second time 24 h later.

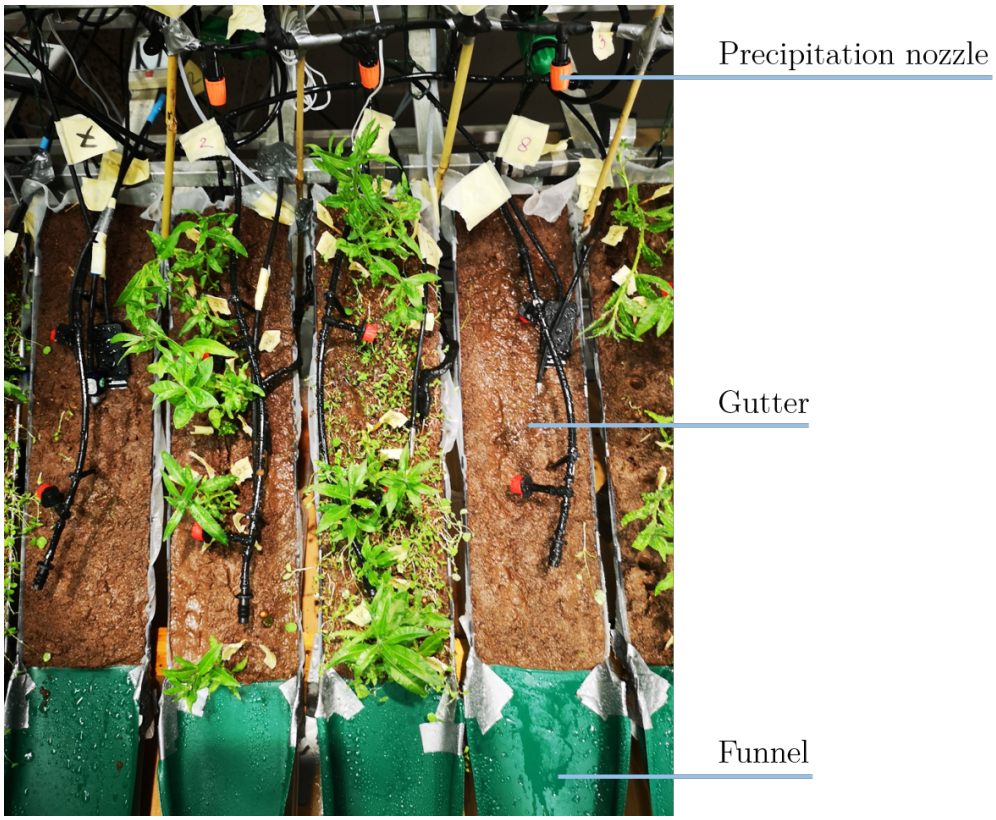

Figure 2.5: *Setup of the laboratory precipitation experiments.*

Chapter 3
Results

In this chapter, the results of the fieldwork and lab experiment are presented. It starts with an overview of the most important findings from the fieldwork in Section 3.1. These are divided into three categories: soil characteristics, dimensions of the LPD and flow through the LPD. The outcomes of the precipitation experiments are presented in Section 3.2. Results of measurements and experiments which did not directly influence the model are presented in Appendices A (fieldwork) and C (lab experiment).

3.1 Fieldwork

Soil characteristics. The average porosity of the nine soil samples was 0.35±0.08. The average percolation rate, found with the falling head test, was 1.14×10^{-3} m/s. Table A.4 gives an overview of the results of all falling head tests. A complete overview of the measured soil characteristics is given in Table A.2.

Dimensions of the LPD. The dimensions of the LPD are schematised in Figure 3.1a. A bundle consists of around 14 cuttings with diameters of 1 cm to 2 cm. The spaces between the cuttings contained soil, but were not completely filled (Figure 3.1b). One of the two branches is connected to a drain which collects water from the upslope area, constituting a base flow through the LPD.

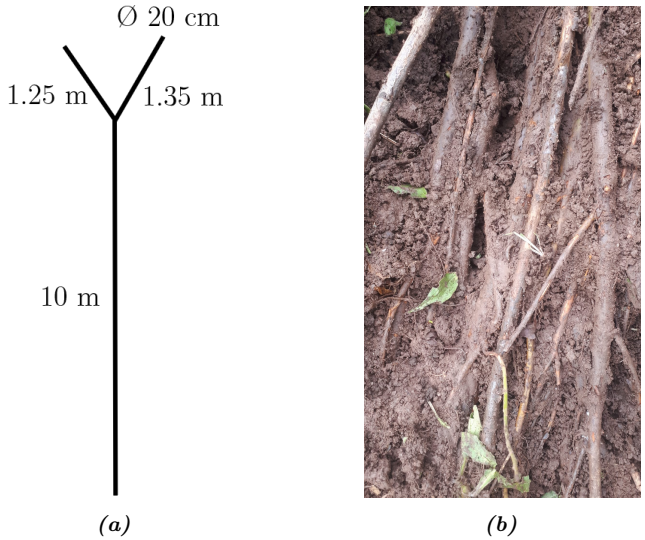

Figure 3.1: *The dimensions of the LPD at the study site.* ***(a)*** *Schematic drawing of the dimensions of the LPD.* ***(b)*** *Photograph of the LPD section that was dug out at the top of the left branch.*

Flow through the LPD. The results of the discharge tests for each measuring day are given in Table 3.1.

Observations at the study site indicated that there was a large difference in plant development between April and June: in June, vegetation was both denser and higher than in April. The last precipitation event before the measurements on 20 and 21 April had occurred on 18 April (0.4 mm) and on 4 April before that (0.2 mm). During the dry period between 4 and 20 April, the average temperature increased by 3 °C. Before the measurements executed on 6 June, rainfall was last measured on 1 June (3.2 mm). The average temperature in the beginning of June was quite constant, about 11 °C. On the second measuring day in April, the discharge had halved compared to the day before. In June, the discharge had decreased by a factor 10 compared to the first day. On all measuring days, tests started in the morning and lasted until the afternoon. Throughout the day, a decrease in discharge was observed (Table A.5). Furthermore, immediately after the execution of the falling head tests the discharge from the LPD visibly increased.

Table 3.1: *Results of the discharge measurements at the study site.*

Date	**Average discharge** (L/h)	**Weather conditions and remarks**
20/04/2022	8.23	*Previous two days:* temperatures around 10 °C, 0.4 mm of rain on 18/04. *During measurement day:* the day was partly sunny without rain. The measured discharge decreased during the day.
21/04/2022	4.30	*Previous two days:* temperatures around 8 °C, no rain. *During measurement day:* the day was partly sunny without rain. The measured discharge decreased during the day.
06/06/2022	0.86	*Previous two days:* temperatures around 12 °C, no rain. *During measurement day:* the day was sunny without rain. Two experiments were executed and the measured discharge was less in the second one.

The water level in the boreholes at locations T and M (Figure 2.1c) was measured from 18 April 2022 till 6 June 2022. The water pressure device at location M (Figure 2.1c) recorded from 18 April till 6 May in the same year. Figure 3.2 shows the measurements and weather conditions on the corresponding dates. Rain events occurred on a total of 21 days. The greatest event occurred on 16 May, with 6.4 mm. The period before this event was the longest dry period: it lasted five days, during which the maximum temperature reached 20.3 °C. The water level measurements at location T show a decrease during this dry period and an increase after the rain event on 16 May. A small peak can also be observed in the measurements at location B. This trend can also be observed around the events on 24-26 April and on 9-10 May. Daily fluctuations in the water level correspond to day- and nighttime: the water level decreased during the day and increased during the night. Later in the measuring period, the water level at location T fluctuated irregularly.

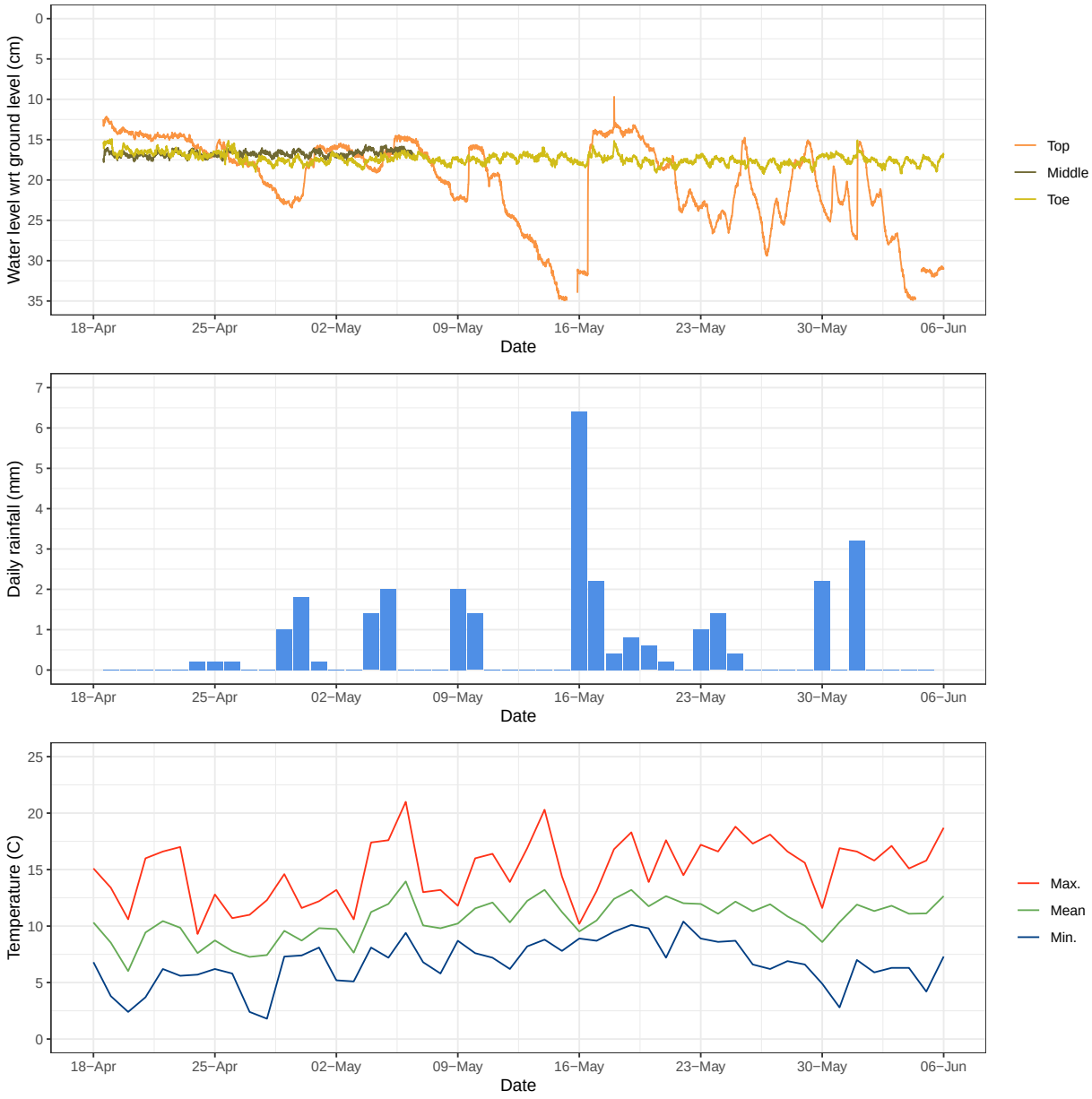

Figure 3.2: *Water level with respect to ground level measured with the water pressure devices at top, middle and bottom of the LPD (top plot). Rainfall (middle plot) and air temperatures (bottom plot) at corresponding dates.*

3.2 Lab Experiment

The water partitioning of the first run of all experiments is depicted in Figure 3.3. The partitioning of the second runs and the results of the soil and lateral flow measurements are given in Appendix C. Gutters 1-3 contained a bundle (LPD), gutters 4-6 contained a bundle and alfalfa seeds (LPD+) and gutters 7-9 only soil (Bare). Table 3.2 contains the ranges and means of the percentages for the first and second run of each experiment.

Some trends pertaining the flow components under different soil and growth conditions can be observed. Less of the total water input volume ended up as runoff if there was a bundle in the soil, compared to the Bare gutters. The fraction that ended up as runoff was the smallest for the LPD+ gutters. Furthermore, this fraction was the greatest in the fourth and fifth experiment, during which the total water input volume was quite high and the pauses between the precipitation intervals were longer compared to the first three experiments. The lateral flow component was smaller in the case of Bare soil. No consistent differences between the LPD and LPD+ gutters can be observed considering this component. Observations during the experiments and lateral flow measurements (Appendix C.2) indicate that lateral flow was measured earlier for the LPD and LPD+ gutters. Moreover, in the Bare gutters, the lateral flow consisted of water drops, whereas in the other gutters a steady stream came from the subsurface. Runoff, on the other hand, started earlier in the Bare gutters. The percolation components were larger for the gutters with a bundle than in those with Bare soil. The LPD+ gutters had the largest percolation components. In most cases, more water percolated from the bottom half of the gutters (toe). The storage component was the largest for the Bare and the smallest for the LPD+ gutters.

The water partitioning of all runs of Experiment 1 is shown in Figure 3.4. The first run was executed 4 h after turning off the regular irrigation, the second run 24 h after the first run and the third run 4 d later. The storage component was larger for almost all gutters in the second run compared to the first run. For almost all gutters, the other components showed a slight decrease. The water partitioning of the third run looks strikingly different compared to that of the first two runs: the storage component was very large for all filling types, but slightly smaller for the LPD+ gutters. Almost all water ended up as percolation; runoff and lateral flow were barely measured.

Table 3.2: *Ranges and means of the fractions of the various flow components of the five precipitation events. These are given as percentages of total water input for each gutter type.*

		First run			Second run		
Type	**Flow component**	**Min.**	**Max.**	**Mean**	**Min.**	**Max.**	**Mean**
LPD	Runoff	0	21	7	0	20	6
	Lateral	18	66	35	4	42	27
	Percolation	8	50	29	10	51	28
	Storage	0	53	29	2	70	39
LPD+	Runoff	0	10	3	0	10	2
	Lateral	14	60	36	18	53	32
	Percolation	27	72	50	17	69	43
	Storage	0	49	11	0	58	23
Bare	Runoff	0	53	20	2	50	24
	Lateral	9	24	16	2	18	13
	Percolation	7	30	18	4	35	17
	Storage	0	71	46	20	92	48

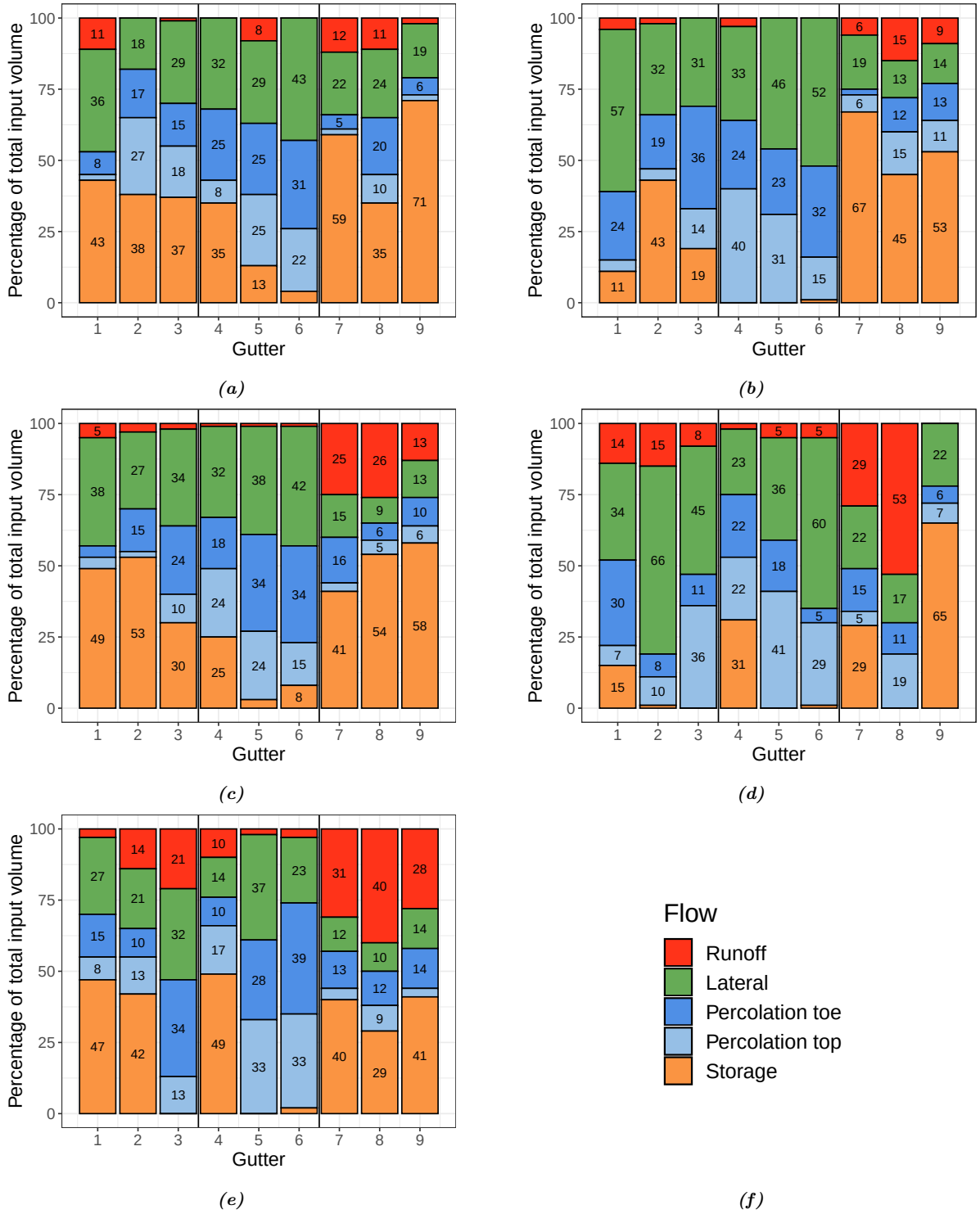

Figure 3.3: *Water partitioning of the first runs of the five precipitation experiments. The initial conditions and input volumes are described in Table 2.1. Gutters 1-3: LPD, gutters 4-6: LPD+ and gutters 7-9: Bare.* ***(a)*** *Experiment 1: 1 interval of* 1 min. ***(b)*** *Experiment 2: 7 intervals of* 1 min *with pauses of* 1 min. ***(c)*** *Experiment 3: 10 intervals of* 30 s *with pauses of* 30 s. ***(d)*** *Experiment 4: 3 intervals of* 1 min *with pauses of* 4 min. ***(e)*** *Experiment 5: 2 intervals of* 2 min *with pauses of* 5 min. ***(f)*** *Legend.*

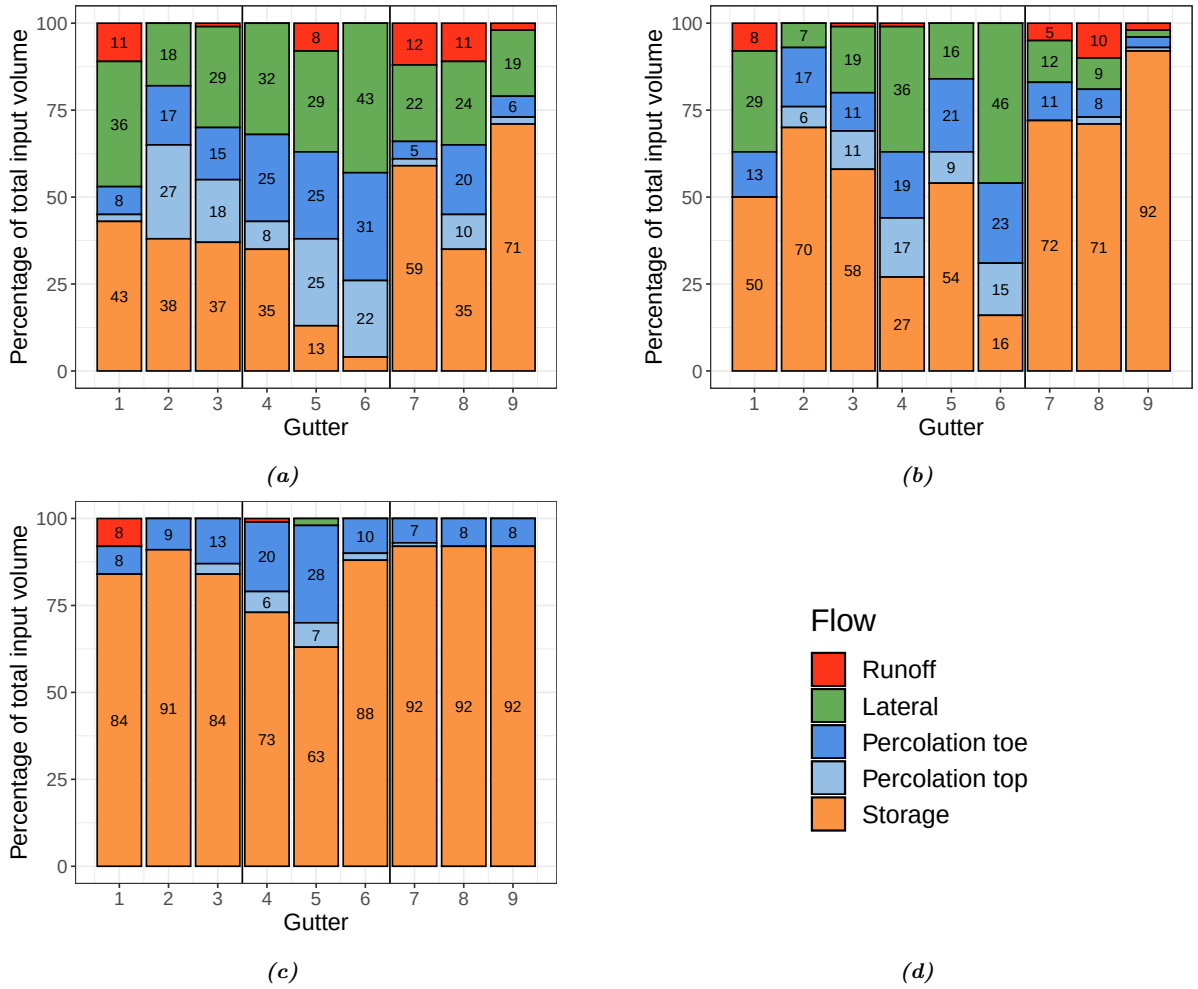

Figure 3.4: *Water partitioning of all runs of precipitation experiment 1: 1 interval of* 1 min. *Gutters 1-3: LPD, gutters 4-6: LPD+ and gutters 7-9: Bare.* ***(a)*** *First run:* 4 h *after turning off the irrigation tanks.* ***(b)*** *Second run:* 24 h *after the first run.* ***(c)*** *Third run:* 4 d *after the second run.* ***(d)*** *Legend.*

Chapter 4
Discussion

An accurate interpretation of the results described in Chapter 3 should concern the malfunctioning during experiments and the limitations of the measuring methods. In this chapter, these malfunctionings and limitations are described and the obtained results are discussed. Section 4.1 deals with the fieldwork and Section 4.2 with the lab experiment.

4.1 Fieldwork

Setup and malfunctioning

The soil samples consisted of soil that was disturbed and the sample rings were sometimes not completely filled, which means that the found porosity could both be smaller and greater than in reality (Tan et al., 2007). Furthermore, the falling head test was executed eight times in the same borehole (Table A.4), causing the soil to compact where the water jet hit. This led to diminished permeability in experiment executions 4-7, after which the pouring location was changed. Therefore, the average of experiments 1-3 and 8 is considered in the discussion.

During the discharge measurements, the water collection was not spill-proof. Furthermore, the installation of the water pressure devices inside the LPD was difficult, possibly leading to installation faults. The temperature and precipitation data that were used to compare the water level measurements to, might have been subject to malfunctioning of the weather station.

Limitations of the methodology

Soil samples were taken close to the LPD at three locations, but were used to characterise and parameterise the behaviour of the LPD itself. The conditions within the LPD, however, are most likely different from those in the soil next to it. In addition, the falling head permeability test usually gives lower values than the permeameter test (Gill et al., 2019), which was attempted but not finished due to malfunctioning of the apparatus.

The dimensions of the LPD were only observed at one of the branches at the top. The bundle could not be dug out entirely (Figure 3.1b), so an estimate of the total number of cuttings in and the diameter of the drain had to be made. The assumption was done that the diameter, number of cuttings and diameter of the cuttings is uniform throughout the entire LPD, which is unrealistic.

The discharge from the LPD was measured on three days of which the first two had quite similar initial conditions. Rainfall did not occur on any of the measuring days and no measurements were done during the dormant season. The water level in the LPD, measured with water pressure devices, was observed every 15 min during 50 days in the same period. Information of multiple years and all seasons is necessary to fully characterise the hydrological behaviour of the LPD.

Discussion of the results

The soil characteristics porosity and saturated hydraulic conductivity were used in the model. The porosity was determined from nine different samples (at three locations and at three depths). The found porosities had a mean of 0.35 and standard deviation of 0.08. Porosity measured by Gonzalez-Ollauri and Mickovski (2017b) was higher: 0.68. However, this value exceeds the range of usually measured porosities for this soil type (Hao et al., 2008). The measured value of 0.35 falls within this range and was therefore used in this study. Saturated hydraulic conductivity was obtained in a previous study through pedotransfer functions with the result $5.82 \times 10^{-5} \pm 1.43 \times 10^{-5}$ m/s (Gonzalez-Ollauri and Mickovski, 2017b). The falling head tests resulted in an average percolation rate of 1.14×10^{-3} m/s, which is two orders of magnitude greater than the value found by Gonzalez-Ollauri and Mickovski (2017b). The pedotransfer functions used in their study tend to underestimate the saturated hydraulic conductivity (Tóth et al., 2015). However, the value found with this method was found to be more representative of reality (Chapuis, 2012) and was therefore further used in this study.

For the model the diameter of the LPD was also of importance. After personal communication with one of the builders of the LPD, it was assumed that the measured 200 mm was representative for the entire LPD. However, as discussed above, in reality the bundle was not perfectly straight and the diameter of the bundle was not constant throughout the entire LPD. The consequences for the flow through the bundle were not taken into account in the conceptualisation of the hydrological behaviour of the LPD (Section 5.2).

The discharge measurements were used to determine a baseflow from upslope (Section 5.3) and to compare model output to. In June, during the third discharge measuring day, the vegetation on the slope had developed significantly since April. Barely any soil was visible and plants were knee- up to breast-height. In April some vegetation was present, but rarely over knee-height and not as dense as in June. The decrease in discharge on the third measuring day compared to the first two is therefore expected to originate from increased evapotranspiration. The LPD drains water both from the part of the slope in which it is located and from upslope. If the entire slope contains more plants, the flow from upslope decreases and the plant water uptake on the LPD plot increases. This theory is strengthened by the fact that the discharge from the LPD decreased throughout each measuring day (Table A.5). Measurements started in the morning and lasted well into the afternoon. As it was sunny and windy, evapotranspiration explains the decrease in discharge after some daylight hours. Daily fluctuations were also observed in the water level measurements, which were used as testing data for the model (Figure 3.2). The water level device which was installed at location M (Figure 2.1c) collected measurements till 6 May only. Up until that point, the water levels at M and B were quite similar, with similar fluctuations. The comparably extreme fluctuations at location T can partly be explained by the precipitation events and temperature. In some cases, e.g. around 23 May, the water level increased after a rainfall event. The dip in temperature before and on 9 May likely resulted in decrease of evapotranspiration, leading to an increase in the water level. However, the differences between levels at location T and the other locations, amount to almost double at some times. The question remains whether this is a result of an installation fault or of other, unidentified processes. These large measurement differences within the small part of the slope (10 m), resulted in the choice to visually compare trends in the water level measurements with the model output data. As the uncertainty in the water level measurements is too great, statistical analysis would not contribute to a better understanding of the hydrological behaviour of a slope with a LPD.

4.2 Lab Experiment

Setup and malfunctioning

Several installation faults influenced the measurements of the lab experiment. In this discussion, the emphasis is on the water measurements, as those are most important for the hydrological characterisation of the LPD.

The regulation of the irrigation drip system was very difficult. Therefore, the water input into the gutters was unreliable, leading to differences in initial conditions of the precipitation events between the nine gutters. Precipitation runs were done for three gutters at the same time. During a run, some water already reached the gutter next to the setup in which rainfall was simulated. Differences between the gutters with LPD (especially between 1 and 2-3) could originate from the difference in initial soil moisture. Initial infiltration is

assumed to occur faster in the case of a greater soil moisture content, as saturated hydraulic conductivity is usually an order of magnitude greater than unsaturated hydraulic conductivity (Tóth et al., 2015). The results do not necessarily indicate this, but that could be the consequence of the uncertainty of water input volume. Protocol was to close the measuring holes in which pH, soil moisture and temperature sensors were inserted for daily monitoring. However, this was forgotten before some runs. The holes facilitated infiltration, presumably increasing percolation and lateral flow. The different flows were measured after (or in the case of lateral flow, during) collection in containers. In some cases, the measured amount of water in the containers was affected by the setup and execution of the experiment. The percolation containers did not only receive water that dripped from the holes in the gutter, but also some water that did not infiltrate and dripped from the sides of the gutters. Furthermore, if the containers were filled with 600 mL or more, spilling was likely to occur. Lastly, the measurement of the lateral flow during the experiments was uncertain due to handmade 100 mL markings on the containers.

Limitations of the methodology

Firstly, the laboratory experiment was built as a miniature of the field. However, the imperfect scaling from field to lab has implications for measurements during the precipitation experiments. The LPD at the study site has a length of approximately 10 m and the ones in the lab were approximately 50 cm, so the lab experiment was built on a scale of 1:20. Accordingly, the average diameter of the bundles in the lab was 3.8 mm and that of the LPD in Catterline was 200 mm. However, the cuttings that were used to build the bundles in the field had diameters of 10 mm to 20 mm, but the bundles in the lab were constructed with cuttings with diameters of 2.7 mm to 12.1 mm (Table C.1). Furthermore, the twigs used for the lab experiment were very straight, allowing for more efficient drainage than in reality. This overrepresentation of empty spaces between the cuttings in the lab experiment was attempted to mitigate by packing the bundle tighter than in the field. Nevertheless, the drainage capacity was likely relatively too large in the lab experiment, allowing for larger lateral flow and percolation volumes than would be the case in the field. However, as this lab experiment was used to gain a first insight into the hydrological behaviour of a slope with a LPD and not for the quantification of its effects, the results of the precipitation experiments are still deemed valuable. Besides, the measurements in the field indicated that the presence of a LPD in a slope does contribute to an increase of the lateral flow component compared to a bare slope. After all, the measured discharge rates would not be observed in a slope without a drainage system. Furthermore, the gutters were prepared by drilling holes to allow for percolation (Figure B.3). The porosity of the soil was not mimicked by the fraction of surface area that was removed by drilling. Especially as the layer of soil in the gutter was so shallow, translating to approximately 50 cm in the field, this low porosity of the gutter may have caused an underrepresentation of the percolation component and an addition to the lateral flow component. On the other hand, the maximum fraction of percolation that was measured, amounted to 72% (Figure 3.3e), which implies that there was no upper limit to the percolation component.

During the precipitation simulations, the input volume of water into the gutters varied due to diverse reasons. Firstly, the rainfall simulator was built with the same equipment as the irrigation system. The three nozzles could not be adjusted as to give exactly equal amounts of water. The assumed total input volume was the average of the average of the three nozzles over 10 calibrations of 1 min (Table C.2). The rightmost nozzle, which was positioned above the Bare gutters (7, 8 and 9), gave approximately 40 mL less than the other two. As the storage component was determined using the assumed total input, this was overestimated for the Bare gutters. Furthermore, the three gutters that were watered simultaneously, were close enough to each other to allow water from one nozzle to reach other gutters (Figure 2.5). The nozzles at the edges both sprayed some water down the side of the setup and into the middle gutter. The spray from the middle nozzle reached both the left and the right gutter. The LPD+ gutters (4, 5 and 6) might therefore have received more water than the others. In addition, the 80% of the total water volume after calibration of the nozzles was assumed to reach the gutters (the reduced amounts are given in Table 2.1). This assumption was made based on the collection of spilled water during both runs of the fifth experiment, amounting to nine measurements. The spillage ranged from 13% to 29% of the input (Table C.3). Lastly, the irrigation system was attached to a tap that was opened and closed manually. Thus, the tap was not opened equally far every time. Differences caused by this are expected to become less significant in the experiments with more intervals.

Discussion of the results

In the LPD gutters, the runoff comprised up to 21% of the total input. For the LPD+ gutters, the fraction of runoff was lower, up to 10% and the in the Bare gutters the runoff constituted up to 53%. The lateral flow part was noticeably smaller in the Bare gutters with up to 24% of the total input. For the other gutters, up to 66% of the total input ended up as lateral flow. Furthermore, a greater fraction of the water percolated in the gutters with a bundle compared to the bare soil: up to 72% vs. 35%. The storage component varied greatly throughout the experiments. This component was called "storage", but was calculated as the water input volume minus the leaving fluxes. As discussed before, the input into the gutters was not constant. The variations in water input resulted in a miscalculation of the storage component: this was too large if the total water input volume was overestimated and too small if it was underestimated. Likewise, the fractions of the other components were under- and overestimated. The water partitioning of the first experiment (Figure 3.4) indicates that the name "storage" for this component does make sense. The initial moisture content was considerably lower for the third run than for the other runs and the fraction of water that ended up in the storage component was considerably larger than in the other cases. The water that did reach the containers during this experiment ended up as percolation; runoff and lateral flow played almost no part. The decrease of shallow lateral flow with decreasingly wet initial conditions was also found by Kim et al. (2005). The differing initial moisture contents during the experiments clarify differences in storage: more pore volume is available for storage if the initial moisture content is lower. Regardless of the over- and underestimations of the components, the observed trends are reflective of reality.

Part II

Numerical Modelling of a Live Pole Drain

Chapter 5
Theoretical Background and Conceptualisation

The aim of this study is to characterise the hydrological behaviour of a LPD. In Part I, a first research into this behaviour was done using observations from the field and a lab experiment. The partitioning of water into runoff, lateral flow, percolation and storage was quantified to give a preliminary understanding of the fluxes leaving the LPD. This chapter focuses on the "inner workings" of the LPD. A numerical model was used to quantify its hydrological behaviour. First, in Section 5.1, the choice for a model type is explained. In Section 5.2, the model that was used in this study is defined, together with the input parameters and forcing data. Different scenarios for model runs are described in Section 5.3. Transient behaviour both at a temporal scale of the LPD's lifetime and within a year are taken into account. Lastly, in Section 5.4, an explanation of the sensitivity analysis of the model output components to the input parameters is given.

5.1 Model Type

Hydrological models can be categorised in many ways, e.g. according to input/output types, simplicity and spatial resolution. A common classification is based on the manner of calculating the output given the input. This classification divides hydrological models into three types: empirical, conceptual and physically based (Devi et al., 2015; Sitterson et al., 2018). Empirical, sometimes referred to as data-driven, models only use data to find the relations between the input and output. They do not regard any properties of the catchment or the physical processes at play (Devi et al., 2015). An example of such an empirical model is an artificial neural network. However, these neural networks generally need a large amount of data to produce an accurate enough model (Sitterson et al., 2018). In a conceptual model, the hydrology is represented by a number of storage reservoirs which are interconnected by simplified equations of the physical processes in the catchment, e.g. rainfall, infiltration and percolation. These are based on water balance equations. These models can be used when limited data is available (Sitterson et al., 2018). Physically based models are mathematical representations of reality, using physically based equations to represent the different processes in the catchment. These equations are derived from the conservation of mass, energy and momentum, combined with the water balance and the kinematics at play. The model parameters are a direct representation of the catchment characteristics and can often be measured. These models are very site specific and need a lot of measurements on a small spatial scale for the input parameters (Sitterson et al., 2018).

In each of these model types, the relations between input and output are modelled differently, yet they all consider the fluxes entering and leaving a certain catchment. Before choosing the model type, this "catchment" should be defined. In this study, the control volume was defined as the LPD and the soil that resides on top (Figure 5.1). If vegetation is present on top of the LPD, this is included in the control volume. The model is not spatially distributed, due to limited data availability and to limit computational time, allowing for rapid iteration and model development.

The choice of the model type also depends on the availability of information on and measurements at the study site. As described in Section 3.1, various soil parameters close to the LPD were measured: bulk density, porosity, etc. Studies by González-Ollauri and Mickovski (2014), Gonzalez-Ollauri and Mickovski (2017a) and Gonzalez-Ollauri and Mickovski (2017b) gave values for various soil- and vegetation-related parameters at the

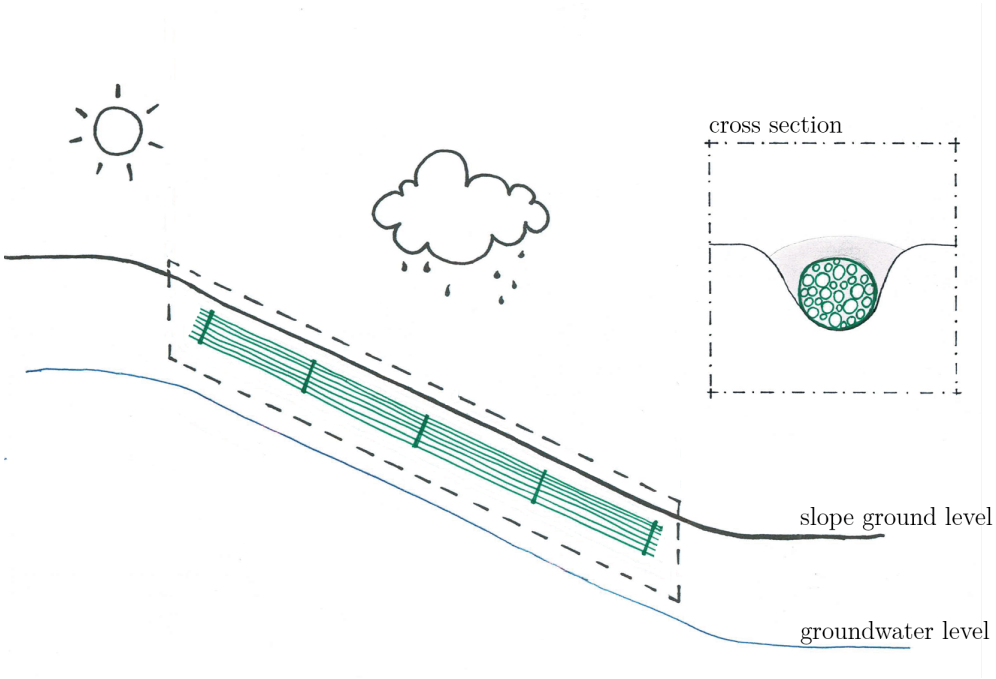

Figure 5.1: *Control volume of the model (inside the dashed box). The green bundle represents the LPD and the box in the upper right corner illustrates the cross-section of the LPD.*

study site. As for meteorological time series, hourly measurements from January 2019 till June 2022 were available. These were provided by a local resident who has access to a weather station. The measurements included precipitation, but solar radiation and potential evaporation data were missing. Therefore, potential evaporation was estimated as described in Section 5.2. Time series to test the model output only exist in the form of the water level measurements (Figure 3.2) and LPD discharge measurements (Table 3.1).

The limited amount of calibration and testing data combined with the quite exhaustive information on the study site's properties gave rise to the choice for a conceptual model with physically based equations that govern the fluxes. These equations include parameters that were measured at the study site, either in this research or in preceding studies. The used spatial scale was up to a few orders of magnitudes smaller than for generally modelled catchments. In order to capture all processes within the slope, the time step used in the model (dt) was set to 1 h.

5.2 Conceptual Model of a Live Pole Drain

As mentioned in Section 5.1, conceptual models are generally based on water balance equations. For an entire catchment, this water balance is given by Equation (5.1).

$$\frac{dS}{dt} = Q_{in} - Q_{out} \tag{5.1}$$

Here, $\frac{dS}{dt}$ is the storage change over time, Q_{in} the sum of the fluxes entering the catchment and Q_{out} the sum of the fluxes leaving the catchment. Q_{in} includes precipitation and Q_{out} discharge from the river and evaporation. Usually, catchments are defined such that the groundwater watershed is equal to the topographical watershed (Bogaard and Greco, 2016), meaning that the aforementioned fluxes are the only ones entering and leaving the system. In this study, however, the defined control volume is part of a hillslope, meaning that Q_{in} and Q_{out} consist of multiple components. The cross-section of a hillslope can be divided into the saturated (below the groundwater table) and unsaturated (above the groundwater table) zone (Lu and Likos, 2004).

Major hydrological processes on and in a hillslope include precipitation, overland flow (both Hortonian and saturation), evaporation, plant water uptake and transpiration, infiltration, lateral flow through the unsaturated zone, seepage and percolation (Lu and Godt, 2013). More vegetation-related processes include canopy interception, throughfall and stemflow (Van Dijk and Bruijnzeel, 2001). The model that was developed for the LPD at Catterline Bay included the processes depicted in Figure 5.2a. This figure illustrates that the storage is made up of the above-ground component canopy interception and the subsurface storage. Q_{in} consists of precipitation and incoming lateral flow. Q_{out} consists of interception evaporation, runoff, evapotranspiration, lateral outflow (or flow through the LPD) and percolation. The water balance of the total model is given in Equation (5.2). Symbols are explained in Figure 5.2. Within the control volume, water partitioning happens between the fluxes stemflow, effective precipitation and infiltration. Mechanical processes such as weathering and erosion are also at play (Lu and Likos, 2004). However, as these processes are not within the scope of this study, they were neglected.

$$\frac{dS}{dt} = P + Q_{L,in} - E_I - Q_{OF,out} - E_{TP} - Q_P - Q_{L,out} \tag{5.2}$$

The conceptual model in this study is also based on the fill-and-spill concept: fluxes entering the control volume are stored (fill) and only when the storage reaches the maximum capacity, a flux leaves this storage component (spill) (Tromp-Van Meerveld and McDonnell, 2006). Usually, the maximum storage capacities are included in the model as empirical parameters for which values are found through calibration, e.g. in the well-known conceptual HBV model (Bergström and Lindström, 2015). However, in this study not enough data was available for testing and calibration, making it necessary to base the maximum storage capacities on physical parameters measured in the field. As mentioned in Section 5.1, the movement of the fluxes between the storage components was also determined with equations which included parameters that were measured in the field or found in previous studies. The equations which describe the aforementioned processes, are given in Appendix D.1.

Two representations of the model can be found in Figure 5.2. Figure 5.2a shows the fluxes and states in a drawing of the slope with fully developed vegetation. Variations in the model as a result of vegetation development and seasonality are described in Section 5.3. The annual evaporation at the study site is 300 mm/yr and mostly occurs during the late spring and the summer months (Marsh and Anderson, 2002). The evaporation was assumed to occur during 6 months (April-September), resulting in an amount of 2 mm/d. Evaporation mostly occurs during daylight hours, so time series with hourly evaporation were made with $E_P = 0$ between 6PM and 8AM and $E_P = 0.2$ mm/h between 8AM and 6PM. The discharge measurements and water level data described in Section 3.1 were used to visually compare the model output to. Furthermore, the water partitioning results from the lab experiments (Section 3.2) were compared to the water partitioning of the model output. As depicted in Figure 5.2b, the model is divided into two parts: Part I comprises the above-ground, vegetation-related processes and Part II the subsurface processes in the control volume. The model algorithm is given in Appendix Appendix D.2 and the assumptions under which the model was created are listed in Table D.3.

Part I

The first part of the model includes the state interception storage, the entering flux precipitation and the fluxes interception evaporation, stemflow and throughfall leaving the control volume. The water balance for these above-ground processes is given in Equation (5.3). Precipitation is entered into the model as hourly input time series. At each time step throughfall, stemflow and evaporation are calculated and used to update the interception storage.

$$\frac{dS_I}{dt} = P - E_I - Q_{st} - P_E \tag{5.3}$$

Part of the precipitation is intercepted and stored by the canopy as interception storage S_I. Another fraction immediately reaches the ground surface as direct throughfall $P_{E,d}$; this partitioning happens by means of the free throughfall coefficient p (Van Dijk and Bruijnzeel, 2001). The precipitation which exceeds the

maximum storage capacity $S_{I,max}$, leaves S_I as indirect throughfall $P_{E,i}$. The sum of direct and indirect throughfall is partitioned into effective precipitation P_E and stemflow Q_{st} through the stemflow fraction p_s (Van Dijk and Bruijnzeel, 2001). The maximum storage capacity is determined with the canopy storage capacity S (Gonzalez-Ollauri and Mickovski, 2017b) and the canopy cover fraction c, which is determined by the Beer-Lambert equation (Maass et al., 1995). The latter depends on the Leaf Area Index LAI and light extinction coefficient kc, allowing for seasonal and longer-scale variations. The interception storage is depleted by evaporation E_I. Solar radiation is assumed to be negligible in time steps during which precipitation occurs, so in that case interception evaporation was set to zero. The equations that govern this part of the model are given in Table D.1.

Part II

The outputs throughfall and stemflow from Part I are inputs for the second part of the model together with the time series for the potential evaporation and precipitation. Part II includes the partitioning of effective precipitation into runoff and infiltration, which enters the subsurface storage together with the stemflow and lateral inflow. Water leaves the storage through evapotranspiration, percolation or flow through the LPD. The water balance for Part II is given in Equation (5.4).

$$\frac{dS_U}{dt} = Q_{st} + Q_{inf} - E_{TP} + Q_{L,in} - Q_P - Q_{L,out} \tag{5.4}$$

First, the stemflow reaches the subsurface storage reservoir S_U. If $S_{U,max}$ would be exceeded, the excess is assumed to leave the system as runoff within the same time step. Afterwards, the effective precipitation P_E is partitioned into runoff $Q_{OF,out}$ and infiltration Q_{inf} according to the model developed by Hawkins and Cundy (1987) as described by Langhans et al. (2011). It is assumed that the infiltration has reached steady state and that the infiltration rate only depends on the rainfall intensity and the average infiltration rate. In this study, the average infiltration rate was replaced with the Van Genuchten-Mualem unsaturated hydraulic conductivity calculated with the Brooks and Corey-Burdine model to predict relative hydraulic conductivity (MVG-BCB) (Kuang et al., 2021) in the case that $S_U < S_{U,max}$. This variable depends on the soil moisture, which in turn depends on the pressure head and hence the storage S_U. In the case that $S_U = S_{U,max}$, all effective precipitation was assumed to end up as runoff.

The incoming lateral flow $Q_{L,in}$ was assumed to consist of two parts. The first part is a constant baseflow Q_{base}, determined with the results from the discharge measurements executed in April and June 2022 (Table 3.1). The second part comprises the runoff from the upslope part of the hill. A simple rainfall-runoff model with a runoff coefficient of 0.2 is used to determine the amount of runoff from the upstream part of the slope. The fraction of water that infiltrates in the upslope part was assumed to percolate, so to not reach the LPD as lateral flow. The evapotranspiration is calculated the potential evaporation E_P. It consists of a soil evaporation and a plant transpiration component. The soil evaporation was assumed to be proportional to the potential evaporation, only limited by the canopy cover, as described by Savabi and Williams (1995). Field observations by Gonzalez-Ollauri and Mickovski (2017a) indicate that the entire root system contributes to plant transpiration, leading to the assumption of a steady transpiration rate. The percolation rate depends on the storage S_U and the maximum percolation rate P_{max}, as commonly used in the conceptual HBV model (Bergström and Lindström, 2015). The lateral flow $Q_{L,out}$ is represented as one-dimensional Darcy flow, including the MVG-BCB unsaturated hydraulic conductivity. The gradient of the pressure head was assumed to be equal to the gradient of the slope. The equations that govern this part of the model are given in Table D.2.

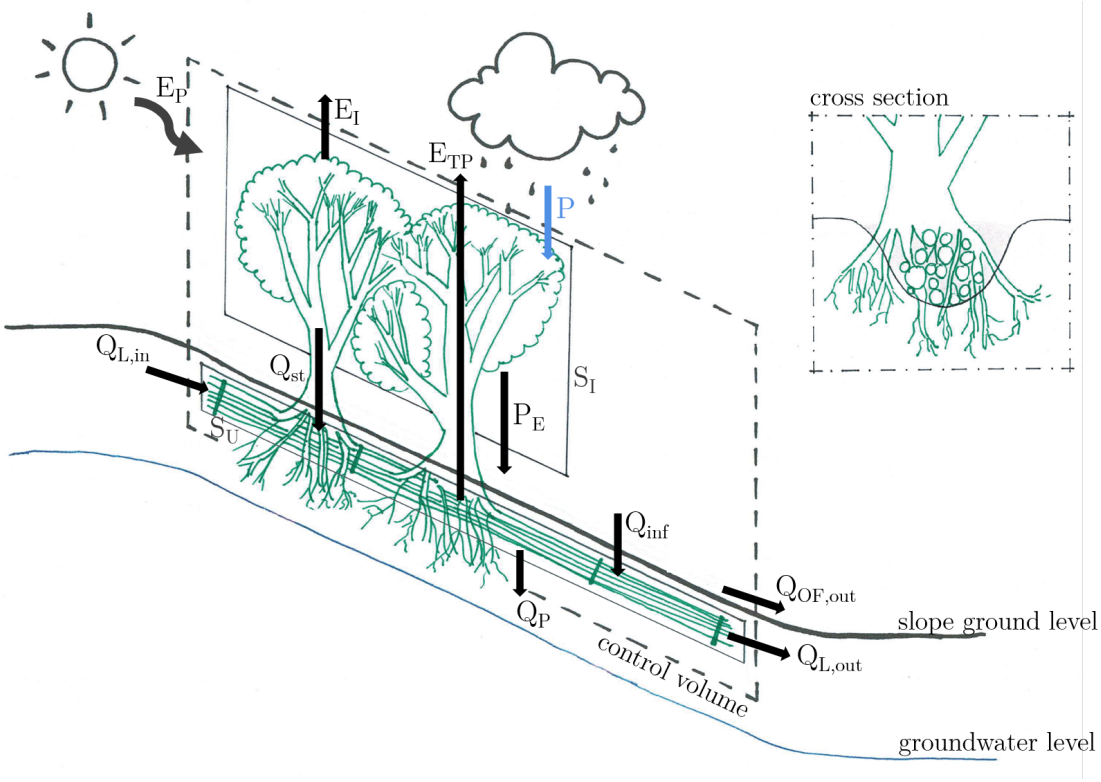

(a)

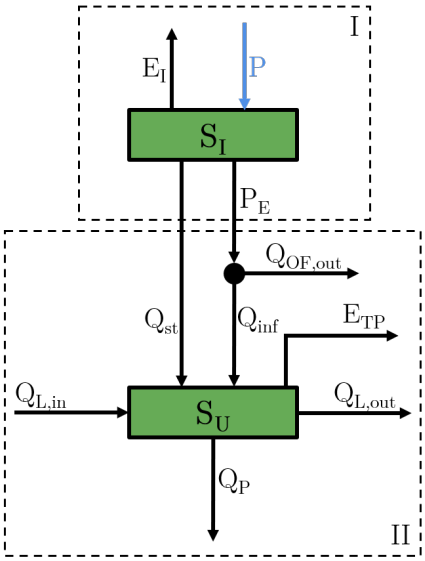

(b)

Symbol	Process
FORCING	
P	Precipitation
E_P	Potential evaporation
STATES	
S_I	Interception storage
S_U	Subsurface storage
FLUXES	
E_I	Interception evaporation
P_E	Throughfall
Q_{st}	Stemflow
$Q_{OF,out}$	Runoff
Q_{inf}	Infiltration
$Q_{L,in}$	Entering lateral subsurface flow
$Q_{L,out}$	Leaving lateral subsurface flow
E_{TP}	Evapotranspiration

(c)

Figure 5.2: *Schematic visualisations of the conceptual model.* ***(a)*** *The fluxes and states depicted in a schematised drawing of the slope.* ***(b)*** *The fluxes depicted with arrows and states/buckets with boxes. The black dot represents the equations used to separate effective precipitation into infiltration and runoff. The model is divided into two parts. Part I comprises the above-ground processes and Part II the subsurface processes.* ***(c)*** *Descriptions of the symbols.*

5.3 Scenarios and Parameter Values

From studies into various tree species, Jacbos et al. (1955) and Meng et al. (2014) found that the life span of forest stands is generally divided into four to six phases, i.e. juvenile sapling, pole, mature (early), mature, mature (late) and overmature. There is a relationship between tree stand age and leaf area index (LAI): the latter increases in the juvenile stages and is at its peak during the beginning of the mature stage, after which it declines (Meng et al., 2014). Accordingly, Marc and Robinson (2007) found that the evaporation and transpiration are higher in the early life stages of a forest stand and later decrease with growing age. Research was done into biomass production of *Salix Viminalis* (Ahman, 1997; Tahvanainen and Rytkönen, 1999), as it is often used for energy production. However, as these studies focus on growing basket willow in optimal conditions to maximize yield, they do not represent a natural development. Studies linking tree size to life phase of *Salix Viminalis* do not exist. Besides, not all trees within a stand develop at the same rate (Tahvanainen and Rytkönen, 1999). Parameters that describe characteristics of willows at the study site were found by Gonzalez-Ollauri and Mickovski (2017b), who assumed adult trees. Therefore, for the hydrological processes concerning LPDs, scenarios were defined at the following phases: Bare, a baseline of a slope without LPD; LPD, just after installation of the LPD and LPD+, a slope with LPD and willows in the mature growth phase.

The 14 input parameters can be divided into three categories: 1) independent of seasons or growth phase (constant), 2) independent on seasons but dependent on the presence of a LPD (LPD-related) and 3) dependent on seasons and growth phase of the willows (vegetation-related). Values for the constant parameters are given in Table 5.1. The first three were generated by the Plant-Best model applied to the study site (Gonzalez-Ollauri and Mickovski, 2017b). The parameter d is described as the diameter of the bundle or the height of the considered soil column in mm.

Table 5.1: *Values of the constant model input parameters. θ_{fc}: soil moisture content at field capacity; k_{sat}: saturated hydraulic conductivity; i: sine of slope inclination; d: diameter LPD or height soil column.*

Parameter	Unit	Value	Source
θ_{fc}	-	0.23	Gonzalez-Ollauri and Mickovski (2017b)
k_{sat}	mm/h	180	Gonzalez-Ollauri and Mickovski (2017b)
i	-	0.50	Gonzalez-Ollauri and Mickovski (2017b)
d	mm	200	This study (Section 3.1)

Parameters whose values only change depending on the presence of a LPD are given in Table 5.2. The porosity for bare soil was determined with the samples taken at the study site (Section 3.1). The porosity was given a higher value in the scenarios with a LPD, as the macropore fraction was assumed larger than in a slope with bare soil. The Van Genuchten parameter n also changes after installation of a LPD or vegetation (Gonzalez-Ollauri and Mickovski, 2017b). The order of magnitude of parameter α was retrieved from a study by Kuang et al. (2021). A value which corresponded with the bulk density and soil type at Catterline was chosen.

Table 5.2: *Values of the LPD-related model input parameters. n_{por}: porosity; n: pore-size distribution; α: Van Genuchten parameter.*

Parameter	Unit	Bare	LPD & LPD+	Source
n_{por}	-	0.35	0.45	This study (Section 3.1)
n	-	3.93	1.51	Gonzalez-Ollauri and Mickovski (2017b)
α	1/mm	0.1	0.01	Kuang et al. (2021)

Values for the season- and life phase-related parameters are given in Table 5.3. The scenarios Bare and LPD do not include vegetation, meaning that the entire Part I of the model reduces to $P_E = P$ (effective

precipitation equals the precipitation). In scenario LPD+ in the dormant season, only stemflow is assumed to influence the effective precipitation. Values for the stemflow (p_s) and free throughfall (p) coefficients were determined on the basis of research at the study site by Gonzalez-Ollauri and Mickovski (2017b). Values for S, kc and LAI were retrieved directly from previous research (Gonzalez-Ollauri and Mickovski, 2017b) and the estimate for Ac' is based on experience from the study site; 80% of the ground area was assumed to be canopy-covered. The baseflow from the upslope part of the hill Q_{base} was estimated with the results from fieldwork (Table 3.1). Measurements from June were used to determine the value for the growing season and the measurements from April were increased to obtain a value for the dormant season, to correct for the presence of vegetation in April.

Table 5.3: *Values of the vegetation-related model input parameters for each scenario. p: free throughfall coefficient; p_s: stemflow fraction; S: canopy storage capacity; Ac': canopy-covered ground area; kc: light extinction coefficient; LAI: Leaf Area Index; Q_{base}: baseflow from upslope.*

Parameter	Unit	Season	Bare	LPD	LPD+	Source
p	-	growing	1	1	0.5	Gonzalez-Ollauri and Mickovski (2017b)
		dormant	1	1	1	
p_s	-	growing	0	0	0.1	Gonzalez-Ollauri and Mickovski (2017b)
		dormant	0	0	0.05	
S	mm/m^2	growing	0	0	0.72	Gonzalez-Ollauri and Mickovski (2017b)
		dormant	0	0	0	
Ac'	m^2	growing	0	0	1.6	Gonzalez-Ollauri and Mickovski (2017b)
		dormant	0	0	0	
kc	-	growing	0	0	0.60	Gonzalez-Ollauri and Mickovski (2017b)
		dormant	0	0	0	
LAI	-	growing	0	0	3.34	Gonzalez-Ollauri and Mickovski (2017b)
		dormant	0	0	0	
Q_{base}	mm/h	growing	0.62	0.62	0.62	This study (Table 3.1)
		dormant	6.2	6.2	6.2	

In total, six model simulations were performed: one for each scenario in both the growing and the dormant season. For the growing season, input time series from May 2022 were used and for the dormant season, input time series from December 2021 were used. Overviews of the input parameter values and input time series for each of the model runs are given in Appendix D.

5.4 Sensitivity Analysis

A local sensitivity analysis of the parameters was executed in order to diagnose which parameters contribute most to the output variability and thus which need additional research to reduce output uncertainty. Sensitive parameters are defined as "those which have a significant influence on assessment results" (Hamby, 1994). This analysis was conducted under the assumption that the model input parameters are independent and it was based on a method by Crick and Hill (1987) as described by Hamby (1994). It is described as a one-at-a-time sensitivity measure, as all parameters are kept constant except one, which is changed repeatedly. For each scenario and season combination, the base-case was defined with the parameter values as described in Section 5.3. One by one, the parameters were sampled 1000 times from a Gaussian distribution. The mean equal was to the base-case value and the standard deviation was 25% of this value. For each parameter, the change in model output was determined by calculating the mean and standard deviation of all 1000 outputs. Afterwards, for all outputs $\neq 0$, the mean of the mean and the mean of the standard deviation were calculated. The means of the standard deviation were reported as a percentage of the base-case in a heat map with an overview of all parameters and model components. A large relative standard deviation indicates a large sensitivity of a model output component to changes in a parameter value.

Chapter 6
Results

The outputs of the model runs for all scenarios in the growing season are presented in this chapter. Outputs for the dormant season can be found in Appendix E.1. Results were similar for the two seasons, the main difference being the evaporation component, which was zero in the dormant season. The data were simulated for one month (May 2022). In this chapter, the third week (15-22 May) is highlighted in the assessment of the slope's predicted reaction to precipitation events of different intensities to allow for some spin-up time and to later compare to the water level measurements (Figure 3.2). First, the model input time series are shown (Figure 6.1), after which several output components are presented (Figure 6.2). Lastly, the water partitioning visualisations for all scenarios in all seasons are shown (Figure 6.3).

6.1 Model Runs

Time Series

The model input time series for a week in the growing season are shown in Figure 6.1 together with the calculated incoming lateral flow, which is a flux that enters the control volume. Daily fluctuations in the potential evaporation rate are visible. It is clear that the incoming lateral flow existed of a baseflow component and a precipitation-related component. Several output components of the model runs for all scenarios in the growing season are depicted in Figure 6.2: runoff, lateral flow, percolation and subsurface storage.

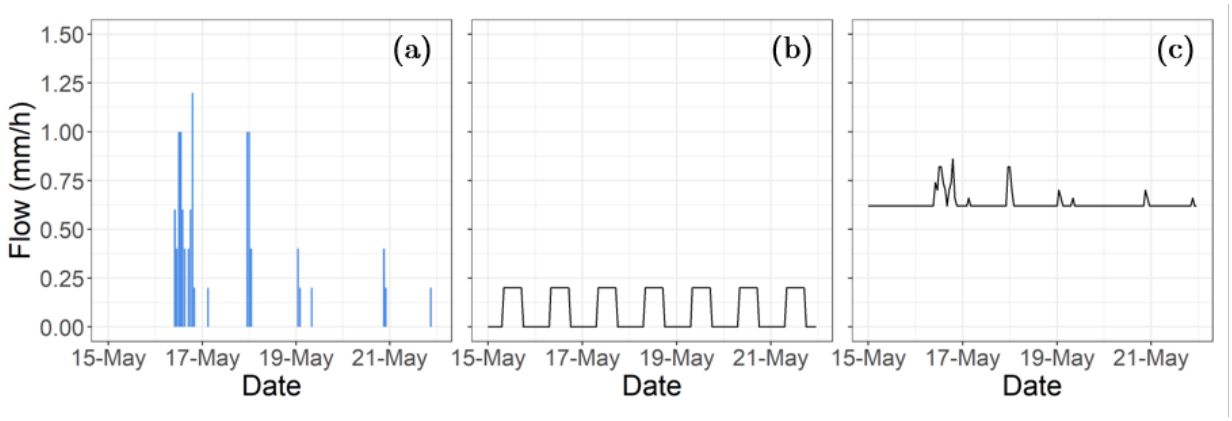

Figure 6.1: *Model input and incoming lateral flow for one week in the growing season. The simulation was done for May 2022 and the third week is shown.* ***(a)*** *Precipitation.* ***(b)*** *Potential evaporation.* ***(c)*** *Incoming lateral flow.*

The peaks in runoff coincided with peaks in precipitation for all three scenarios, but they were up to five times higher in the Bare scenario. For both LPD and LPD+, the runoff never exceeded 0.25 mm/h. For these two scenarios, the lateral flow fluctuated around a baseflow of approximately 0.25 mm/h with peaks which coincided with precipitation events. The fluctuations corresponded to those in the evaporation component.

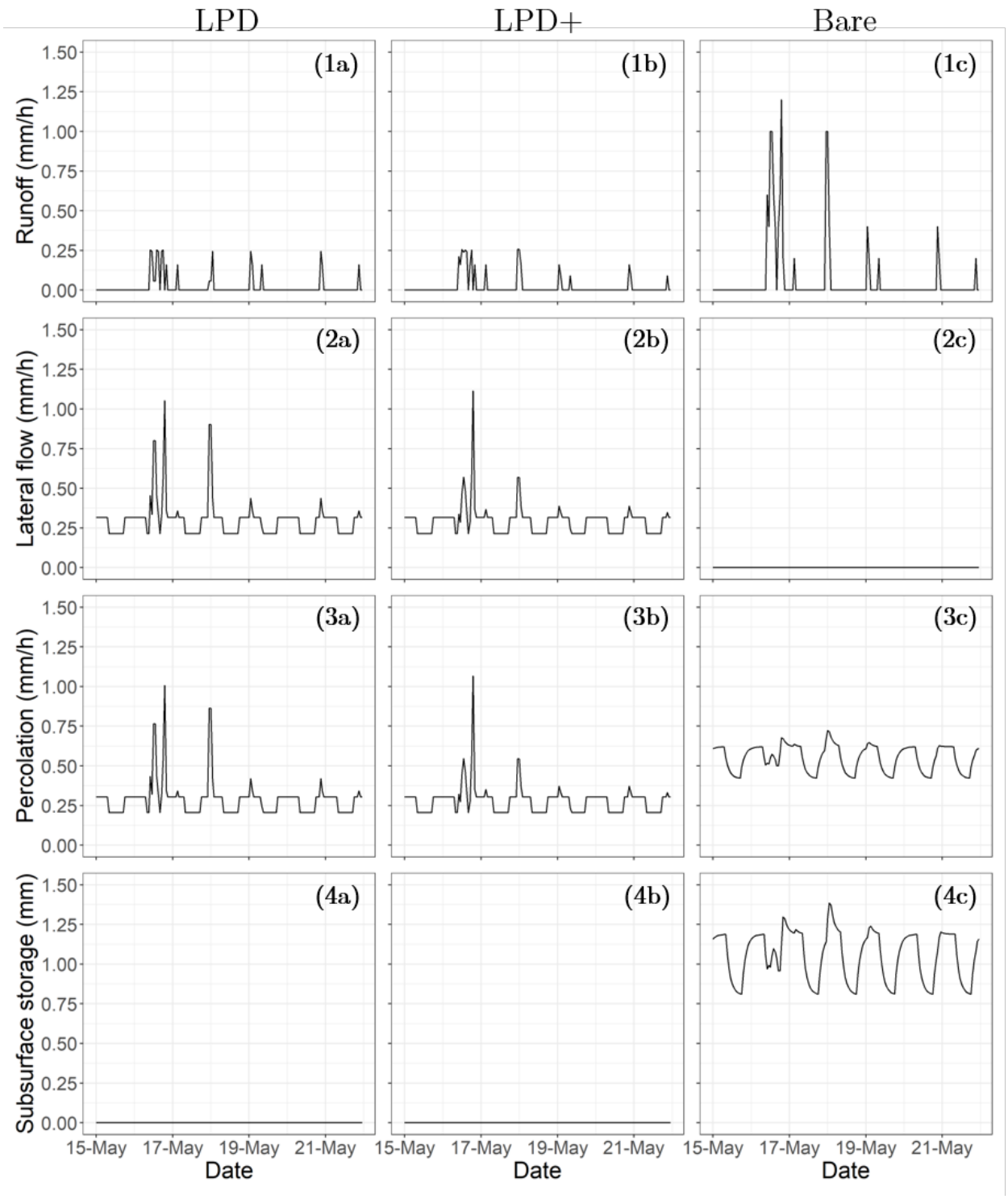

Figure 6.2: *Model output for one week in the growing season. The simulation was done for May 2022 and the third week is shown.* ***(1)*** *Runoff.* ***(2)*** *Lateral flow.* ***(3)*** *Percolation.* ***(4)*** *Subsurface storage.* ***(a)*** *LPD.* ***(b)*** *LPD+.* ***(c)*** *Bare.*

In the Bare scenario, none of the water which entered the control volume left as lateral flow. In this scenario, however, the percolation component was larger than in the other two. In the LPD and LPD+ scenarios, the

percolation fluctuated around 0.25 mm/h with peaks which correspond to precipitation events. The patterns and amounts of runoff, lateral flow and percolation were almost equal in these two scenarios, with slightly smaller peaks at lower precipitation intensities and larger peaks at higher precipitation intensities in the LPD+ scenario. Fluctuations in percolation were less regular and even than in the Bare scenario. The subsurface storage remained zero throughout the entire week in the scenarios with a LPD, meaning that the model predicted that all incoming water drained from the control volume within each time step of 1 h. Up to 1.7 mm of water was stored in the Bare scenario, with fluctuations which coincide with the evaporation. Once again, small peaks at the times of precipitation peaks are visible.

Water Partitioning

The results of the water partitioning of the entire model run for both seasons are shown in Figure 6.3. In the dormant season, outflow only happened in the form of runoff, lateral flow or percolation. A very small amount stayed in the control volume as storage. In the growing season, evapotranspiration made up 13% of the total output volume for all scenarios and interception evaporation played a very small role in the LPD+ case. In both seasons, more water ended up as runoff in the Bare scenario than in the scenarios with a LPD. All runoff components were larger in the growing season. Furthermore, lateral flow was zero for the Bare scenario in both seasons: the largest part of the water ended up as percolation. In the scenarios LPD and LPD+, the lateral flow component was slightly larger than the percolation component; both components comprised up to 50% of the total input volume in the dormant season and up to 43% in the growing season.

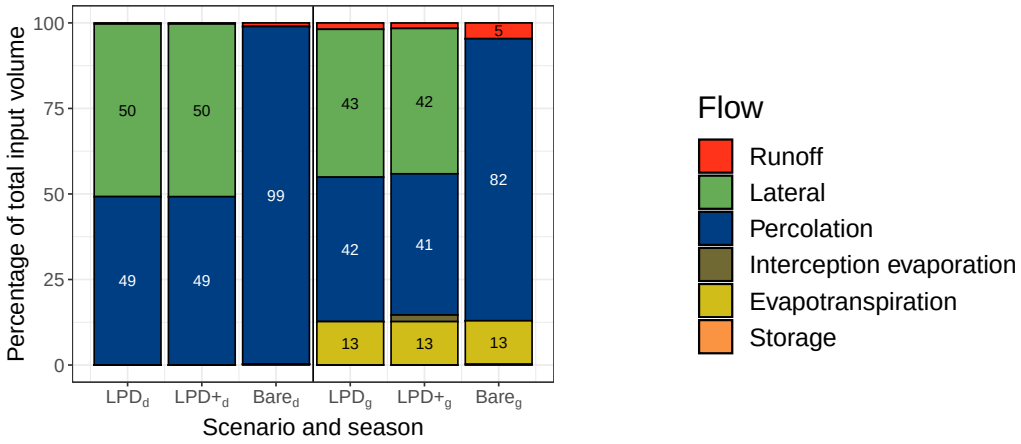

(a) *(b)*

Figure 6.3: ***(a)*** *Water partitioning into fluxes leaving the system as percentages of the monthly input volume for all model runs. Left three bars: dormant season. Right three bars: growing season.* ***(b)*** *Legend.*

6.2 Sensitivity Analysis

The results of the sensitivity analysis for LPD+ scenario in the growing season are presented as a heatmap in Figure 6.4. None of the model output components were sensitive to the sine of the slope inclination i. Evapotranspiration E_{TP} and incoming lateral flow $Q_{L.in}$ were only sensitive to the baseflow from upslope Q_{base}. Other model components were influenced by multiple parameters. Especially the subsurface storage S_U was sensitive to many parameters, with relative standard deviations ranging from 27% to 319%. The Van Genuchten parameter n had the most influence on change in the subsurface storage. This parameter also influenced the lateral flow $Q_{L.out}$, percolation Q_P, runoff $Q_{OF.out}$ and infiltration Q_{inf}. In addition, the subsurface storage was sensitive to the diameter of the LPD d and the porosity n_{por}, which also influenced the lateral flow $Q_{L.out}$ and percolation Q_P. The same model components were sensitive to the soil moisture content at field capacity θ_{fc}. Runoff and infiltration, effective precipitation, stemflow, interception storage and evaporation were sensitive to the free throughfall coefficient p. Both the canopy storage capacity S and the canopy-covered ground area Ac' also influenced these components.

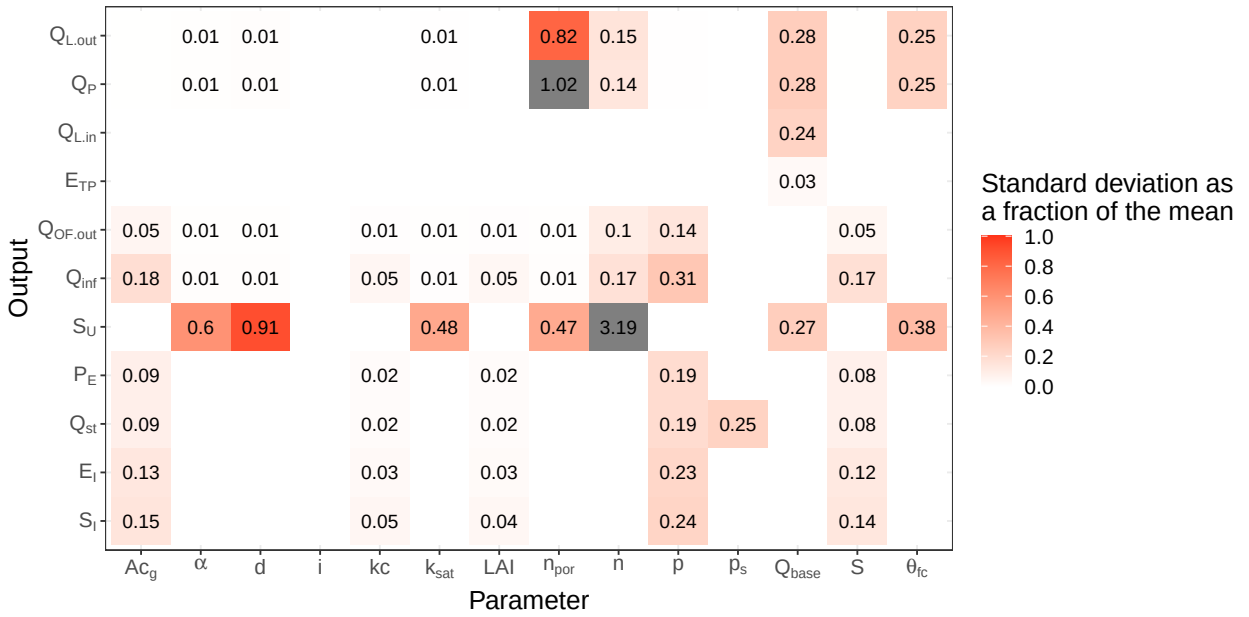

Figure 6.4: *Heatmap of the sensitivity of model outputs to the change in input parameter values. The scenario is LPD+ in the growing season. Values are standard deviations of the base-case as fraction of the mean. Explanations of the output component symbols are given in Figure 5.2c. Explanations of the parameter symbols are given in Tables 5.1, 5.2 and 5.3.*

Chapter 7
Discussion

In Section 7.1, the limitations of the methodology are explained. This explanation includes the conceptualisation of the model, the assumptions that were made (Table D.3) and their presumed effects on the model output. Furthermore, the methodology of the sensitivity analysis is considered. In Section 7.2, the model output time series and the water partitioning are discussed and a nuanced interpretation of the results is given.

7.1 Limitations of the method

Hydrological processes and their numerical representation in this study

Firstly, input potential evaporation time series were created assuming that evaporation only occurs in April-September and between 8AM and 6PM during those months. In many hydrological models, potential evaporation is determined using an equation that takes the solar radiation as one of its inputs (Penman et al., 1948; Priestley and Taylor, 1972). In these models, variations in evaporation within seasons and, depending on the temporal resolution, within the day, are accounted for. However, daily values of evapotranspiration are of a small order of magnitude compared to e.g. subsurface storage. Bergström and Lindström (2015) found that detailed potential evaporation estimates are unnecessary for successful model predictions. Besides, annual evaporation in Scotland is low, meaning that its influence on the model output is limited.

The vegetation-related model components consist of canopy interception, throughfall, stemflow and interception evaporation. The maximum storage capacity was based on a study by Gonzalez-Ollauri and Mickovski (2017b). It depends on the parameters canopy storage capacity, canopy covered ground area, LAI and light extinction coefficient, which account for more than one third of the input parameters. The choices for the most influential parameter values are discussed in Section 7.2. Interception by litter was not taken into account, while it has been found to constitute up to 5% of annual rainfall (Helvey and Patric, 1965). Interception by trunks and branches was also neglected, while over half of the total interception has been found to consist of trunk storage (Herwitz, 1985). Thus, the maximum interception storage was presumably underestimated in this study. Furthermore, the indirect throughfall is assumed to occur only when the maximum interception storage capacity is exceeded. This might have led to an overestimation of p (Van Dijk and Bruijnzeel, 2001), because it was determined based on regression between throughfall and rainfall, rather than the rainfall needed to saturate the canopy (Gonzalez-Ollauri and Mickovski, 2017a). Interception evaporation was assumed to occur only in time steps with zero precipitation, but evaporation can still occur during those times.

Partitioning of effective precipitation into infiltration and runoff was done by means of the Hawkins and Cundy (1987) model. In this model, the infiltration capacity parameter represents the average of the hydraulic conductivities in the field. It is assumed that the wetting front has travelled far enough for the effect of suction on infiltration capacity to become very small. Normally, this infiltration capacity is determined empirically (Langhans et al., 2011), but in this study, it was substituted with the MVG-BCB unsaturated hydraulic conductivity. The effects of changes of the empirical Van Genuchten parameters are described in Section 7.2. Research by Langhans et al. (2011) showed that increased precipitation intensity leads to increased infiltration capacity. In this study, the infiltration capacity only depends on the degree of filling of the subsurface storage. Precipitation intensity is not taken into account, which means that the infiltration

capacity might be overestimated in case of low intensity events and underestimated in case of high intensity events. Furthermore, ponding or surface storage was neglected in this study; effective precipitation that reaches the ground is immediately available for infiltration/runoff partitioning. In reality, a delay occurs at the beginning of a precipitation event before infiltration and runoff start (Mishra et al., 2003). This delay is not represented in the model and runoff and infiltration are therefore overestimated at the start of precipitation events. Lastly, resistance to overland flow was not taken into account. The time step of 1 h was assumed to be large enough for this not to affect the results significantly. Runoff from the part of the hill upslope of the LPD was assumed to enter the control volume as lateral flow. As the LPD is located very close to the ground level and is Y-shaped at the upslope end, it was assumed to collect and drain runoff from upslope. This assumption was also included in the Bare scenario, though it is unlikely that in that case, runoff from upslope enters the control volume as lateral flow. The incoming lateral flow volume was therefore overestimated for the Bare scenario; it would have been more representative of reality to include an incoming overland flow component. The runoff coefficient which was used to determine the fraction of precipitation that reaches the LPD as incoming lateral flow was based on commonly used values for rural areas (Allen et al., 1998). It actually increases with precipitation intensity, but as the value of 0.2 is already on the high side for rural areas (Rodríguez-Blanco et al., 2012), the runoff coefficient was assumed constant.

Subsurface storage capacity $S_{U,max}$ was simplified to the product of the porosity n_{por} and the depth of the soil column or diameter of the LPD d. This implies that the soil is considered a homogeneous continuum. Macropores were not taken into account, but the value of n_{por} varied according to the presence of a LPD to account for this phenomenon. Water leaves the subsurface storage as either evapotranspiration, percolation or lateral flow. Evapotranspiration is limited by the available water in the subsurface storage after it is recharged with stemflow, infiltration and incoming lateral flow. It consists of a soil evaporation and plant transpiration component. The latter is assumed zero in the scenarios without vegetation (Bare and LPD). Water from the entire soil column with depth d was assumed to be available for both soil evaporation and plant transpiration, while in reality the depth available for soil evaporation is limited based on soil type (Gonzalez-Ollauri and Mickovski, 2017b). This results in equal amounts of evapotranspiration in all scenarios.

Percolation is limited by the maximum percolation rate P_{max} and depends on the degree of filling of the subsurface storage. P_{max} is determined with $S_{U,max}$, d and the soil moisture content at field capacity θ_{fc}. Field capacity is defined as "the amount of water held in the soil after the excess gravitational water has drained away [...]" (Veihmeyer and Hendrickson, 1931). Therefore, it was assumed that the amount of water draining from S_U could not exceed the difference between $S_{U,max}$ and $d \cdot \theta_{fc}$. However, the value of P_{max} was not compared to the saturated hydraulic conductivity, which is determinative for the velocity of water movement through soil (Chapuis, 2012; Ghestem et al., 2011). P_{max} could exceed k_{sat}, which would lead to an overestimation of the percolation component. Furthermore, macropores are not explicitly accounted for in the model, but these affect flow through the soil (Beven and Germann, 1982). In reality, the macropore fraction is expected to increase after installation of a LPD. Therefore, the value of n_{por} was increased for the scenarios that include a LPD. This is reflected in the value of $S_{U,max}$ and thus in that of P_{max}.

Lastly, lateral flow through the soil column or LPD is determined with one-dimensional Darcy flow, in which a homogeneous soil column is assumed. As explained above, this is not realistic. Another assumption is that the gradient in hydraulic head equals the slope gradient. In reality, this is not the case (Wallach and Zaslavsky, 1991).

Sensitivity analysis

The sensitivity analysis was executed under the assumption that all parameters are independent. In reality, groups of parameters are related to each other, e.g. the vegetation-related p, p_s, S, Ac', kc and LAI. This method, however, was merely implemented to determine the comparative sensitivity of the model to the various parameters (Hamby, 1994). For insight into this sensitivity, the one-by-one assessment of the parameters is sufficient. Furthermore, for the creation of the heatmap (Figure 6.4), only model output that was greater than zero was taken into account. This was done because most of the fluxes are zero in case of zero precipitation, regardless of parameter values. Taking into account these zero values would lead to an underestimation of sensitivity, because zero values would not change as a result of the varying parameter values. However, some model output components, e.g. the subsurface storage S_U, are zero for almost the entire run. In that case, the

value of the relative standard deviation which is shown in the heatmap (Figure 6.4) was determined based on a limited amount of time steps and not very representative for the entire model run. Lastly, it is important to note that the sensitivity analysis was only run for the LPD+ scenario in the growing season, in which all processes are included in the model. In the dormant season or other scenarios, part of the parameters is zero. The other, non-zero parameters might have a larger influence on the model output components than it seems from Figure 6.4.

7.2 Discussion of the results

The limitations discussed in Section 7.1 are specific for the model used in this study. However, other choices in terms of numerical representation of hydrological processes, would have led to other limitations. The aim of the modelling in this research is to compare the trends in a slope with LPD to the trends in a slope with Bare soil. Obtaining values and amounts that exactly reflect reality is therefore not the main concern and the discussion of the model outputs comprises the observed trends. It is centred around the model runs of the LPD+ scenario in the growing season. The model output components (Figure 6.2) are discussed one by one, including the results from the sensitivity analysis. Comparison to the other scenarios and seasons is done on the basis of the water partitioning (Figure 6.3). Parameters and model output which concern the design of the LPD are discussed more in-depth than the physical parameters, as the former are important for application of the measure.

The calculated runoff for the Bare scenario is up to five times larger than that for the scenarios with a LPD (Figure 6.2). The runoff depends on the Van Genuchten parameters, which are empirical and have not been determined for this study site specifically. However, the observed difference in runoff between the scenarios corresponds to expectations, as the LPD causes an increase in porosity. Higher porosity soils are more permeable and more susceptible to infiltration compared to lower porosity soils (Lipiec et al., 2006). If the LPD is installed at ground level and only loosely covered by soil, water can infiltrate very easily, resulting in zero to very little runoff. Furthermore, vegetation causes resistance to overland flow (Kadlec, 1990). This characteristic was not captured in the model setup, but it confirms the realistic truth of the difference in runoff between the scenarios. Figure 6.3 shows that the calculated fraction of water input volume which ended up as runoff was smaller in the dormant season for all scenarios. In reality, the increased resistance to overland flow by vegetation presumably leads to a decrease of the runoff component in the growing season in the LPD+ scenario. In the Bare scenario, 5% of the input volume ended up as runoff, which is low considering commonly found values for runoff coefficients for rural areas, which often exceed 0.10 (Allen et al., 1998). Nevertheless, the observed trends are representative of reality.

The differences in output time series of lateral flow between the different scenarios are evident: the model predicts zero lateral flow for the Bare scenario and flows up to 1.1 mm/h for the LPD and LPD+ scenarios (Figure 6.2). In the Bare scenario, all water which enters the subsurface storage leaves as either soil evaporation or percolation. Some of it stays behind in the soil. It seems that the unsaturated hydraulic conductivity is (almost) zero for the Bare scenario. This is confirmed by the fact that infiltration is zero in this case (Figure E.6c). However, infiltration and (shallow) lateral flow are usually non-zero on steep slopes (Kim et al., 2005). For the other two scenarios, the predicted regimes are very similar and follow the daily fluctuations which are influenced by the evapotranspiration. That water is predicted to infiltrate, becomes clear from the peaks that correspond to precipitation events. The sensitivity analysis shows that the lateral flow is very sensitive to changes in porosity (Figure 6.4). This parameter determines the volume available for subsurface storage. As this storage is predicted to empty within each time step, more available water results in more lateral flow. A value of 0.45 was assumed for this parameter in the scenarios with a LPD, opposed to 0.35 in the Bare scenario. The latter value was determined through fieldwork and the former value was derived from that. In reality, the porosity of the soil/LPD volume is uncertain. Design of the LPD has impact on this parameter, as the macropore fraction is dependent on the diameters and packing of the cuttings, the amount of cuttings used to form a bundle and their curvature. Usually, the larger the diameters of the cuttings, the more efficient the drainage of water occurs (Ghestem et al., 2011). The other parameter that follows directly from the design of the LPD is the diameter of the bundle. Its influence on the lateral flow seems minimal (Figure 6.4), whereas it was expected that a larger drain would lead to increased flow. An explanation for this

is that the smallest drain size determined in the sensitivity analysis is already large enough to accommodate the emptying of the subsurface storage. Figure 6.3 shows that the lateral flow can be up to 50% of the outflow for the LPD and LPD+ scenarios. Kim et al. (2005) found, for a slightly steeper slope, that in wet initial conditions, up to 56% of precipitation can end up as lateral flow, even without the presence of a LPD. In the growing season this fraction is smaller, which is in line with expectations because part of the water evaporates.

Both scenarios with a bundle show very similar trends in the percolation rate (Figure 6.2). In the model, this flux was determined before the lateral outflow was calculated. If the order of appearance of these fluxes had been interchanged, there would have been no water left in the storage for percolation. In reality, these processes happen simultaneously and water which is flowing through the drain, might still be available for percolation. However, as mentioned above, the percentage of water which ends up as lateral flow in the LPD and LPD+ scenarios is representative of a hillslope without a LPD. Therefore, the percolation component was presumably overestimated. For the Bare scenario, the percolation makes up almost the entire outflow volume (Figure 6.3). The lateral flow being zero in each time step for this scenario, which would not likely be the case in reality (Kim et al., 2005), also points to an overestimation of the percolation component. The difference in percolation between the scenarios is striking. In the interpretation of this partitioning difference, multiple processes play a role. On the one hand, the lateral flow component is likely smaller in the Bare scenario compared to the other two scenarios. This leaves more water for percolation. On the other hand, the increase in macroporosity in the latter scenarios can lead to an increase in percolation (Ghestem et al., 2011). This uncertainty is discussed further in Chapter 8.

As mentioned before, the subsurface storage empties within each time step if there is a bundle present, leading to a predicted storage of zero (Figure 6.2). In the Bare scenario, some water is stored. The storage follows daily fluctuations which correspond to soil evaporation. Some small peaks occur at the times of precipitation events. These are governed by the variable part of the incoming lateral flow, as none of the precipitation infiltrates in this scenario. The change in storage over time for the entire model run is very close to zero, meaning that the model predicts all water to leave the control volume over time. With 200 mm, the considered soil layer is very shallow. Therefore, it is likely that all water leaves the system through evaporation, percolation or laterally.

Part III

Synthesis, Conclusions and Recommendations

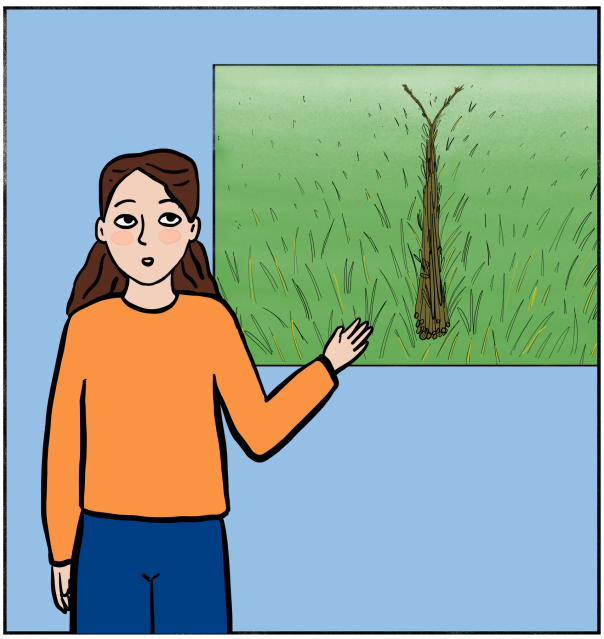

Chapter 8
Synthesis

In this chapter, the results of the fieldwork, lab experiment and model runs are compared and discussed together. First, the water partitioning results of both the lab precipitation simulations and the model runs are compared and the most important similarities and differences are discussed. Afterwards, the water level measurements at the study site are compared to the model output of the lateral flow component.

During the interpretation and comparison of the results from fieldwork, laboratory experiment and model runs, it is important to keep the following in mind. Firstly, the scaling from field to lab (Chapter 4) presumably led to overestimation of the percolation and lateral flow in the lab experiment. Secondly, the names for the scenarios (LPD, LPD+ and Bare) were used to describe both the gutter fillings in the lab experiment and the model run scenarios. However, LPD+ as a description of gutter filling means a bundle and alfalfa seeds and as a model scenario it means a LPD of which the willows have developed to the mature growth phase. During the lab experiment willows grew in both the LPD and LPD+ gutters. Although this could have caused differences between model and lab experiment in evapotranspiration in the LPD cases, this process is assumed to be negligible in the laboratory precipitation experiments because of the limited runtime of the experiments. Thirdly, the water partitioning after precipitation in the lab was calculated for each experiment, which never lasted over 45 min. The model runs were done for a month with hourly time steps and include rainfall events as well as dry periods. These events were of moderate intensity in May 2022, whereas the simulated events in the lab were very intense, which was necessary to be able to observe and measure flows. Differences in precipitation intensity logically lead to changes in the flow components, which is neglected in this comparison. Furthermore, in the lab experiment the input of precipitation was simulated by a nozzle at the upslope end of the gutter to mimic the incoming lateral flow which was also included in the model. Fourthly, the control volumes in the lab experiment were the entire gutters, which included bundles as well as surrounding soil on the bottom, top and at the sides. The discharge measurements in the field also included some soil at the sides of the LPD. In the numerical model, the control volume was defined as the LPD with the soil and vegetation on top. Lastly, the discharge measurements (Table 3.1) were used in the model for the baseflow from upslope. This should be considered during the comparison of the lateral outflow model output and the measured discharge in Catterline. All mentioned differences in conditions and methodologies naturally lead to differences in results, but in this synthesis the focus is on the observed trends which provide information on the hydrological behaviour of a slope with a LPD. Regardless of the discrepancies between the fieldwork, laboratory experiment and model runs, the same processes are at play at the study site and in the lab and those processes were captured by a numerical model. The resulting trends are therefore assumed comparable.

These trends are illustrated by the water partitioning results of the lab experiment (Figure 3.3) and the model runs (Figure 6.3). Three similar trends can be observed. Firstly, the runoff component was smaller in the scenarios with a LPD, indicating that more water infiltrated in these cases. As discussed in Section 7.2, this can be explained by the increased porosity compared to Bare soil conditions. Secondly, the lateral flow component was larger if a LPD was present. Observations during both fieldwork and precipitation experiments indicated that the flow from the LPD was a steady stream, while in the Bare gutters water dripped slowly from the subsurface. This increase in lateral flow is presumed to be the result of preferential flow along the willow cuttings. Thirdly, the model output (Figure 6.2), lab experiment observations and observations in the field all showed very instantaneous responses of the lateral flow to changes in the water volume entering the control volume. This is indicative of the rapid drainage of water by the LPD.

Four main differences between the found water partitionings were identified. Firstly, more water ended up as runoff in the laboratory experiment than predicted by the model, especially in the Bare scenario. This can partly be explained by the high intensity and amount of precipitation, leading to saturation excess overland flow. Accordingly, the first experiment included the smallest input volume and in this case, less water ended up as runoff than in the other experiments. Furthermore, the lab experiment results show that in the LPD+ gutters the least water ended up as runoff. Although it was not modelled, the resistance to overland flow due to vegetation can be observed in practice. Secondly, the modelled lateral flow component was zero for the Bare scenario, but it was measured in the lab. Even during daily irrigation and monitoring, flow from the subsurface was measured in all gutters. In reality, lateral is expected to play a role on a bare slope (Kim et al., 2005), but not as large as in the presence of a LPD. Thirdly, in the lab experiment more water ended up as percolation in the gutters with a bundle, but the opposite was predicted by the model. As discussed in Section 7.2, the presence of a LPD could lead to an increase in percolation through preferential flow. However, Ghestem et al. (2011) also state that the flow direction is very dependent on the root architecture. Just after installation of a LPD, most preferential flow paths are parallel to the ground surface and would therefore contribute to the lateral flow, not necessarily to percolation. During tree growth, the orientation of the macropores changes, e.g. if not all cuttings in the LPD stay alive or when roots develop vertically. Lastly, more water is stored in the subsurface in the Bare scenario, compared to the scenarios with a drain. The presence of a LPD leads to the rapid drainage of infiltrated water and incoming lateral flow.

The water level measurements (Figure 3.2) and model output of the lateral flow component in the LPD+ scenario in the growing season (Figure 6.2.2b) were also compared. It should be recalled that the water level measurements are quite uncertain (Section 4.1), but this comparison is once again focused on trends, not on amounts and values. In both the field measurements and the model output, daily fluctuations corresponding to evapotranspiration are visible. These were also noticeable during the discharge measurements (Table 3.1): during the day, the flow from the LPD decreased. Furthermore, peaks which correspond to precipitation events can be observed in the results of both methodologies. This illustrates the rapid drainage of incoming water. The most important differences include that flow predicted by the model is quite constant (with exceptions for the peaks) due to the baseflow that governs the lateral flow, whereas larger-than-daily frequencies can be observed in water level measurements at both top and toe. Differences between the water level measurements are quite large, but they all show fluctuations in the water level beyond those within a day. This is not the case for the model run: the fluctuations happen around a constant value of 0.25 mm/h with exception from some peaks during rainfall. This can be explained by the similar nature of the incoming lateral flow, which includes a baseflow which sustains this outflow of 0.25 mm/h. In reality, this baseflow is not constant, as was discussed in Section 7.1.

Chapter 9
Conclusions

The aim of this study is to characterise the hydrological behaviour of a LPD. The research question is: ***What is the hydrological behaviour of a Live Pole Drain?*** Three methodologies were implemented to answer this question. Fieldwork was executed at an Open Air Lab in Scotland, where a LPD is located in a hillslope. There, the porosity of the soil, the dimensions of the LPD and flow from the LPD were measured. Soil and willow cuttings were gathered at the study site to build a lab experiment. This experiment consisted of nine gutters with three different fillings: a LPD, a LPD plus alfalfa seeds and bare soil. The experiment setup was used to run five precipitation simulations with varying intensities and durations. From these experiments, the partitioning of input water into runoff, lateral flow, percolation and storage was determined. Findings from the field and the lab were used to conceptualise the hillslope hydrology to create a numerical model which predicts partitioning of precipitation into runoff, lateral flow, interception evaporation, evapotranspiration, percolation and storage.

This model was used to answer the first subquestion: *Can the hydrological behaviour of a LPD be represented by a numerical model?* A first version of a conceptual model was created. It does not accurately predict the sizes of fluxes, but is helpful in gaining insight into the aspects of LPD design which are of importance for the flow through the LPD. These aspects are the macropore fraction within and the diameter of the drain. The macropore fraction is determined by the diameters and packing of the cuttings, the amount of cuttings used to form a bundle and their curvature. A larger macropore fraction results in more lateral flow. The diameter of the drain also influences the flow through the LPD, although a minimum diameter which depends on the intensity of the precipitation, seems to be sufficient for the rapid drainage of the incoming water. The predicted partitioning into lateral flow and percolation was not completely reliable. However, the model simulations gave a first insight into the differences between a slope with a LPD and a bare slope.

The comparison of the predicted trends to the findings from the lab experiment and measurements at the study site, was used to answer the second subquestion: *What is the hydrological response to a rain event of a hillslope with a LPD compared to that of a bare slope?* In the Bare setups and scenarios less input water ended up as lateral flow, compared to those with a LPD. More instantaneous reactions of lateral flow to precipitation events were observed in the presence of a LPD. Correspondingly, less water infiltrated and therefore more water ended up as runoff in the Bare scenarios. The rapid drainage by the LPD also led to a smaller volume of water stored in the soil compared to a Bare slope.

What is the hydrological behaviour of a Live Pole Drain?

The answers to the subquestions and the results from all three methodologies confirm the expected effect of drainage through preferential flow by the LPD. It accommodates rapid infiltration of precipitation and consequent drainage, also of water which enters the drain at the upslope end. Furthermore, the presence of a LPD results in a decrease of runoff. After vegetation development, the runoff decreases even further. Vegetation also leads to an increase of evapotranspiration, resulting in a decrease of the size other fluxes leaving the slope. A definitive conclusion on the effect of a LPD on percolation cannot be drawn, as the findings from the lab experiment and the model runs indicated opposite reactions.

Chapter 10
Recommendations

This study has provided a first insight into the effects of Live Pole Drains on hillslope hydrology. Further research to enhance the understanding of these effects is needed to make this measure for shallow landslides safely applicable.

First of all, a more realistic quantification of the hydrological processes must be obtained for the assessment of slope stability. It is still unclear which part of the infiltrated and incoming lateral water ends up as lateral flow and which part as percolation. As percolation contributes to the forming of landslides, it is important to acquire a better understanding of the effects of a LPD on the sizes of these fluxes. The improved model can function as a tool for the quantification of the hydrological processes. The accuracy of the model's predictions can be enhanced after evaluation of the used equations and algorithm. The model components are interchangeable and can be replaced with possibly more suitable numerical representations of the processes. Improvement of the model can also be obtained through calibration with data. Useful data include discharge and water level measurements, runoff measurements and values of variables such as soil moisture and matric suction, which can also be used to quantify soil stability (González-Ollauri and Mickovski, 2014). Protocols must be developed for the gathering of these data to make this process reproducible. Application of such protocols on a plot with bare soil is advisable, as it would make comparison of a bare slope and a slope with LPD on a real-life spatial scale possible.

Secondly, these protocols can also be applied to gain more insight into the effects of the LPD design on the hydrological processes. By performing tests on slopes with LPDs with different cutting sizes and assemblies, the effects of the macropore fraction can be analysed. The results from this study indicate that the LPD at the study site is large enough to rapidly drain precipitation of low to moderate intensities. It is recommended to test LPDs of varying diameters with precipitation intensities which have triggered landslides in the past. The improved model can also be used to find the minimal LPD diameter which is needed to accommodate high enough flows for landslide prevention.

Lastly, it is advised to study the transient behaviour of a LPD. Several changes are expected to occur regarding the LPD's structure during its lifetime: some cuttings will probably not survive and leave macropores after decomposition and vegetation will develop both above and below ground. The analysis of the deconstruction of the lab experiment can provide a first insight into the survival rate of the cuttings and the cross section of the bundle after the initial months. Some effects of trunks and the canopy were assessed in this study, but the effects of roots were neglected. As roots affect the direction of preferential flow (Ghestem et al., 2011) and could therefore contribute to increases in lateral flow and percolation, analysis of their development would contribute to a better understanding of the long-term effects of a LPD. This analysis could be performed by doing a literature review into the development of forest stands on a hillslope. The monitoring of plant development will also lead to a better understanding of the maintenance needed, making the application of LPDs more realistic.

Bibliography

Ahman, I. (1997). Growth, herbivory and disease in relation to gender in Salix viminalis L. *Oecologia*, (111):61–68.

Allen, R., Pereira, L., Raes, D., Fao, M. S., Rome, u., and 1998, u. (1998). Crop evapotranspiration-Guidelines for computing crop water requirements-FAO Irrigation and drainage paper 56. *scscourt.org*.

Bergström, S. and Lindström, G. (2015). Interpretation of runoff processes in hydrological modelling—experience from the HBV approach. *Hydrological Processes*, 29(16):3535–3545.

Beven, K. and Germann, P. (1982). Macropores and water flow in soils. *Water Resources Research*, 18(5):1311–1325.

Bogaard, T. A. and Greco, R. (2016). Landslide hydrology: from hydrology to pore pressure. *Wiley Interdisciplinary Reviews: Water*, 3(3):439–459.

Chapuis, R. P. (2012). Predicting the saturated hydraulic conductivity of soils: a review. *Bulletin of Engineering Geology and the Environment 2012 71:3*, 71(3):401–434.

Cohen-Shacham, E., Walters, G., Janzen, C., and Maginnis, S. (2016). Nature-based solutions to address global societal challenges. *IUCN: Gland, Switzerland*, 97:2016–2036.

Crick, M. and Hill, M. (1987). The role of sensitivity analysis in assessing uncertainty. Technical report.

Devi, K., Ganasri, B., and Dwarakish, G. (2015). A Review on Hydrological Models. *Aquatic Procedia*, 4:1001–1007.

Epps, R. and Head, K. H. (2006). *Manual of soil laboratory testing Volume 2: Permeability, Shear Strength and Compressibility tests Third Edition*, volume 2.

Fitts, C. R. (2002). *Groundwater Science*. Academic Press.

Ghestem, M., Sidle, R. C., and Stokes, A. (2011). The Influence of Plant Root Systems on Subsurface Flow: Implications for Slope Stability. *BioScience*, 61(11):869–879.

Gill, L., Knappe, J., and Morrissey, P. (2019). A comparison of falling head vs constant head percolation tests using field results and numerical modeling to determine the hydraulic conductivity of soils. *Geophysical Research Abstracts*, 21:1–1.

González-Ollauri, A. and Mickovski, S. B. (2014). Integrated Model for the Hydro-Mechanical Effects of Vegetation Against Shallow Landslides. *EQA - International Journal of Environmental Quality*, 13:37–59.

Gonzalez-Ollauri, A. and Mickovski, S. B. (2017a). Hydrological effect of vegetation against rainfall-induced landslides. *Journal of Hydrology*, 549:374–387.

Gonzalez-Ollauri, A. and Mickovski, S. B. (2017b). Plant-Best: a novel plant selection tool for slope protection. *Ecological Engineering*, 106(A):154–173.

Gonzalez-Ollauri, A. and Mickovski, S. B. (2017c). Shallow landslides as drivers for slope ecosystem evolution and biophysical diversity. *Landslides*, 14(5):1699–1714.

Hamby, D. (1994). A review of techniques for parameter sensitivity analysis of environmental models. *Environmental monitoring and assessment*, 32(2):135–154.

Hao, X., Ball, B., Culley, J., Carter, M., and Parkin, G. (2008). Soil density and porosity. *Soil sampling and methods of analysis*, 2:179–196.

Hawkins, R. H. and Cundy, T. W. (1987). Steady-State Analysis of Infiltration and Overland Flow for Spatially-Varied Hillslopes. *JAWRA Journal of the American Water Resources Association*, 23(2):251–256.

Head, K. H. (1994). *Manual of soil laboratory testing*, volume 1. Pentech Press.

Head, K. H. and Epps, R. J. (2014). *Manual of soil laboratory testing. Volume 3, Effective stress tests*, volume 3.

Helvey, J. D. and Patric, J. H. (1965). Canopy and litter interception of rainfall by hardwoods of eastern United States. *Water Resources Research*, 1(2):193–206.

Herwitz, S. R. (1985). Interception storage capacities of tropical rainforest canopy trees. *Journal of Hydrology*, 77(1-4):237–252.

Jacbos, Maxwell, Ralph, and e.a. (1955). Growth habits of the eucalypts. *Growth habits of the eucalypts*.

Kadlec, R. H. (1990). Overland Flow in Wetlands: Vegetation Resistance. *Journal of Hydraulic Engineering*, 116(5):691–706.

Kim, H. J., Sidle, R. C., and Moore, R. D. (2005). Shallow lateral flow from a forested hillslope: Influence of antecedent wetness. *CATENA*, 60(3):293–306.

Kuang, X., Jiao, J. J., Shan, J., and Yang, Z. (2021). A modification to the van Genuchten model for improved prediction of relative hydraulic conductivity of unsaturated soils. *European Journal of Soil Science*, 72(3):1354–1372.

Langhans, C., Govers, G., Diels, J., Leys, A., Clymans, W., Putte, A. V. d., and Valckx, J. (2011). Experimental rainfall–runoff data: Reconsidering the concept of infiltration capacity. *Journal of Hydrology*, 399(3-4):255–262.

Lipiec, J., Kuś, J., Słowińska-Jurkiewicz, A., and Nosalewicz, A. (2006). Soil porosity and water infiltration as influenced by tillage methods. *Soil and Tillage Research*, 89(2):210–220.

Lu, N. and Godt, J. W. (2013). *Hillslope Hydrology and Stability*. Cambridge University Press, Cambridge.

Lu, N. and Likos, W. J. (2004). *Unsaturated Soil Mechanics*. John Wiley & Sons, Inc.

Maass, J., Vose, J. M., Swank, W. T., and Martínez-Yrízar, A. (1995). Seasonal changes of leaf area index (LAI) in a tropical deciduous forest in west Mexico. *Forest Ecology and Management*, 74(1-3):171–180.

Marc, V. and Robinson, M. (2007). The long-term water balance (1972–2004) of upland forestry and grassland at Plynlimon, mid-Wales. *Hydrology and Earth System Sciences*, 11(1):44–60.

Marsh, T. J. and Anderson, J. L. (2002). Assessing the water resources of Scotland—perspectives, progress and problems. *Science of The Total Environment*, 294(1-3):13–27.

Meng, W., Bogaard, T., and van Beek, R. (2014). How the stabilizing effect of vegetation on a slope changes over time: A review. *Landslide Science for a Safer Geoenvironment*, 1:363–372.

Mishra, S. K., Tyagi, J. V., and Singh, V. P. (2003). Comparison of infiltration models. *Hydrological Processes*, 17(13):2629–2652.

Moayedi, H., Huat, B. B., Ali, T. A. M., Asadi, A., Moayedi, F., and Mokhberi, M. (2011). Preventing landslides in times of rainfall: Case study and FEM analyses. *Disaster Prevention and Management: An International Journal*, 20(2):115–124.

Norwegian Geotechnical Institute (2016). LaRiMit.

Penman, H. L., Ey, H., Lovell, J. S., Banwell, A. C. B., Mccready, D. F., Pawsey, L., Payne-S Cott, J. L., ; N Yquist, R., Pawsey, H., Payne-Scott, J. L., and Mccready, R. (1948). Natural evaporation from open water, bare soil and grass. *Proceedings of the Royal Society of London. Series A. Mathematical and Physical Sciences*, 193(1032):120–145.

Polster, D. F. and Bio, R. P. (1997). Proceedings of the 21 st Annual British Columbia Mine Reclamation Symposium in Cranbrook, BC, 1997. The Technical and Research Committee on Reclamation.

Priestley, C. and Taylor, R. (1972). On the assessment of surface heat flux and evaporation using large-scale parameters. *Monthly Weather Review*, 100(2):81–92.

Rodríguez-Blanco, M. L., Taboada-Castro, M. M., and Taboada-Castro, M. T. (2012). Rainfall–runoff response and event-based runoff coefficients in a humid area (northwest Spain). *https://doi.org/10.1080/02626667.2012.666351*, 57(3):445–459.

Savabi, M. R. and Williams, J. R. (1995). Chapter 5. Water Balance and Percolation. In: USDA-Water Erosion Prediction Project, NSERL Report #10. Technical report, West Lafayette, Indiana.

Sidle, R. C. and Bogaard, T. A. (2016). Dynamic earth system and ecological controls of rainfall-initiated landslides. *Earth-Science Reviews*, 159:275–291.

Silvia, F. G., Mauro, P., Colin, R., and Stark, P. (2008). The rainfall intensity-duration control of shallow landslides and debris flows: an update. 5:3–17.

Sitterson, J., Knightes, C., Parmar, R., Wolfe, K., Avant, B., Overview, A., and Muche, M. (2018). An overview of rainfall-runoff model types. page 41.

Tahvanainen, L. and Rytkönen, V. M. (1999). Biomass production of Salix viminalis in southern Finland and the effect of soil properties and climate conditions on its production and survival. *Biomass and Bioenergy*, 16(2):103–117.

Tan, T., Phoon, K. K., Hight, D., and Leroueil, S. (2007). *Characterisation and Engineering Properties of Natural Soils*, volume 3. Taylor & Francis Group, Boca Raton.

Tóth, B., Weynants, M., Nemes, A., Makó, A., Bilas, G., and Tóth, G. (2015). New generation of hydraulic pedotransfer functions for Europe. *European Journal of Soil Science*, 66(1):226–238.

Tromp-Van Meerveld, H. J. and McDonnell, J. J. (2006). Threshold relations in subsurface stormflow: 2. The fill and spill hypothesis. *Water Resources Research*, 42(2):2411.

Van Dijk, A. I. and Bruijnzeel, L. A. (2001). Modelling rainfall interception by vegetation of variable density using an adapted analytical model. Part 1. Model description. *Journal of Hydrology*, 247(3-4):230–238.

Van Genuchten, M. (1980). A Closed-form Equation for Predicting the Hydraulic Conductivity of Unsaturated Soils. *Soil Science Society of America*.

Varnes, D. J. (1978). Slope movement types and processes. *Special report*, 176:11–33.

Veihmeyer, F. and Hendrickson, A. (1931). The moisture equivalent as a measure of the field capacity of soils. *Soil Science*, 32(3):181–194.

Voor de Poorte (2022). Meteorological time series of Catterline, Scotland, UK.

Wallach, R. and Zaslavsky, D. (1991). Lateral Flow in a Layered Profile of an Infinite Uniform Slope. *Water Resources Research*, 27(8):1809–1818.

Yan, L., Xu, W., Wang, H., Wang, R., Meng, Q., Yu, J., and Xie, W. C. (2019). Drainage controls on the Donglingxing landslide (China) induced by rainfall and fluctuation in reservoir water levels. *Landslides*, 16(8):1583–1593.

Part IV

Appendices

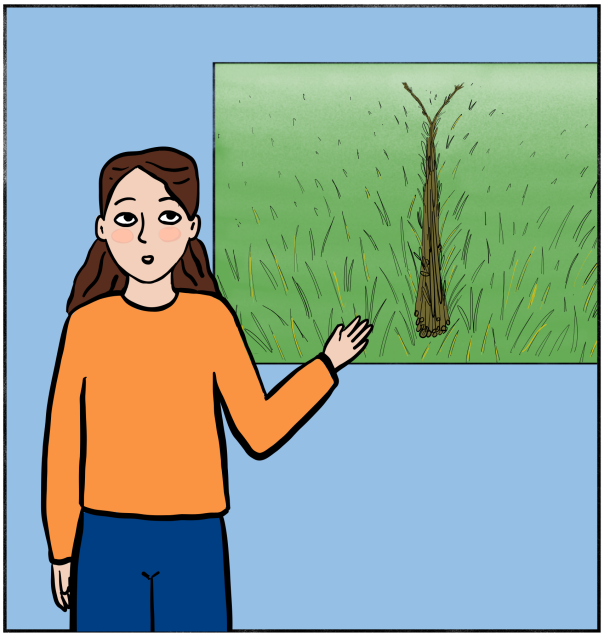

Appendix A
Fieldwork

A.1 Methodology Additional Fieldwork

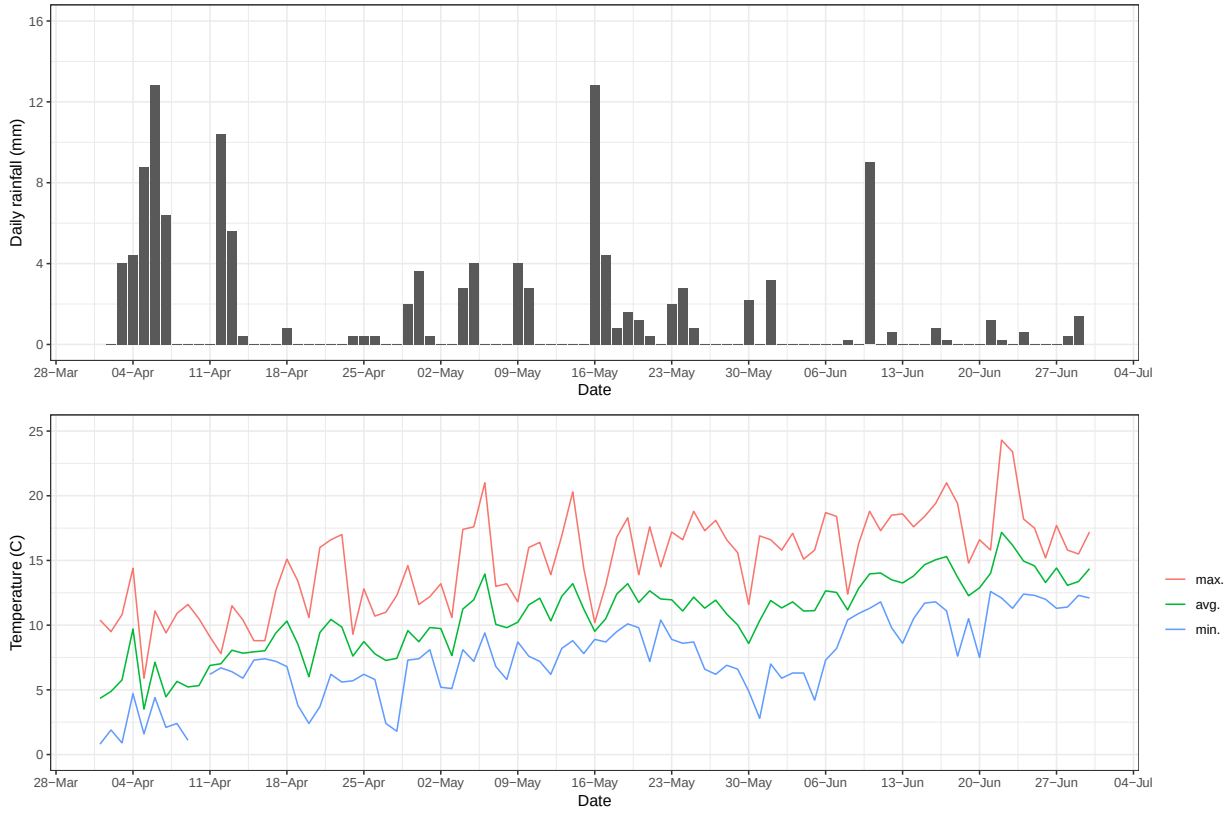

Figure A.1: *Daily rainfall and temperature at the study site in April, May and June 2022*

Table A.1: *Measurements and tests executed in the field or on samples collected in the field. The locations T, M and B are depicted in Figure 2.1c.*

Test or Measurement	**Method**	**Locations or Samples**
Bulk density	Standard	On the 9 samples TI-III, MI-III, BI-III
Moisture content	Standard	On the 9 samples TI-III, MI-III, BI-III
Moisture content	In the field with a Delta-T HH150 sensor	At three locations T, M, B
Vane shear test	In the field with a vane shear test apparatus	At three locations T, M, B
Direct shear test	On dry samples with a Matest shear box	On samples TII, MII and BII
Porosity	Standard	On the 9 samples TI-III, MI-III, BI-III
Organic Matter content	Standard	On the 9 samples TI-III, MI-III, BI-III
Particle Size Distribution	Dry sieving and hydrometer test	On samples TII, MII and BII
Falling head test	In a borehole Ø60 mm, depth 175 mm with 1.9 L	At one location in between T and M
Dimensions LPD	Measuring tape and ruler	Diameter of LPD and cuttings and number of cuttings at the top of the right branch
Discharge from LPD	Measure volume of water (L) discharged from LPD over time	At the toe of the LPD
Water level in LPD	With 3 TD- and 1 Baro-Diver (model DI801, Van Essen Instruments)	In boreholes at T, M and B
Tree height	Laser rangefinder, ENTS method	On the study site
Diameter at breast height	Measuring tape, from circumference at breast height (1.4 m)	
No. primary branches		
No. secondary branches		
Stem lean from vertical	Laser rangefinder	
Branch insertion angles	Laser rangefinder and level app on smartphone	

A.2 Results Additional Fieldwork

Soil characteristics. A summary of the results obtained from the lab and field test on the samples taken on the three locations T, M, B and horizons (I), (II), (III) is given in Table A.2. The results from the direct shear test are presented in Figure A.2.

Table A.2: *Overview of the results of lab and field soil tests on the samples taken from locations Top (T), Middle (M) and Bottom (B) and the horizons I-III. ρ: bulk density (Mg/m^3); MC_{lab}: moisture content measured in the lab (%); MC_{field}: moisture content measured in the field (%); ρ_{dry}: dry bulk density (Mg/m^3); n_{por}: porosity (-); σ_{field}: shear strength measured with the vane test (N/mm^2); OM: organic matter content (%).*

Sample	ρ	MC_{lab}	MC_{field}	ρ_{dry}	n_{por}	σ_{field}	OM
TI	1.43	61		0.89	0.38		10.68
TII	1.75	24	60.5	1.41	0.19	50.0	4.23
TIII	1.66	50		1.13	0.32		6.16
MI	1.33	70		0.78	0.41		9.71
MII	1.46	54	67.8	0.95	0.35	50.5	6.83
MIII	1.55	67		0.93	0.40		6.97
BI	1.01	51		0.67	0.34		7.58
BII	1.33	91	69.4	0.70	0.48	50.5	10.32
BIII	1.79	44		1.24	0.31		4.43

The particle size distribution of the samples TIII, MIII and BIII is displayed in Figure A.3. The samples were too small for a hydrometer test. Therefore, the particle size distribution of the lab experiment soil is used to calculate hydraulic conductivity from pedotransfer functions.

Tree architecture. The willows ranged from 2 to 7 metres in height, with diameters between 0.6 and 25 cm. A complete overview of the measurements is shown in Table A.3.

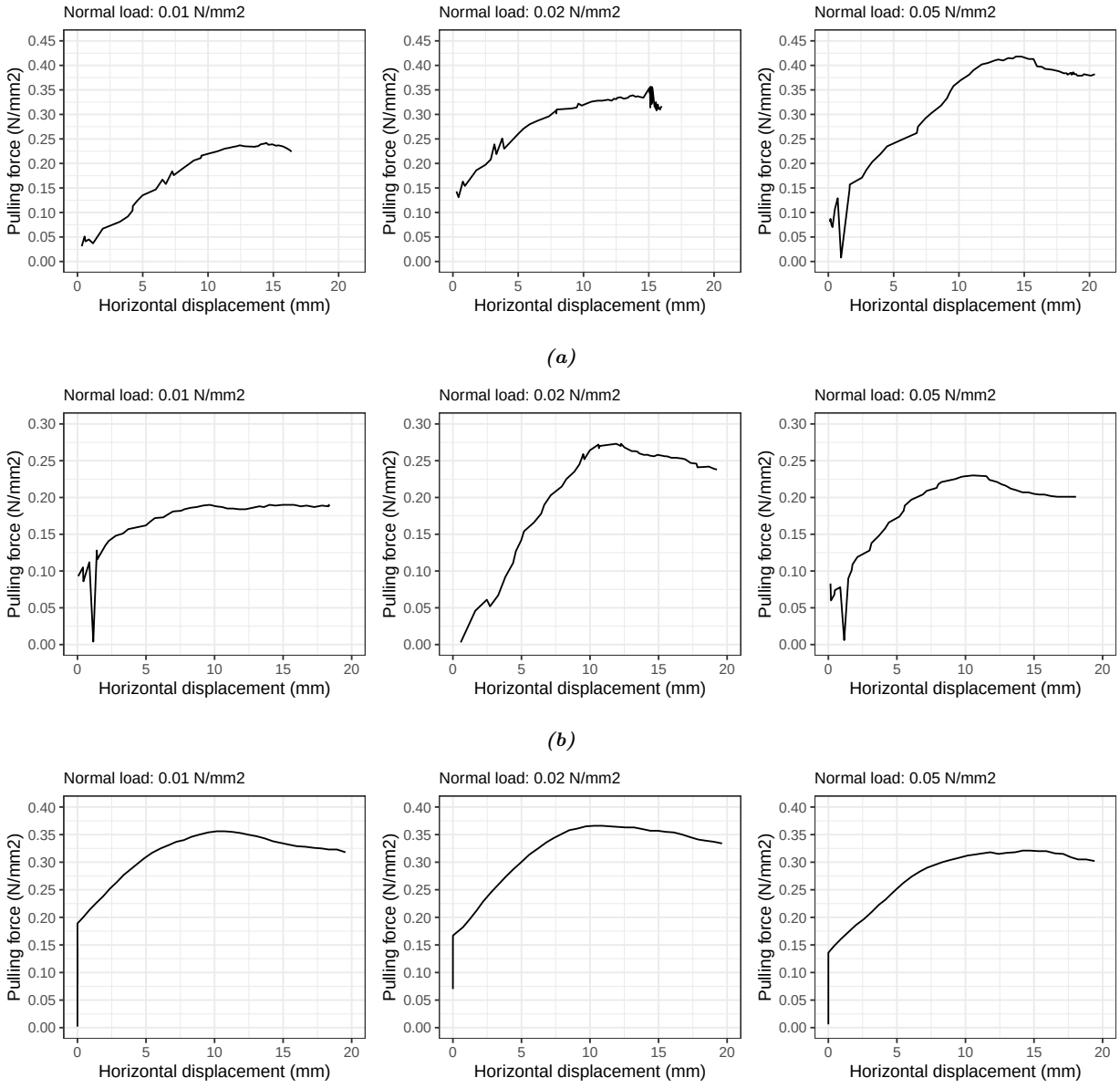

Figure A.2: *Results of the direct shear tests on samples taken from the top* **(a)**, *middle* **(b)** *and bottom* **(c)** *along the length of the LPD at the study site.*

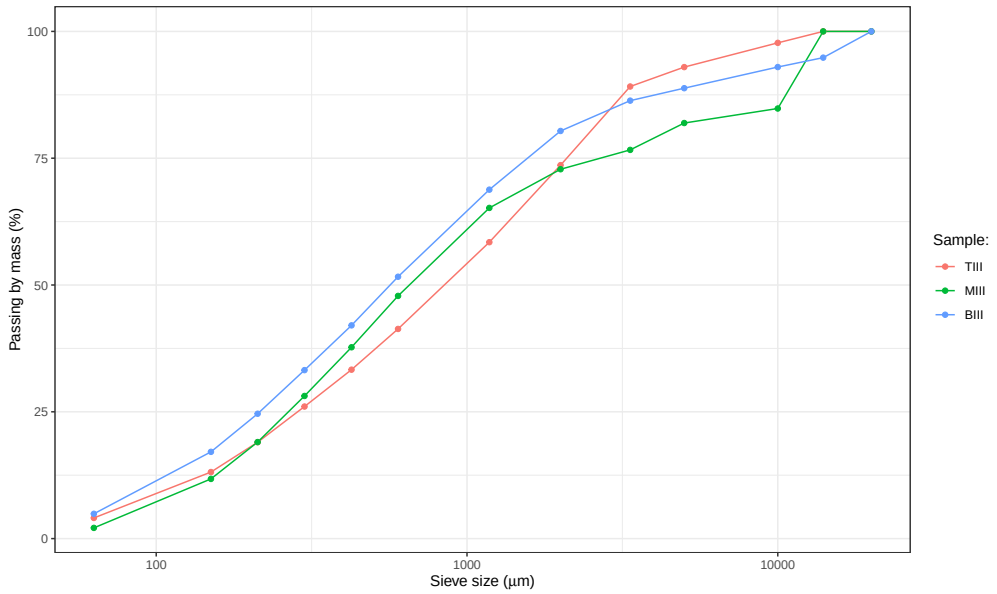

Figure A.3: *Particle size distribution of samples taken from the top (T), middle (M) and bottom (B) along the length of the LPD at the study site.*

Table A.3: *Traits of 10 Salix Viminalis individuals at the study site. DBH: diameter at breast height* (m)*; Ht: tree height* (m)*; #P: number of primary branches; #S: number of secondary branches; SL: stem lean from vertical (°); minBr: minimum branch insertion angle (°); maxBr: maximum branch insertion angle (°); avBr: average branch insertion angle (°); LAI: leaf area index; #stems: number of stems/trunks.*

Tree	**DBH**	**Ht**	**#P**	**#S**	**SL**	**minBr**	**maxBr**	**avBr**	**#stems**
W1	0.0874	5.38	43	205	20.2	-22.55	56.75	30.43	2
W2	0.0509	2.45	38	92	45.3	-38.6	79.45	30.62	1
W3	0.0955	2.94	44	113	84.9	0.09	74.47	34.95	2
W4	0.2546	7.64	47	220	37.05	-26.5	92.15	51.55	1
W5	0.0883	2.69	89	200	48.1	-71.35	85.75	20.15	4
W6	0.105	3.23	52	121	43.75	-17.5	95.35	43.14	2
W7	0.0064	2.23	15	21	24.95	8.05	69.55	30.65	1
W8	0.106	4.61	94	135	40.45	3.55	84.7	45.73	2
W9	0.0518	3.54	38	54	41	22.75	86.4	54.12	2
W10	0.0473	2.07	33	55	21.05	-18.4	72.8	29.12	2
Min	0.0064	2.07	15	21	20.2	-71.35	56.75	20.15	1
Max	0.2546	7.64	94	220	84.9	22.75	95.35	54.12	4
Average	0.0893	3.68	49.3	122	40.68	-16.05	79.74	37.05	1.9

A.3 Results Falling Head and Discharge Tests

The results of the eight falling head experiments are given in Table A.4. After the first three repetitions, the bottom of the borehole was affected due to the water load. During the last (eighth) test, the location of pouring was changed. The average percolation rate of experiments 1, 2, 3 and 8 is 1.14×10^{-3} m/s. The results of all discharge tests are presented in Table A.5.

Table A.4: *Results of the eight falling head tests executed at the study site.*

Experiment	**Percolation rate** (m/s)
1	1.26×10^{-3}
2	1.09×10^{-3}
3	1.10×10^{-3}
4	8.40×10^{-4}
5	8.12×10^{-4}
6	5.78×10^{-4}
7	6.76×10^{-4}
8	1.09×10^{-3}

Table A.5: *Results of the discharge tests executed at the study site.*

Date	**Experiment**	**Discharge** (L/h)
20/04/2022	1	9.03
	2	8.78
	3	7.91
	4	7.73
	5	7.72
21/04/2022	1	4.70
	2	4.73
	3	4.65
	4	4.43
	5	4.04
	6	3.84
	7	3.69
06/06/2022	1	0.96
	2	0.75

Appendix B
Lab Experiment Protocol

This appendix is a shorter version of the protocol that was developed for the lab experiment. It includes the building of the setup, the soil tests that were performed, the monitoring of the vegetation development and the execution of the precipitation experiments.

B.1 Equipment and Materials

- Soil collection: shovel, plastic bag, oven, oven trays, hammer, buckets, sieve (2 mm).
- Bundles: loppers, plastic bags, bucket, refrigerator, gardening twine, vernier callipers, painter's tape, permanent marker.
- Set-up: half round PVC gutters to make 9 parts with length 500 mm (diameter: 115 mm), permanent marker, duct tape, painter's tape, steel ruler, drill, 4 mm and 5 mm bits, shelving rack (height: 132 mm, depth: 34.5 cm, width: 140 cm, vertical spacing of shelves: 18.8 cm), nylon mesh, scissors, galvanised wire (diameter 1.1 mm), 10 S-hooks, rope, table (width at least equal to width shelving rack, depth 67.5 cm), alfalfa seeds, wooden beam (length: 140 cm, width: 4.5 cm, height: 9.4 cm).
- Growing: LED grow lamp (spectrum 660 nm to 665 nm, 3000 K, 34 500 lm, 200 W), plug-in timer.
- Monitoring: 36 containers (650 mL) of which 9 have markings every 100 mL, 9 soil moisture sensors (6 of SEN0193 and 3 of SEN0308), 9 temperature probes (107 Campbell Scientific Temperature Sensor), data logger, 9 tensiometers (T5), pH sensor, humidity sensor, moisture content sensor (Delta-T HH150), nail clippers, tooth picks, pencil, painter's tape, ruler (length: 30 cm).
- Irrigation and precipitation: 3 equal-sized 25 L tanks with outlet diameter: 4.5 cm, irrigation system, hose, lighter.

B.2 Building of the Setup

B.2.1 Soil

Collect approximately 50 kg of soil at the study site. Take a sample for bulk density analysis before air drying and store in the fridge. Air dry the soil at the lab for 4 to 6 days (Figure B.1a). Oven dry the soil at 100 °C for 12 h to 24 h if not completely dry after air drying. Break the soil with hammers (Figure B.1b). Take a soil sample for the particle size distribution test. Sieve 18 kg of soil under 2 mm. Run the following tests: soil bulk density, soil moisture content, particle size distribution, plasticity (liquid limit, plastic limit, plasticity index), soil organic matter, soil shear strength (Table B.1). Use protocols by Head (1994), Epps and Head (2006) and Head and Epps (2014).

Table B.1: *Measurements and tests executed during the preparation and building phase of the lab experiment.*

Measurement	Remarks
Bulk density (Mg/m^3)	Before drying and sieving.
Moisture content (%)	Before drying and sieving.
Particle Size Distribution	After drying, before sieving.
Liquid limit (%)	After drying and sieving.
Plastic limit (%)	After drying and sieving.
Organic matter (%)	After bulk density and soil moisture.
Shear strength (N/mm^2)	For unsieved, dry soil and unsieved soil at three different moisture contents.
Volume of the irrigation drops (mL)	Recorded for each nozzle and per gutter.
Diameters of the cuttings in the bundles (mm)	Recorded per bundle.
Diameters of each bundle (mm)	Recorded for each gutter.
Diameters of the stakes (mm)	Recorded for each gutter.
Mass of soil added in each gutter (kg)	-

B.2.2 Willow cuttings

Collection and storage

Collect approximately 170 cuttings with diameters of 2 mm to 14 mm at the study site. The bottom of a clipping is the part that was connected to the tree and the top is the other end. Preserve half of the cuttings in water: 50% to 80% of the willow should be covered by water, refresh the water daily. Preserve half of the cuttings in the fridge at 5 °C to 10 °C until the assembly of the bundles.

Assembly of the bundles

With painter's tape, make a length marking on the floor of 140 cm. Mark every 10 cm: start with 0 and end with 14 (Figure B.2a). Cut each willow cutting to a length of 450mm: check the bottom if it looks healthy. If so, cut off the top end. Otherwise, clip off the bottom end until it looks healthy and then clip the top end to obtain the desired length. Measure the diameter of each cutting with vernier callipers at the middle and sort according to the tape markings on the floor (Figure B.2a). Sort the cuttings into 6 bundles of 15 twigs with a similar size distribution (Figure B.2b). All bottom ends should be at one side of the bundle. After assembling the 6 bundles, take note of the diameter of all twigs of each bundle. Tie the bundles with gardening twine at 10 cm from each end, as tightly as possible (Figure B.2b). Label the bundles from 1 to 6. Use a string and measuring tape to measure the circumference of each bundle at the middle. Make sure the circumferences are approximately equal. Using fresh cuttings, cut 12 live stakes with a diameter of 6 mm to 7 mm. The bottom end should be cut in a point. Clip the top end so the total length is 7 cm.

B.2.3 Gutters

Preparation

Cut the gutters into 9 parts with length 500 mm and label from 1 to 9. Drill a 5 mm hole in each gutter to be able to hang them with a S-hook (Figure B.3). The hole should be drilled at the centre of the gutter (width-wise) at 15 mm from the edge. Also drill 4 mm holes according to the pattern in (Figure B.3b).

Close the upslope end of each gutter with duct tape and the other end with nylon mesh supported by galvanised wire (Figure B.4a). Line the bottom of each gutter with a piece of nylon mesh (60 cm × 20 cm) to avoid passing of fine particles through the holes (Figure B.4a). For each gutter, make 2 barriers to redirect percolation to the containers by cutting 2 pieces of duct tape (20 cm), folding in half but leaving a strip of 2 cm

(a) *(b)*

Figure B.1: *Preparation of the soil.* ***(a)*** *Air drying.* ***(b)*** *Hammering and sieving of the soil.*

(a) *(b)*

Figure B.2: *Preparation of the bundles.* ***(a)*** *Sorting of the willow cuttings according to diameter.* ***(b)*** *The assembled bundles, tied tightly.*

and sticking in place. One piece should be stuck at the downslope end of the gutter, below the last hole in the centre and the other below the hole just downslope of the middle of the gutter, length-wise (Figure B.4b). Now, the gutters are ready for filling.

Filling with soil and bundles

Bare, gutters 7-9. Using beakers, fill each gutter with approximately 2 kg of soil. Measure and record the mass of the used soil for each gutter. Compact the soil evenly with a putty knife or trowel. Install the flexible funnel on top of the soil to redirect runoff (Figure B.5). Water gently with 800 mL (Figure B.6e). Be careful not to displace the soil.

LPD, gutters 1-3; LPD+, gutters 4-6. Fill each gutter with approximately 1 kg of soil (Figure B.6a), making an indent in the centre (length-wise) and compacting with a putty knife or trowel (Figure B.6b). The soil layer should be approximately 2 cm thick throughout the gutter. Place a bundle in the centre of the indent (Figure B.6c). The bottom ends of the cuttings coincide with the upslope end of the gutter. Fill the indents along the sides of the bundle with soil, compacting evenly. Cover the LPD with soil until a layer of 0.5 cm is formed on top (Figure B.6d). Compact evenly. Install the flexible funnel on top of the soil to redirect runoff. Water gently with 800 mL (Figure B.6e). Be careful not to displace the soil. *Only for gutters 4-6: evenly distribute* 6 g *of alfalfa seeds over the soil (Figure B.6f).* Vertically place 2 live stakes in gutter,

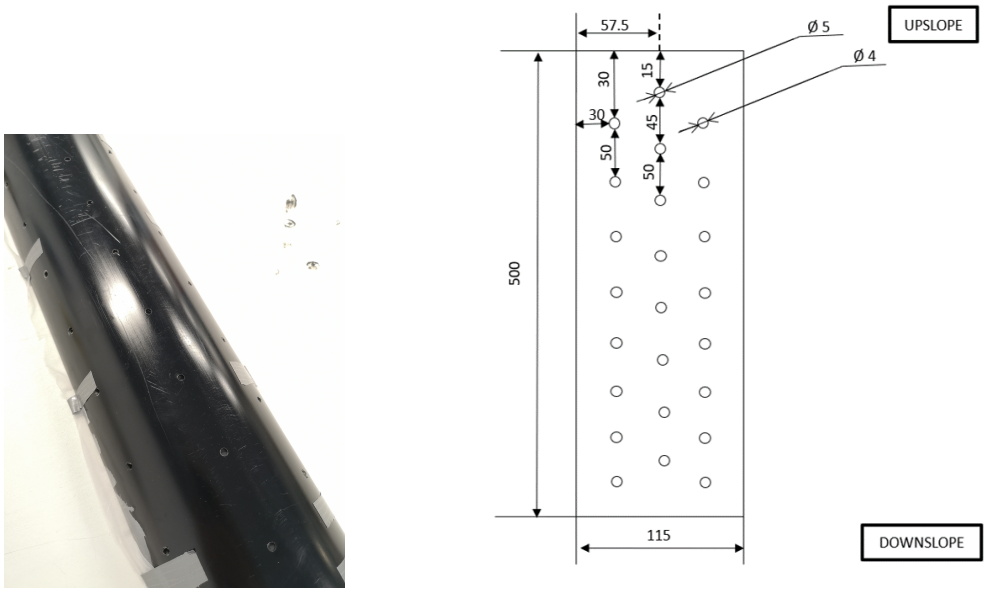

(a) *(b)*

Figure B.3: *Pattern of holes in the gutters.* ***(a)*** *Photograph of the outside of the gutter.* ***(b)*** *Schematic drawing of the pattern. Units are* mm. *Measurements are given following the curve of the gutter. Centre distances are given. The sketch does not respect real proportions.*

17 cm from the upslope and 11 cm from the downslope end, pushing down to the bottom of the gutter.

B.2.4 Experiment setup

The setup is shown in Figure 2.4. It should be built to allow for easy refilling of the water tanks, monitoring (photographing of vegetation growth, measuring soil characteristics and water volume from the containers) and simulation of rainfall events (photographing/filming of simulation and data collection). Place the shelving rack and a table to create a slope gradient (30°) for the 9 setups. Hang 9 S-hooks from the shelving rack to and attach the gutters. Use the wooden beam to lift the downslope end of the gutters, so percolation and lateral flow can be collected in the plastic containers. Install a lower shelf in front of the table for placement of the runoff containers. Place the containers (Figure 2.4). Place the irrigation systems, elevated with 2 support stakes per setup. The first nozzle is placed 20 cm downslope of the gutter top and the second one 40 cm downslope of the gutter top. Insert a soil moisture sensor, tensiometer and temperature probe in the middle of each gutter.

B.2.5 Irrigation system

Daily watering

The system should be built with three tanks supplying water to the gutters with a dripping system. Each tank supplies water to 3 gutters, and each gutter has 2 red nozzles (Figure B.7). Cut tube into 9 pieces of 15 cm, 9 pieces of 20 cm and 9 pieces of 4 cm. For each gutter, connect: 1 end closure + 4 cm + 1 barbed tee + 1 nozzle + 15 cm tube + 1 barbed tee + 1 nozzle + 20 cm tube. Now cut tube into 3 pieces of 12 cm, 3 pieces of 7 cm, 3 pieces of 5 cm, 3 pieces of 30 cm and 6 pieces of 4 cm. For each tank supplying water to 3 gutters, connect: drip system for 1 gutter + flat tee pipe connector + 12 cm tube + flat tee pipe connector + drip system for 1 gutter + 5 cm tube + flat tee pipe connector and 30 cm tube to connect with tank + 7 cm tube + flat tee pipe connector + drip system for 1 gutter. Connect a 4 cm tube and an end closure at each end side. Connect the final 3 drip systems to the tanks. The final distance between the top of the tank and the upslope end of the gutters is approximately 62 cm.

(a)

(b)

Figure B.4: *Preparation of the gutters.* ***(a)*** *Lining of the gutter with mesh.* ***(b)*** *Redirection of percolation with tape.*

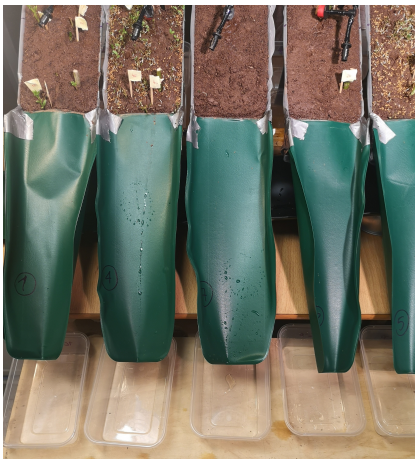

Figure B.5: *Installation of the funnels which redirect runoff.*

Precipitation simulation

Build a framework with four bamboo sticks, three of which are vertical and one horizontal to connect the sticks at the top (Figure B.8). The distance between the vertical stick should be just enough to fit a gutter in between. The height of the horizontal stick should be the distance from the table to the top of the gutter plus 20 cm. Connect the orange nozzles to tubes and with one extra tube in the middle to connect to a hose that is connected to the tap. Calibrate the nozzles according to the protocol in the box below.

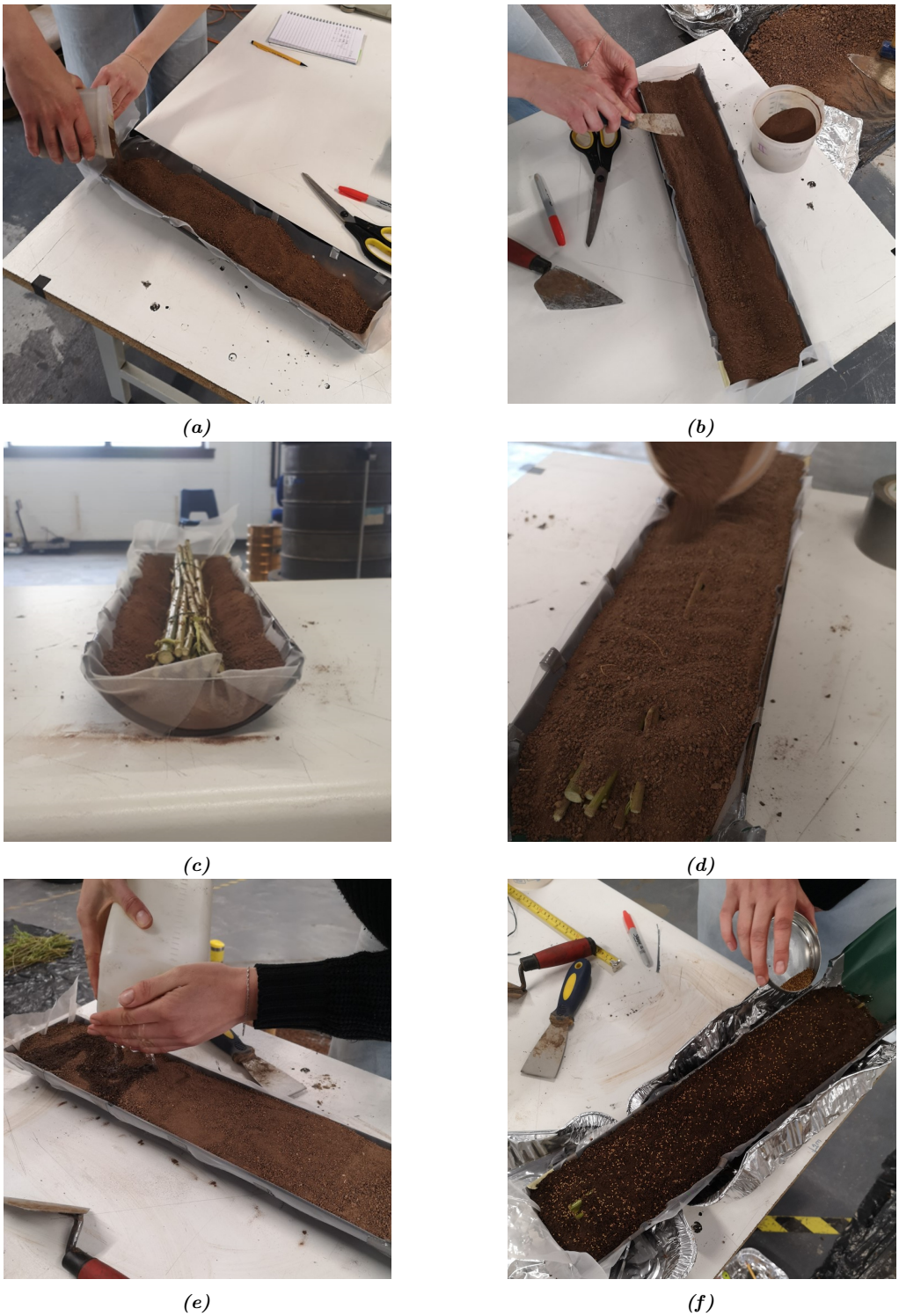

(a) ***(b)*** ***(c)*** ***(d)*** ***(e)*** ***(f)***

Figure B.6: *Filling of the gutters with soil and a bundle.* ***(a)*** *Bottom layer of soil.* ***(b)*** *Making an indent to place the bundle in and compacting.* ***(c)*** *The placement of the bundle in the gutter.* ***(d)*** *Covering the bundle with a soil layer.* ***(e)*** *Gently watering of the compacted soil.* ***(f)*** *Sowing alfalfa seeds.*

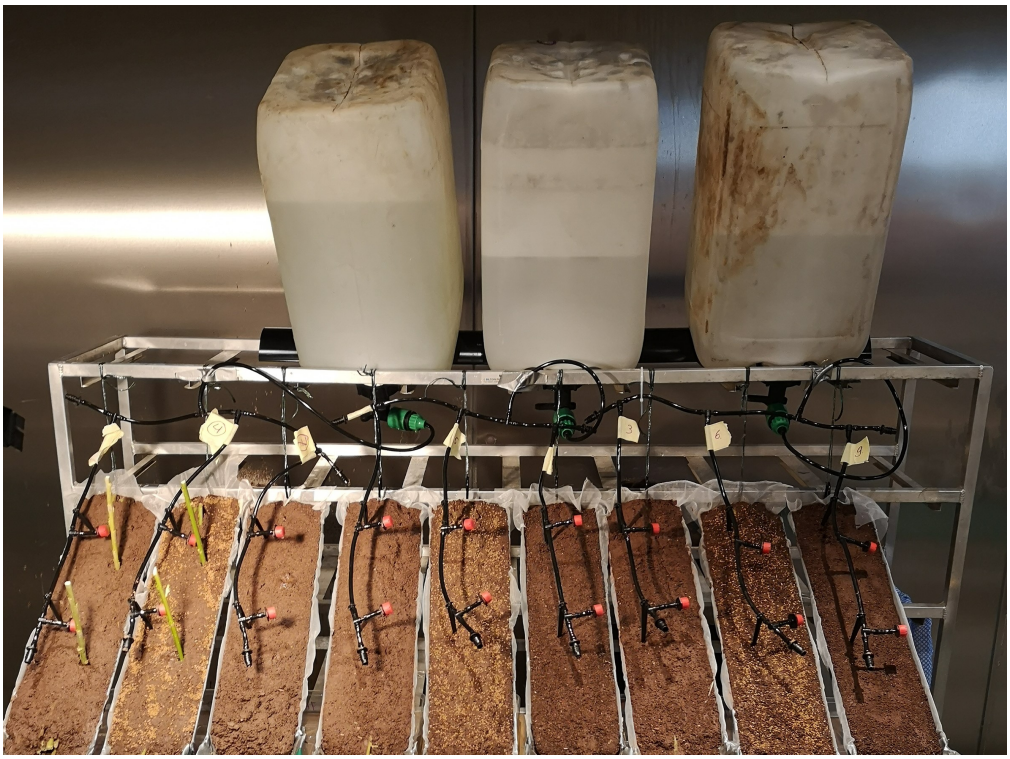

Figure B.7: *Installation of the irrigation system in the gutters.*

Protocol for calibration of the precipitation simulator

Materials

- Irrigation system for rainfall simulation
- 3 measuring cylinders of 1 L
- Permanent marker
- Painter's tape
- Pencil
- Stopwatch

Protocol

1. Label each of the three nozzles 1-3 with painter's tape and pencil.
2. Connect the irrigation system to the tap with the hose.
3. Turn the tap on and adjust the nozzles such that the water is a spray, not a single beam.
4. Mark the tap with a permanent marker such that it can be opened equally far for each experiment.
5. Place a measuring cylinder under each of the nozzles. Turn the tap on to the marking for a duration of approximately 20 s and adjust the nozzles such that their outflow volumes are (almost) equal. Their outflow volumes should be approximately 100 mL in 20 s. Repeat as many times as needed.
6. Make sure the cylinders are empty before starting a calibration sequence. Place each nozzle in a cylinder. Start the stopwatch while opening the tap to the marking. After one minute, stop the stopwatch while closing the tap.
7. Measure and record the volume in each of the cylinders. Discard the water.
8. Repeat steps 6 and 7 ten times. Determine the average volume per minute from each nozzle and the overall average volume per minute.

Figure B.8: *Precipitation simulation setup.*

B.3 Monitoring

Table B.2: *Overview of regularly monitored processes and parameters during the lab experiment.*

Measurements	Frequency	Remarks
Percolation (mL)	Daily	
Runoff (mL)	Daily	
Lateral flow (mL)	Three times per day	During the night this was collected in groups of 4 or 5 gutters.
Soil pH	Daily	At three locations in each gutter.
Soil moisture (%)	Daily	At three locations in each gutter.
Soil moisture with sensor (%)	Every 5 min	All gutters.
Soil temperature (°C)	Daily	At three locations in each gutter.
Soil temperature with sensor (°C)	Every 5 min	Not installed in one gutter with bare soil.
Matric suction (kPa)	Every 5 min	In the three leftmost gutters.
Ambient temperature (°C)	Twice daily	To monitor the growing conditions.
Humidity (%)	Twice daily	To monitor the growing conditions.
Plant height (mm)	Daily	Recorded for each plant.
Plant location	Once	To map the plants in the gutter.
Number of sprouts from stake	Daily	
Stem diameter (mm)	Biweekly	For 3 stems per gutter.
Number of leaves on a stem	Biweekly	For the same 3 stems per gutter.
LAI willows	Biweekly	For 5 leaves from 5 different stems from each gutter.
Root biomass	Weekly	For one stem per column.
LAI alfalfa	Biweekly	With ImageJ.

B.4 Precipitation Simulations

Each rainfall experiment is conducted for two or three different soil conditions - (i) moist soil, 4 h without watering; (ii) 24 h after first run, without any other watering; (iii) 4 days after second run, without any other watering (Table 2.1). The protocol is as follows.

1. At 9AM of the day of the first run, close the tanks to stop water supply to the gutters.
2. Wait 4 h before starting the first run.
3. Take photos and videos of the entire process.
4. Place the rainfall simulation system at the top of three gutters, 5 cm from the upper edge of the gutter (Figure B.8).
5. Place a cover (for example an aluminium baking sheet) between the trios of gutters to avoid spilling of water to another trio during a rainfall event.
6. Wipe the funnels with a cloth.
7. Check if percolation, subsurface flow and surface runoff containers are in place and empty.
8. Make sure stems' labels are stable and steady to avoid displacement with the runoff.
9. Take the environmental chamber's temperature and humidity.

10. Measure soil temperature and moisture at top, middle and toe of each of the three gutters; take note of the time.
11. With your fingers, gently close the holes used to take daily measurements in the soil.
12. Check if the drip system's nozzles are not too close to the soil surface; twist them up to not be an obstruction to runoff.
13. When the rainfall event starts, note the time (for later assessment of data collected by sensors).
14. After 30 s, record the volume in each of the three subsurface flow containers. Do this every 30 s until 1 min after the end of the event.
15. Note down observations during the event.
16. After the determined duration of rainfall, close the tap and note the time (for later assessment of data collected by sensors).
17. From the last 30 s-interval lateral flow measurement, take the measurement every 2 min until 30 min after the end of the event.
18. About 10 min after the end of the event, measure soil temperature and moisture at top, middle and toe of the three gutters.
19. Measure the mass of 18 empty aluminium containers.
20. 30 min after the end of the event, measure all the outflow volumes, noting down the time. Percolation: measure the volume inside the containers with a measuring cylinder. Lateral flow and runoff: transfer the contents of the plastic containers to aluminium containers and measure their masses.
21. Let the samples dry for 24 h at 100 °C and measure their masses.
22. About 24 h after the end of the event, repeat steps 3-21. Possibly repeat 4 days after the second run.

After the last run, open the tanks for constant irrigation and let the gutters restabilise for at least 2 days before running the rainfall simulations with another intensity.

Appendix C
Lab Experiment Results

C.1 Building of the Setup

All gutters contained approximately 1.9 kg of soil with a bulk density of 1.7 Mg/m^3 and the bundles had an average cross-section of 470 mm^2. The diameters of the cuttings varied from 2.7 mm to 12.1 mm. The space between the cuttings made up 58% of the cross-sections on average, assuming circular cross-sections and that the twigs were completely straight. The measurements of the calibration of the precipitation simulation device are presented in Table C.2. The average input volume per gutter was 314 mL/min.

Table C.1: *Characteristics of the nine gutters of the lab experiment.*

	LPD			**LPD+**			**Bare**		
	1	**2**	**3**	**4**	**5**	**6**	**7**	**8**	**9**
Diameter bundle (mm)	38	35	39	36	39	39			
Min. diameter twigs (mm)	3.6	3.7	2.8	2.7	4.0	3.6			
Max. diameter twigs (mm)	10.5	11.5	11.8	9.6	12.1	10.9			
Avg. diameter twigs (mm)	6.0	6.2	6.0	5.9	6.1	5.8			
Mass soil (kg)	1.94	1.96	1.88	1.88	1.79	1.95	1.93	1.80	1.95

Table C.2: *Measurements during calibration of the precipitation simulation system. The runtime of each sequence was* 1 min.

	Volume from nozzle (mL)			
Run	**1**	**2**	**3**	**Average**
1	330	325	290	315
2	335	345	285	322
3	320	325	285	310
4	340	325	290	318
5	325	340	285	317
6	320	330	280	310
7	315	330	280	308
8	340	350	270	320
9	325	350	280	318
10	320	325	270	305
Avg.	327	335	282	**314**

Table C.3: *Spillage during precipitation experiment 5 as a percentage of the total nozzle output volume per three gutters.*

	Spilled (%)		
Gutters	**Run 1**	**Run 2**	**Average**
1,4,7	29	18	23.5
2,5,8	15	24	19.5
3,6,9	13	20	16.5
Avg.	19	21	**20**

C.2 Precipitation Simulations

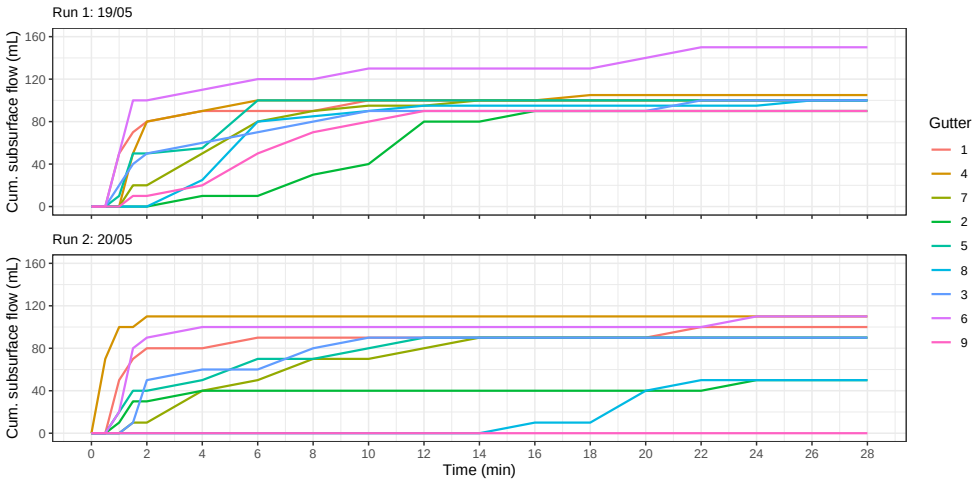

Figure C.1: *Cumulative lateral flow over time of the first two runs of precipitation experiment 1.*

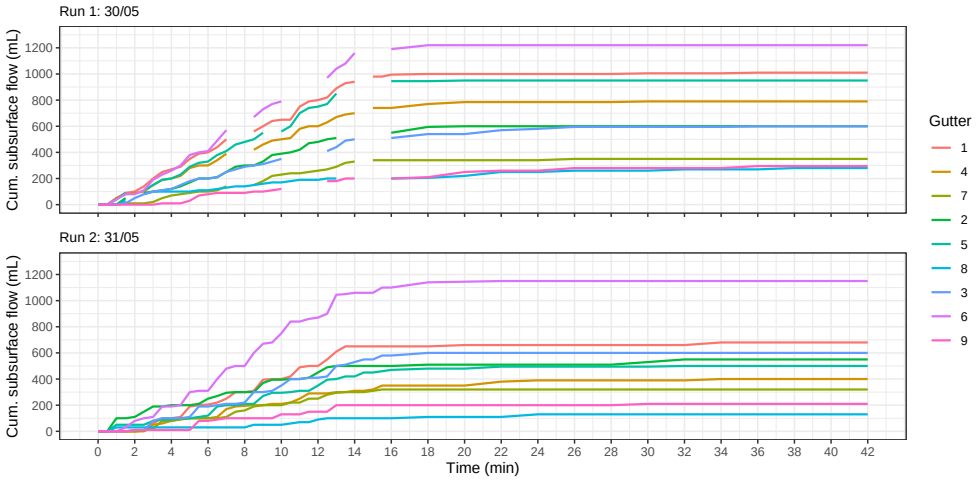

Figure C.2: *Cumulative lateral flow over time of the first two runs of precipitation experiment 2.*

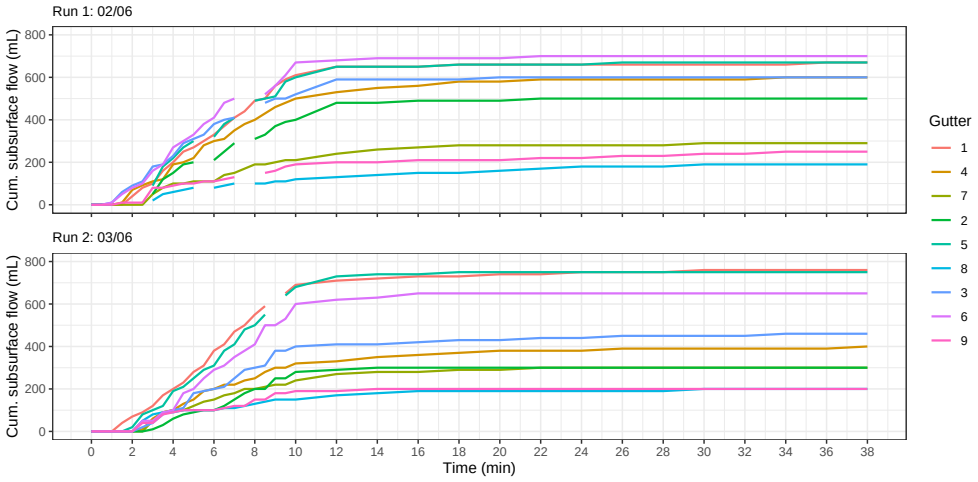

Figure C.3: *Cumulative lateral flow over time of the first two runs of precipitation experiment 3.*

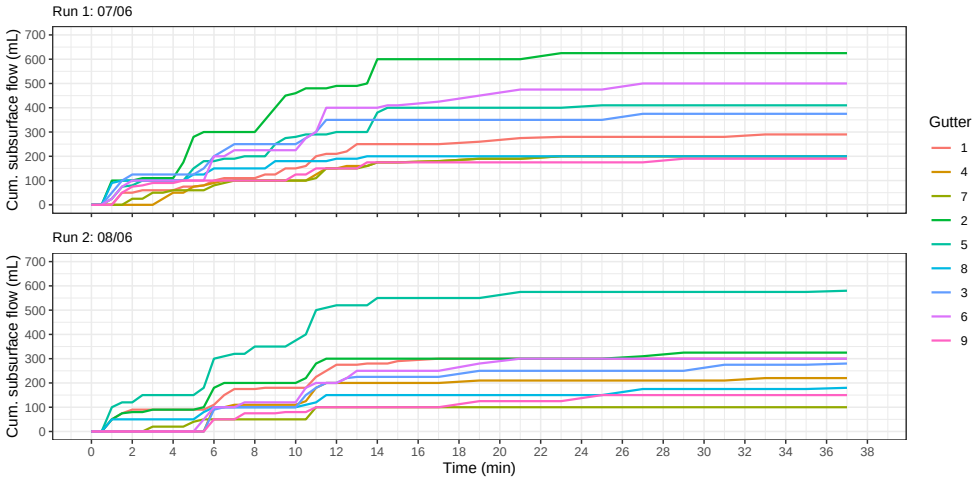

Figure C.4: *Cumulative lateral flow over time of the first two runs of precipitation experiment 4.*

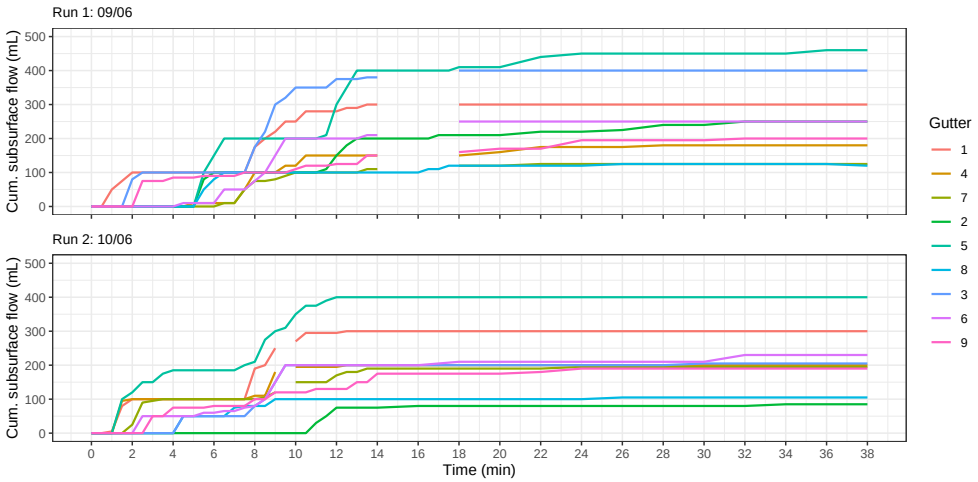

Figure C.5: *Cumulative lateral flow over time of the first two runs of precipitation experiment 5.*

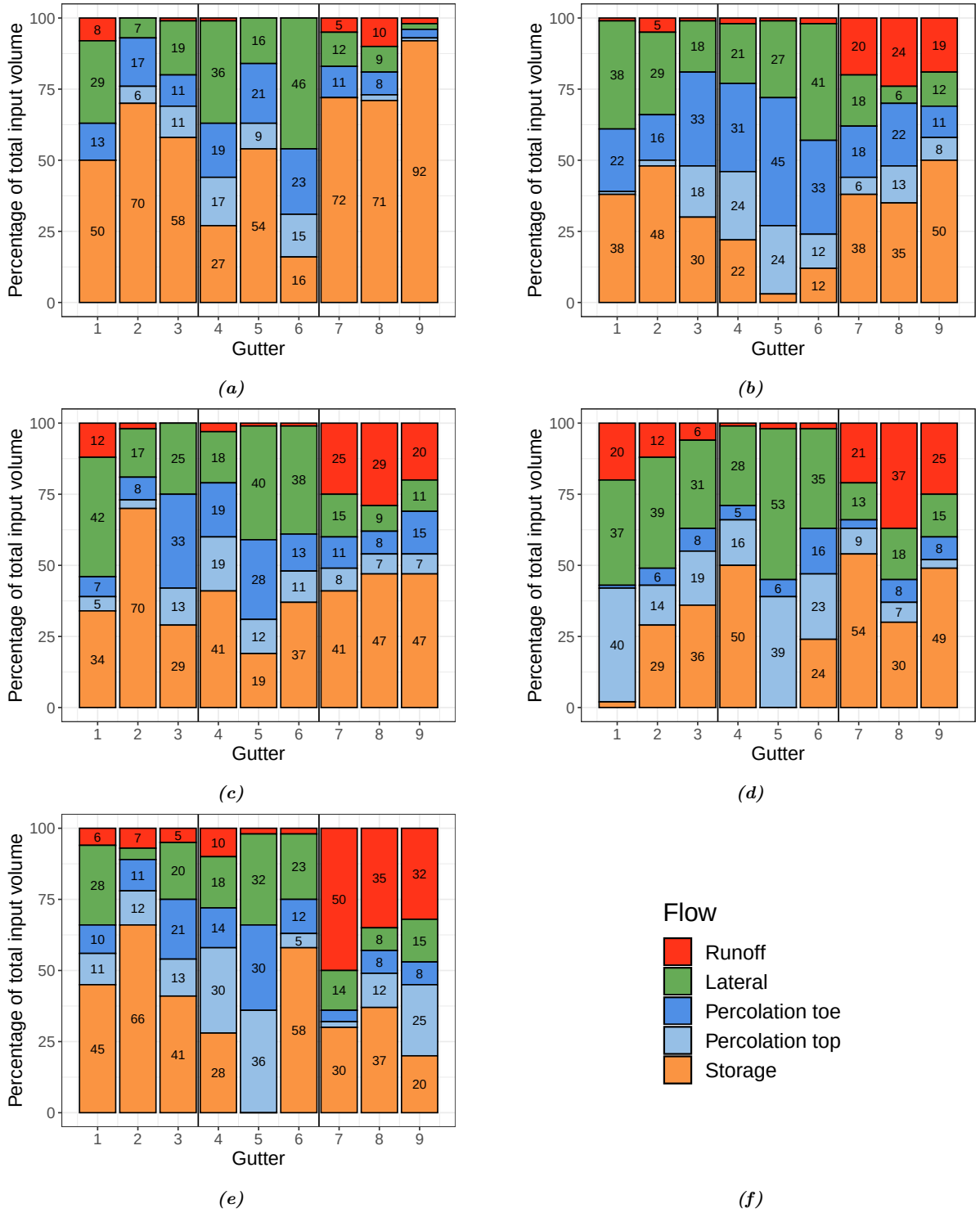

Figure C.6: *Water partitioning of the second runs of the five precipitation experiments. The initial conditions are described in Table 2.1. Gutters 1-3: LPD, gutters 4-6: LPD+ and gutters 7-9: Bare.* ***(a)*** *Experiment 1: 1 interval of* 1 min. ***(b)*** *Experiment 2: 7 intervals of* 1 min *with pauses of* 1 min. ***(c)*** *Experiment 3: 10 intervals of* 30 s *with pauses of* 30 s. ***(d)*** *Experiment 4: 3 intervals of* 1 min *with pauses of* 4 min. ***(e)*** *Experiment 5: 2 intervals of* 2 min *with pauses of* 5 min. ***(f)*** *Legend.*

Appendix D
Model Setup

This appendix includes further elaboration on the model setup, which was presented in Section 5.2. Appendix D.1 contains the equations of the model. The R code which was developed for the model simulations and the sensitivity analysis is presented in Appendix D.2. Lastly, the assumptions made during the conceptualisation of the slope, are listed in Appendix D.3.

D.1 Equations

Table D.1: *Equations of Part I of the model.*

Equation	Sources	Variables/Parameters
(1) $P_{E,d} = pP$	Van Dijk and Bruijnzeel (2001)	$P_{E,d}$: direct throughfall (mm/h) p: free throughfall coefficient (-) P: precipitation (mm/h
(2) $P_{E,i} = \max(\frac{S_I - S_{I,max}}{dt}, 0)$	This study	$P_{E,i}$: indirect throughfall (mm/h) S_I: interception storage (mm) $S_{I,max}$: maximum interception storage (mm) dt: time step (h)
(3) $Q_{st} = p_s(P_{E,d} + P_{E,i})$	Van Dijk and Bruijnzeel (2001)	Q_{st}: stemflow (mm/h) p_s: stemflow fraction (-)
(4) $P_E = P_{E,d} + P_{E,i} - Q_{st}$	Van Dijk and Bruijnzeel (2001)	P_E: effective precipitation (mm/h
(5) $E_I = min(E_P, \frac{S_I}{dt})$	This study	E_I: interception evaporation (mm/h) E_P: potential evaporation (mm/h)
(6) $S_{I,max} = \frac{S}{c} A'_c$	Gonzalez-Ollauri and Mickovski (2017b)	S: canopy storage capacity (mm/m^2) c: canopy cover fraction (-) A'_c: canopy covered ground area (m^2)
(7) $c = 1 - \exp(-kcLAI)$	Maass et al. (1995)	kc: light extinction coefficient (-) LAI: Leaf Area Index (-)

Table D.2: *Equations of Part II of the model.*

Equation	Sources	Variables/Parameters
(8) $S_{U,max} = n_{por}d$	This study	$S_{U,max}$: maximum subsurface storage (mm) n_{por}: porosity (-) d: diameter of the bundle (mm)
(9a) $k_r(S_U) = \frac{1-(\alpha S_U)^{(n-1)}(1+(\alpha S_U)^n)^{-m}}{(1+(\alpha S_U)^n)^{\frac{m}{2}}}$	Van Genuchten (1980)	$k_r(S_U)$: relative unsaturated hydraulic conductivity (mm/h) α: van Genuchten parameter (mm^3/mm) S_U: subsurface storage (mm) n: pore-size distribution parameter (-)
(9b) $m = 1 - \frac{1}{n}$	Van Genuchten (1980)	
(9c) $k(S_U) = k_r(S_U) \cdot k_{sat}$	Van Genuchten (1980)	k_{sat}: saturated hydraulic conductivity (mm/h)
(10a) $Q_{inf} = P_E \cdot k(S_U) \cdot (1 - \exp(-P_E/k(S_U)))$	Hawkins and Cundy (1987)	Q_{inf}: infiltration (mm/h) P_E: throughfall (mm/h)
(10b) $Q_{OF,out} = P_E - Q_{inf}$	This study	$Q_{OF,out}$: runoff (mm/h) $Q_{L,in}$: incoming lateral flow (mm/h)
(11) $Q_{L,in} = 0.2P + Q_{base}$	This study	P: precipitation (mm/h) Q_{base}: baseflow from upslope part (mm/h)
(12) $E_{SP} = E_P \cdot \exp(-0.4LAI)$	Savabi and Williams (1995)	E_{SP}: soil evaporation (mm/h) E_P: potential evaporation (mm/h) LAI: Leaf Area Index (-)
(13) $E_T = E_P(1 - \frac{E_{SP}}{E_P})$	Savabi and Williams (1995)	E_T: plant transpiration (mm/h)
(14) $E_{TP} = E_{SP} + E_T$	Savabi and Williams (1995)	E_{TP}: evapotranspiration (mm/h)
(15) $P_{max} = (S_{U,max} - d\theta_{fc})dt$	This study	P_{max}: maximum percolation rate (mm/h) θ_{fc}: soil moisture content at field capacity (-)
(16) $Q_P = P_{max} \cdot \frac{S_U}{S_{U,max}}$	Bergström and Lindström (2015)	Q_P: percolation (mm/h)
(17) $Q_{L,out} = (k(S_U) \cdot S_U \cdot i)/d$	Fitts (2002)	$Q_{L,out}$: flow through LPD (mm/h) i: sin of inclination of slope (-)

D.2 Algorithm

R Packages

- ggplot2
- patchwork
- lubridate
- dplyr
- xts
- matrixStats

Input parameter values for the scenarios and seasons

```
# Names of the parameters
parnames <- c('th.fc', 'ksat', 'i', 'd', 'n', 'n.genuchten', 'alpha',
    'Qbase', 'p', 'ps', 'S', 'Ac.g', 'kc', 'LAI')

# LPD
parvec.LPD.d <- c(0.23, 180, 0.5, 200, 0.45, 1.51, 0.01, 6.2, 1, 0,
    0, 0, 0, 0)
parvec.LPD.g <- c(0.23, 180, 0.5, 200, 0.45, 1.51, 0.01, 0.62, 1, 0,
    0, 0, 0, 0)

# LPD+
parvec.LPDplus.d <- c(0.23, 180, 0.5, 200, 0.45, 1.51, 0.01, 6.2, 1,
```

```
        0.05, 0, 0, 0, 0)
    parvec.LPDplus.g <- c(0.23, 180, 0.5, 200, 0.45, 1.51, 0.01, 0.62, 0.5,
        0.1, 0.72, 1.6, 0.6, 3.34)

    # Bare
    parvec.Bare.d <- c(0.23, 180, 0.5, 200, 0.35, 3.93, 0.1, 6.2, 1, 0, 0,
        0, 0, 0)
    parvec.Bare.g <- c(0.23, 180, 0.5, 200, 0.35, 3.93, 0.1, 0.62, 1, 0, 0,
        0, 0, 0)
```

Reading of meteorological data

```
    read.data.func <- function(month, year){
        # Read data for given month and year
        filename <- paste('weather_data/', month, substr(year, 3, 4),
            'log.txt', sep='')
        month.data <- read.table(filename, sep=',', dec='.', header=F)

        col.names <- c('Day.Month.Year', 'Hour.Minute', 'temp', 'RH',
            'dewpoint', 'moving.avg.windspeed', 'highest.wind.gust',
            'avg.wind.bearing', 'current.rainfall.rate', 'cum.rainfall',
            'sea.level.pressure', 'rainfall.counter', 'inside.temp',
            'inside.humidity', 'lastest.wind.speed', 'wind.chill',
            'heat.index', 'UV.index', 'solar.radiation',
            'evapotranspiration', 'annual.evapotranspiration',
            'apperent.temp', 'theoretical.max.solar.radiation',
            'cum.daily.hours.of.sunshine', 'wind.bearing',
            'RG-11.rain.today', 'cum.daily.rainfall', 'feels.like',
            'humidex')

        colnames(month.data) <- col.names
        month.data$datetime <- as.POSIXct(paste(month.data$Day.Month.Year,
                                month.data$Hour.Minute),
                                format='%d/%m/%y %H:%M')
        month.data['Day.Month.Year'] <- NULL
        month.data['Hour.Minute'] <- NULL
        datetime <- month.data['datetime']

        rainfall.permin <- rep(0, times=length(datetime))
        rain.data <- data.frame(datetime, rainfall.permin)

        for(i in 1:(length(month.data[,1])-1)){
            difference <- month.data[i+1, 'cum.rainfall'] - month.data[i,
                        'cum.rainfall']
            rain.data[i, 'rainfall.permin'] <- month.data[i+1,
                    'cum.rainfall'] - month.data[i, 'cum.rainfall']
        }

        rain.data$rainfall.permin[which(rain.data$rainfall.permin < 0)] <- 0
        rain.xts <- xts(rain.data$rainfall.permin, rain.data$datetime)
        ends <- endpoints(rain.data$datetime, 'hours', 1)
        hourly.rain.data <- period.apply(rain.xts, ends, sum)
        hourly.rain.data <- align.time(hourly.rain.data, 3600)
        hourly.rain.data <- data.frame(index(hourly.rain.data),
            coredata(hourly.rain.data))
        colnames(hourly.rain.data) <- c('datetime', 'rain(mm)')
        return(hourly.rain.data)
    }
```

Functions

```
    # INTERCEPTION STORAGE
    # Eq. 1 direct throughfall
    eq.PE.d <- function(P, p){
        PE.d <- p * P
        return(PE.d)
```

```
    }

    # Eq. 2 indirect throughfall
    eq.PE.i <- function(SI, SI.max, dt=1){
        PE.i <- max(c((SI - SI.max) / dt, 0))
        return(PE.i)
    }

    # Eq. 3 stemflow
    eq.Qst <- function(PE.d, PE.i, ps){
        Qst <- ps * (PE.d + PE.i)
        return(Qst)
    }

    # Eq. 4 total throughfall
    eq.PE <- function(PE.d, PE.i, Q.st){
        PE <- PE.d + PE.i
        return(PE)
    }

    # Eq. 5 interception evaporation
    eq.EI <- function(P, EP, SI, dt=1){
        if(P == 0){
            EI <-min(c(EP, SI/dt))
        }else{
            EI <- 0
        }
        return(EI)
    }

    # Eq. 6 maximum interception storage
    eq.SI.max <- function(S, c.c, Ac.g){
        if(S == 0){
            SI.max <- 0
        }else{
            SI.max <- S / c.c * Ac.g
        }
        return(SI.max)
    }

    # Eq. 7 canopy cover fraction
    eq.c.c <- function(kc, LAI){
        c.c <- 1 - exp(-kc * LAI)
        return(c.c)
    }

    # Eq. Part I
    part.I <- function(P, EP, SI, SI.max, p, ps, dt=1){
        # Interception and stemflow
        PE.d <- eq.PE.d(P, p)
        SI = SI + (1 - p) * P
        PE.i <- eq.PE.i(SI, SI.max, dt)
        Qst <- eq.Qst(PE.d, PE.i, ps)
        PE <- eq.PE(PE.d, PE.i, Q.st)
        EI <- eq.EI(P, EP, SI, dt)
        SI <- SI - (PE.i + EI)

        return(c(SI, EI, Qst, PE))
    }

    # INFILTRATION AND RUNOFF
    # Eq. 8 Maximum subsurface storage
    eq.SU.max <- function(n, d){
        SU.max <- n * d
        return(SU.max)
    }


```

```
    # Eq. 9 Van Genuchten for unsaturated hydraulic conductivity
    eq.kr <- function(SU, alpha, n.genuchten){
        m <- 1 - 1/n.genuchten
        numerator <- (1 - (alpha * SU)^(n.genuchten-1) *
            (1 + (alpha * SU)^n.genuchten)^(-m))^2
        denominator <- (1 + (alpha * SU)^n.genuchten)^(m/2)
        kr <- numerator / denominator
        return(kr)
    }

    # Eq. 10 inf. submodel
    inf.submodel <- function(SU, PE, SU.max, k.th){
        fs <- k.th * (1 - exp(-PE / k.th))
         Qinf <- min(c(PE * fs, PE))
        QOF.out <- PE - Qinf
        return(c(Qinf, QOF.out))
    }

    # LATERAL INFLOW
    # Eq. 11 Incoming lateral flow
    eq.QL.in <- function(P, Qbase){
        QL.in <- 0.2 * P + Qbase
        return(QL.in)
    }

    # EVAPOTRANSPIRATION
    # Eq. 12 soil evaporation
    eq.ESP <- function(EP, LAI){
        ESP <- min(EP * exp(-0.4 * LAI))
        return(ESP)
    }

    # Eq. 13 transpiration
    eq.ET <- function(EP, ESP){
        if(EP == 0){
            return(0)
        }
        ET <- (1 - ESP / EP) * EP
        return(ET)
    }

    # Eq. 14 evapotranspiration
    eq.ETP <- function(ESP, ET){
        return(ESP + ET)
    }


    # PERCOLATION
    # Eq. 15 Maximum percolation rate
    eq.P.max <- function(SU.max, d, th.fc, dt=1){
         P.max <- (SU.max - th.fc * d) / dt
        return(P.max)
    }

    # Eq. 16 Percolation
    eq.QP <- function(SU, SU.max, P.max){
        QP <- P.max * SU / SU.max
        return(QP)
    }

    # LATERAL FLOW
    # Eq. 17 Lateral outflow
    eq.QL.out <- function(SU, SU.max, k.th, d, ksat, i){
        if(SU < SU.max){
            QL.out <- (k.th * SU * i) / d
        }else{
            QL.out <- (ksat * SU * i) / d
        }
```

```
        return(QL.out)
    }

    # Eq. Part II
    part.II <- function(P, EP, SU, PE, Qst, SU.max, P.max, LAI, d, Qbase,
    alpha, n.genuchten, ksat, i){
        # Update SU with stemflow
        QOF.out <- max(c(0, SU + Qst - SU.max))
        SU <- min(c(SU + Qst, SU.max))

        # Determine infiltration and runoff
        kr <- eq.kr(SU.max - SU, alpha, n.genuchten)
        k.th <- kr * ksat
        Qinf.OFout <- inf.submodel(SU, PE, SU.max, k.th)
        Qinf <- Qinf.OFout[1]
        QOF.out <- QOF.out + Qinf.OFout[2]
        SU <- SU + Qinf

        # Determine incoming lateral flow
        QL.in <- eq.QL.in(P, Qbase)
        SU <- SU + QL.in

        # Determine evapotranspiration
        ESP <- eq.ESP(EP, LAI)
        ET <- eq.ET(EP, ESP)
        ETP <- eq.ETP(ESP, ET)
        ETP <- min(c(SU, ETP))
        SU <- SU - ETP

        # Determine percolation
        QP <- eq.QP(SU, SU.max, P.max)
        SU <- SU - QP

        # Determine lateral flow
        kr <- eq.kr(SU.max - SU, alpha, n.genuchten)
        k.th <- kr * ksat
        QL.out <- min(c(eq.QL.out(SU, SU.max, k.th, d, ksat, i), SU))
        SU <- SU - QL.out
        return(c(SU, Qinf, QOF.out, ETP, QL.in, QP, QL.out))
    }

    # MODELRUNNER
    modelrunner <- function(parvec, dt=1, year, month){
        Pdata <- read.data.func(month, year) #hourly data in mm
        Pdata[is.na(Pdata[,2]), 2] <- 0
        EPdata <- Pdata # hourly data in mm
        colnames(EPdata) <- c('datetime', 'evap.mm')
        EPdata[,2] <- 0
        if(month != 'Dec'){
            timevec <- format(as.POSIXct(EPdata$datetime), format = '%H:%M')
            time.mask <- which(timevec >= '08:00' & timevec < '18:00')
            EPdata[time.mask, 2] <- 0.2
            rm(timevec); rm(time.mask)
        }
        rm(month); rm(year)

        SI <- NULL
        SI[1] <- 0
        SU <- NULL
        SU[1] <- 0
        EI <- NULL
        Qst <- NULL
        PE <- NULL
        Qinf <- NULL
        QOF.out <- NULL
        ETP <- NULL
        QL.in <- NULL
        QP <- NULL
```

```
        QL.out <- NULL

        th.fc <- parvec[1]
        ksat <- parvec[2]
        i <- parvec[3]
        d <- parvec[4]
        n <- parvec[5]
        n.genuchten <- parvec[6]
        alpha <- parvec[7]
        Qbase <- parvec[8]
        p <- parvec[9]
        ps <- parvec[10]
        S <- parvec[11]
        Ac.g <- parvec[12]
        kc <- parvec[13]
        LAI <- parvec[14]

        c.c <- eq.c.c(kc, LAI)
        SI.max <- eq.SI.max(S, c.c, Ac.g)
        SU.max <- eq.SU.max(n, d)
        P.max <- eq.P.max(SU.max, d, th.fc, dt=1)

        for(i in 1:length(Pdata[,1])){
            above.ground <- part.I(Pdata[i, 2], EPdata[i, 2], SI[i],
                SI.max, p, ps, dt)
            SI[i+1] <- above.ground[1]
            EI[i] <- above.ground[2]
            Qst[i] <- above.ground[3]
            PE[i] <- above.ground[4]

            below.ground <- part.II(Pdata[i, 2], EPdata[i, 2], SU[i],
                PE[i], Qst[i], SU.max, P.max, LAI, d, Qbase, alpha,
                n.genuchten, ksat, i)
            SU[i+1] <- below.ground[1]
            Qinf[i] <- below.ground[2]
            QOF.out[i] <- below.ground[3]
            ETP[i] <- below.ground[4]
            QL.in[i] <- below.ground[5]
            QP[i] <- below.ground[6]
            QL.out[i] <- below.ground[7]
        }

        df <- cbind(Pdata, EPdata[,2])
        colnames(df) <- c('datetime', 'Pdata', 'EPdata')
        df$SI <- SI[1:(length(SI)-1)]
        df$EI <- EI
        df$Qst <- Qst
        df$PE <- PE
        df$SU <- SU[1:(length(SU)-1)]
        df$Qinf <- Qinf
        df$QOF.out <- QOF.out
        df$ETP <- ETP
        df$QL.in <- QL.in
        df$QP <- QP
        df$QL.out <- QL.out

        return(df)
    }
```

Sensitivity Analysis

```
    # Input parameters
    parnames <- c('th.fc', 'ksat', 'i', 'd', 'n', 'n.genuchten', 'alpha',
        'Qbase', 'p', 'ps', 'S', 'Ac.g', 'kc', 'LAI')
    parvec <- c(0.23, 180, 0.5, 200, 0.45, 1.51, 0.01, 0.62, 0.5, 0.1, 0.72,
        1.6, 0.6, 3.34)

```

```
    # Baseline run
    df.base <- modelrunner(parvec, 'May', '2022')

    # Loop for model runs with varying parameter values
    N <- 1000
    for(i in 1:length(parvec)){
        c.names <- c('datetime', 'R1')
        df.SI <- data.frame(Pdata[,1], 0)
        colnames(df.SI) <- c.names
        rm(c.names)
        df.EI <- df.SI
        df.Qst <- df.SI
        df.PE <- df.SI
        df.SU <- df.SI
        df.Qinf <- df.SI
        df.QOF.out <- df.SI
        df.ETP <- df.SI
        df.QL.in <- df.SI
        df.QP <- df.SI
        df.QL.out <- df.SI

        parvec.samp <- parvec
        for(j in 1:N){
            parvec.samp[i] <- rnorm(1, mean=parvec[i], sd=0.25*parvec[i])
            df.samp <- modelrunner(parvec.samp, 'May', '2022')
            df.samp$Pdata <- NULL
            df.samp$EPdata <- NULL
            df.SI[paste('R', j, sep='')] <- df.samp$SI
            df.EI[paste('R', j, sep='')] <- df.samp$EI
            df.Qst[paste('R', j, sep='')] <- df.samp$Qst
            df.PE[paste('R', j, sep='')] <- df.samp$PE
            df.SU[paste('R', j, sep='')] <- df.samp$SU
            df.Qinf[paste('R', j, sep='')] <- df.samp$Qinf
            df.QOF.out[paste('R', j, sep='')] <- df.samp$QOF.out
            df.ETP[paste('R', j, sep='')] <- df.samp$ETP
            df.QL.in[paste('R', j, sep='')] <- df.samp$QL.in
            df.QP[paste('R', j, sep='')] <- df.samp$QP
            df.QL.out[paste('R', j, sep='')] <- df.samp$QL.out
            rm(df.samp)
        }
        write.csv(df.SI, paste('sensitivity_analysis/', parnames[i],
            '_SI.csv', sep=''), row.names=F)
        write.csv(df.EI, paste('sensitivity_analysis/', parnames[i],
            '_EI.csv', sep=''), row.names=F)
        write.csv(df.Qst, paste('sensitivity_analysis/', parnames[i],
            '_Qst.csv', sep=''), row.names=F)
        write.csv(df.PE, paste('sensitivity_analysis/', parnames[i],
            '_PE.csv', sep=''), row.names=F)
        write.csv(df.SU, paste('sensitivity_analysis/', parnames[i],
            '_SU.csv', sep=''), row.names=F)
        write.csv(df.Qinf, paste('sensitivity_analysis/', parnames[i],
            '_Qinf.csv', sep=''), row.names=F)
        write.csv(df.QOF.out, paste('sensitivity_analysis/', parnames[i],
            '_QOF.out.csv', sep=''), row.names=F)
        write.csv(df.ETP, paste('sensitivity_analysis/', parnames[i],
            '_ETP.csv', sep=''), row.names=F)
        write.csv(df.QL.in, paste('sensitivity_analysis/', parnames[i],
            '_QL.in.csv', sep=''), row.names=F)
        write.csv(df.QP, paste('sensitivity_analysis/', parnames[i],
            '_QP.csv', sep=''), row.names=F)
        write.csv(df.QL.out, paste('sensitivity_analysis/', parnames[i],
            '_QL.out.csv', sep=''), row.names=F)
        rm(list=c('df.SI', 'df.EI', 'df.Qst', 'df.PE', 'df.SU', 'df.Qinf',
            'df.QOF.out', 'df.ETP', 'df.QL.in', 'df.QP', 'df.QL.out'))
    }

    # Analysis of output
    df.sensitivity <- data.frame(SI=rep(0, 14),
```

```
                              EI=rep(0, 14),
                              Qst=rep(0, 14),
                              PE=rep(0, 14),
                              SU=rep(0, 14),
                              Qinf=rep(0, 14),
                              QOF.out=rep(0, 14),
                              ETP=rep(0, 14),
                              QL.in=rep(0, 14),
                              QP=rep(0, 14),
                              QL.out=rep(0, 14),
                              row.names=parnames)

    outputnames <- c('SI', 'EI', 'Qst', 'PE', 'SU', 'Qinf', 'QOF.out', 'ETP',
        'QL.in', 'QP', 'QL.out')
    outputunits <- c('(mm)', '(mm/h)', '(mm/h)', '(mm/h)', '(mm)', '(mm/h)',
        '(mm/h)', '(mm/h)', '(mm/h)', '(mm/h)', '(mm/h)')

    for(i in 1:length(parvec)){
        for(j in 1:length(outputnames)){
            df.analysis <- read.table(paste('sensitivity_analysis/', parnames[i],
                '_', outputnames[j],  '.csv', sep=''), sep=',', header=T)
            df.analysis$mean <- rowMeans(df.analysis[,
                names(df.analysis) != 'datetime'])
            df.analysis$sd <- rowSds(as.matrix(df.analysis[,
                names(df.analysis) != 'datetime']))
            df.analysis$datetime <- as.POSIXct(df.analysis$datetime,
                format='%Y-%m-%d %H:%M')
            analysis.mean <- mean(df.analysis$mean[df.analysis$mean != 0])
            analysis.sd <- mean(df.analysis$sd[df.analysis$mean != 0])

            df.sensitivity[parnames[i], outputnames[j]] <- analysis.sd / analysis.mean
            rm(df.analysis); rm(analysis.mean); rm(analysis.sd)
        }
    }
```

D.3 Assumptions

Table D.3: *Model assumptions*

Model Part	Assumptions
IN GENERAL	The catchment is lumped, i.e. no spatial variability. Erosion is not taken into account.
INPUT	
Precipitation	All precipitation is rain, snowfall is not taken into account. The rainfall is steady. Rain is uniformly distributed over the control volume's surface area.
Potential evaporation	Evaporation only occurs in the months April-September. It only occurs between 8AM and 6PM. During those hours, potential evaporation is steady, at a rate of 0.2 mm/h.
PART I	
Interception storage	Litter interception is not taken into account. Foliage is randomly distributed in the canopy. Leaf inclination angles are spherically distributed in space. Interception only happens by the canopy, not by trunks and stems.

Model Part	Assumptions
Throughfall	Direct throughfall is a fraction of the precipitation rate. Indirect throughfall only occurs if the interception storage is full. Indirect throughfall comprises the excess rainfall that cannot be stored by the canopy. Dripfall is not taken into account.
Stemflow	Stemflow is a fraction of the throughfall.
Interception evaporation	Interception evaporation happens at the rate of potential evaporation. It is zero in time steps during which precipitation occurs.
PART II	
Subsurface storage	The maximum storage capacity consists of all pores in the soil.
Infiltration	All effective precipitation is available for infiltration. All water that infiltrates immediately reaches the subsurface storage. If the storage is full, water does not infiltrate and becomes runoff. The infiltration submodel was developed for the steady-state case. The average infiltration rate for the slope equals the unsaturated hydraulic conductivity if the subsurface storage is not full. It equals the saturated hydraulic conductivity if the storage is full.
Runoff	All water that does not infiltrate, leaves the system as runoff. It does not infiltrate downslope.
Incoming lateral flow	The runoff from the upslope part of the hill enters the system as lateral flow. This runoff is 20% of the precipitation. Another part of the incoming lateral flow consists of a baseflow from uphill.
Evapotranspiration	The soil evaporation is limited by the height of the soil column (d).
Percolation	The maximum percolation rate is limited by the maximum subsurface storage and soil moisture content at field capacity. Beta in the Bergström and Lindström (2015) submodel equals 1.
Flow through LPD	The gradient in hydraulic head is parallel to the slope gradient. The pressure head equals the subsurface storage. The LPD is represented by a homogeneous soil column. The unsaturated hydraulic conductivity is used if the subsurface storage is not full. At the downslope end, water can flow freely from the LPD. The flow through the LPD is steady.

Appendix E
Model Simulation Results

This appendix includes the input and output time series of all executed model simulations. The input and results for the dormant season are shown in Appendix E.1 and those for the growing season are shown in Appendix E.2.

E.1 Dormant Season

Input

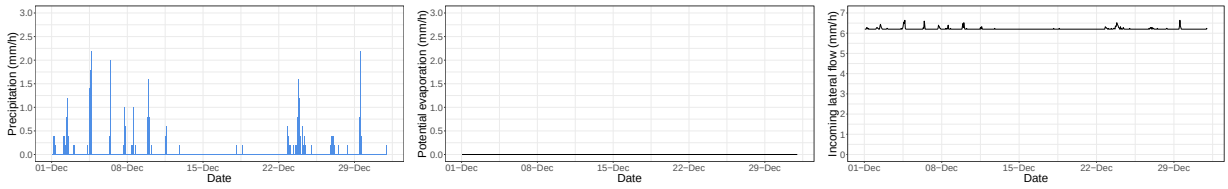

(a) ***(b)*** ***(c)***

Figure E.1: *Model input and incoming lateral flow for one month in the dormant season. The simulation was done for December 2021.* ***(a)*** *Precipitation.* ***(b)*** *Potential evaporation.* ***(c)*** *Incoming lateral flow.*

Output

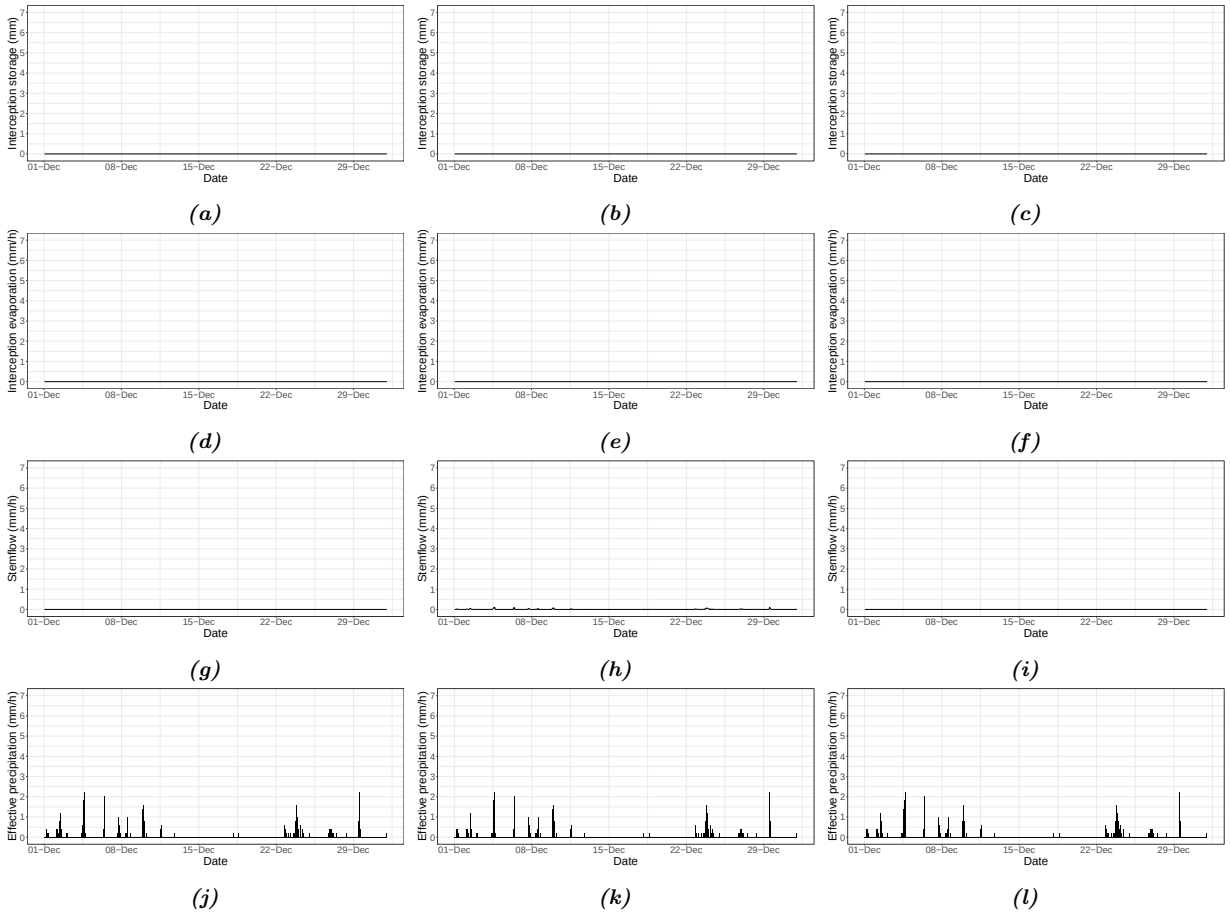

Figure E.2: *Output of Part I of the model for one month in the dormant season. The simulation was done for December 2021.* ***(a)*** *LPD: interception storage.* ***(b)*** *LPD+: interception storage.* ***(c)*** *Bare: interception storage.* ***(d)*** *LPD: interception evaporation.* ***(e)*** *LPD+: interception evaporation.* ***(f)*** *Bare: interception evaporation.* ***(g)*** *LPD: stemflow.* ***(h)*** *LPD+: stemflow.* ***(i)*** *Bare: stemflow.* ***(j)*** *LPD: effective precipitation.* ***(k)*** *LPD+: effective precipitation.* ***(l)*** *Bare: effective precipitation.*

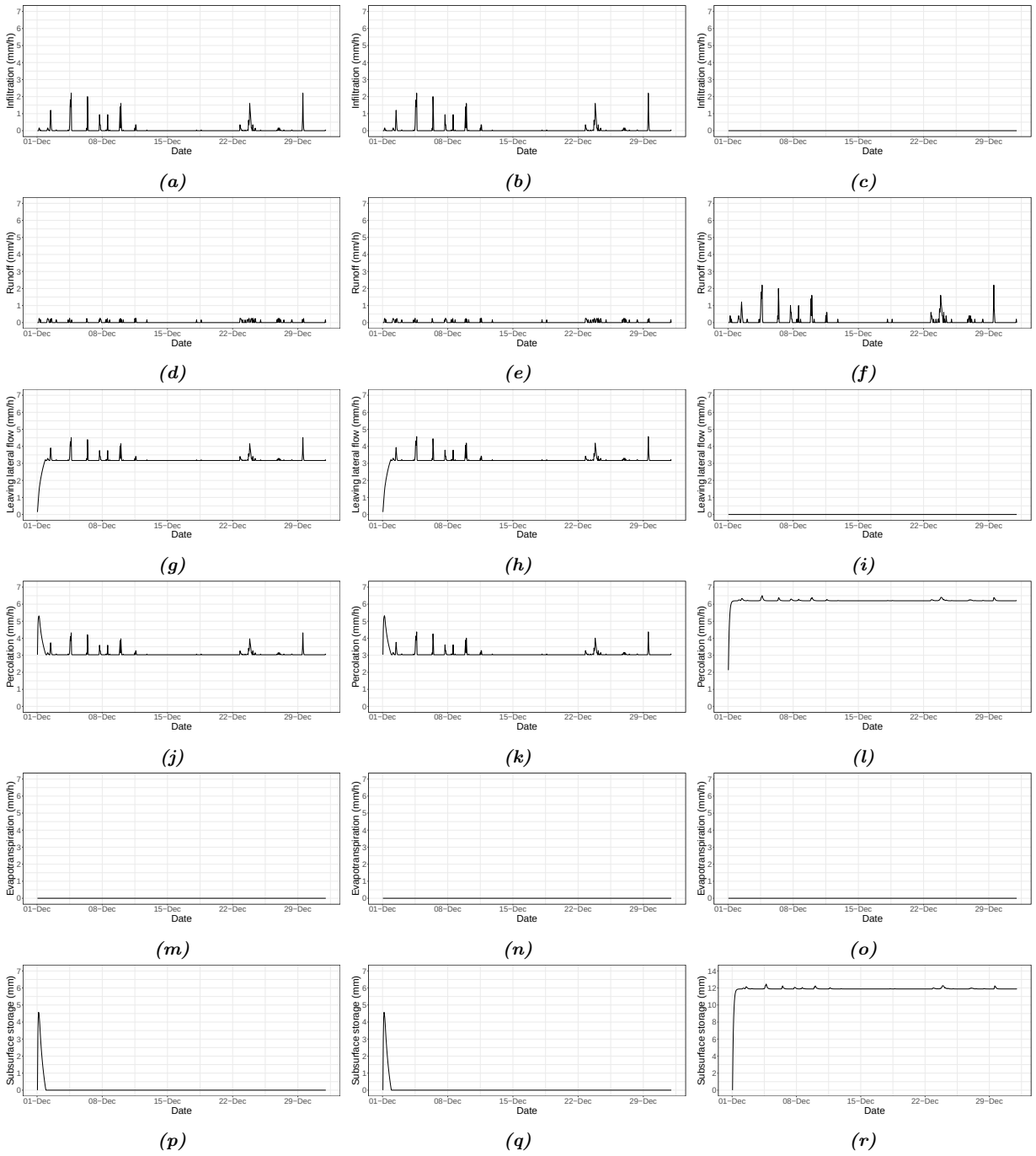

Figure E.3: *Output of Part II of the model for the dormant season. The simulation was done for December 2021.* ***(a)*** *LPD: infiltration.* ***(b)*** *LPD+: infiltration.* ***(c)*** *Bare: infiltration.* ***(d)*** *LPD: runoff.* ***(e)*** *LPD+: runoff.* ***(f)*** *Bare: runoff.* ***(g)*** *LPD: lateral flow.* ***(h)*** *LPD+: lateral flow.* ***(i)*** *Bare: lateral flow.* ***(j)*** *LPD: percolation.* ***(k)*** *LPD+: percolation.* ***(l)*** *Bare: percolation.* ***(m)*** *LPD: evapotranspiration.* ***(n)*** *LPD+: evapotranspiration.* ***(o)*** *Bare: evapotranspiration.* ***(p)*** *LPD: evapotranspiration.* ***(q)*** *LPD+: evapotranspiration.* ***(r)*** *Bare: evapotranspiration.* ***(s)*** *LPD: subsurface storage.* ***(t)*** *LPD+: subsurface storage.* ***(u)*** *Bare: subsurface storage.*

E.2 Growing Season

Input

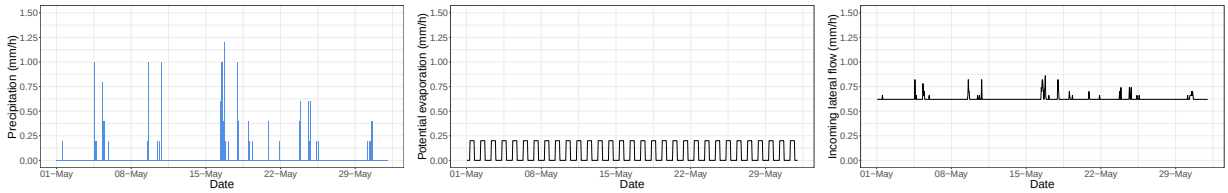

Figure E.4: *Model input and incoming lateral flow for one month in the growing season. The simulation was done for May 2022.* ***(a)*** *Precipitation.* ***(b)*** *Potential evaporation.* ***(c)*** *Incoming lateral flow.*

Output

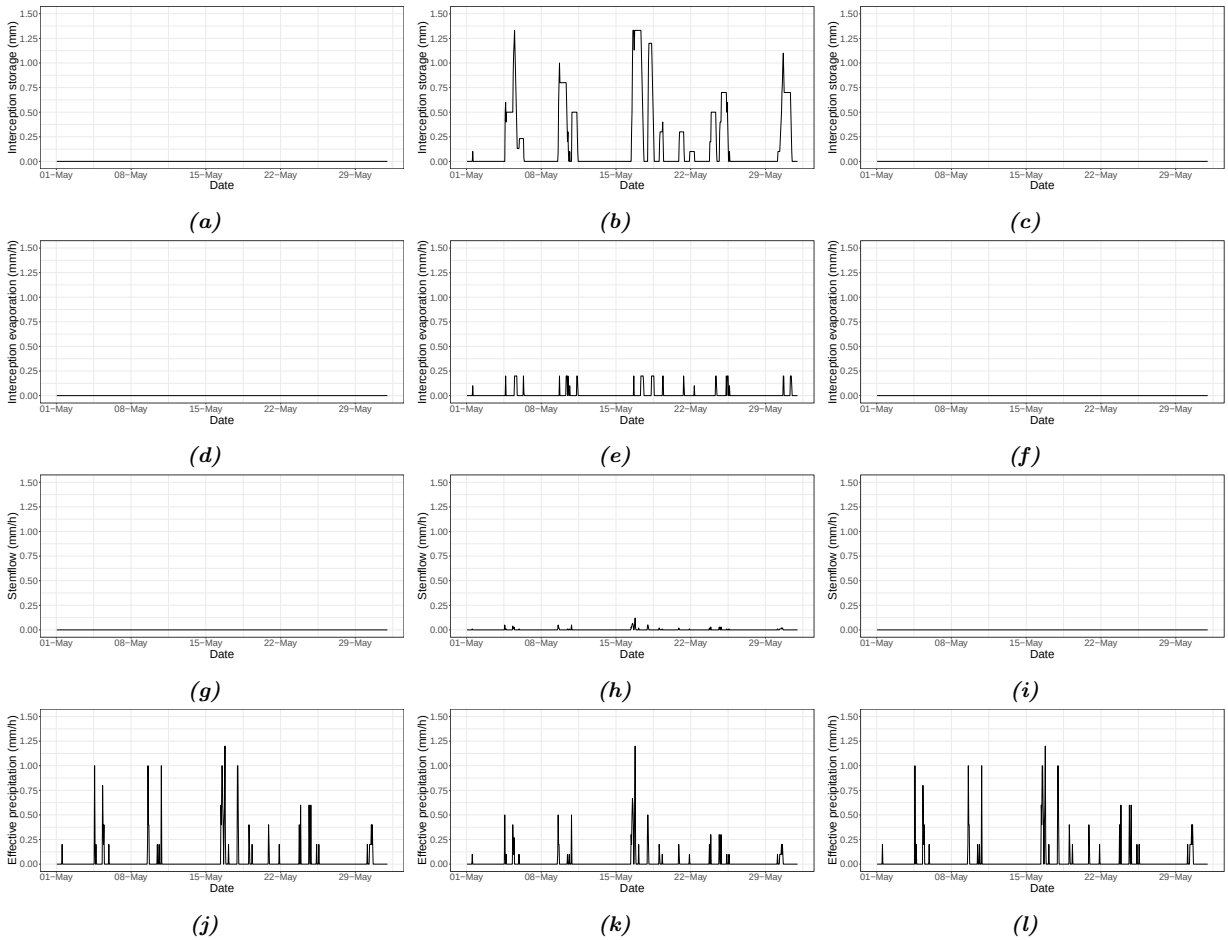

Figure E.5: *Output of Part I of the model for the growing season. The simulation was done for May 2022.* ***(a)*** *LPD: interception storage.* ***(b)*** *LPD+: interception storage.* ***(c)*** *Bare: interception storage.* ***(d)*** *LPD: interception evaporation.* ***(e)*** *LPD+: interception evaporation.* ***(f)*** *Bare: interception evaporation.* ***(g)*** *LPD: stemflow.* ***(h)*** *LPD+: stemflow.* ***(i)*** *Bare: stemflow.* ***(j)*** *LPD: effective precipitation.* ***(k)*** *LPD+: effective precipitation.* ***(l)*** *Bare: effective precipitation.*

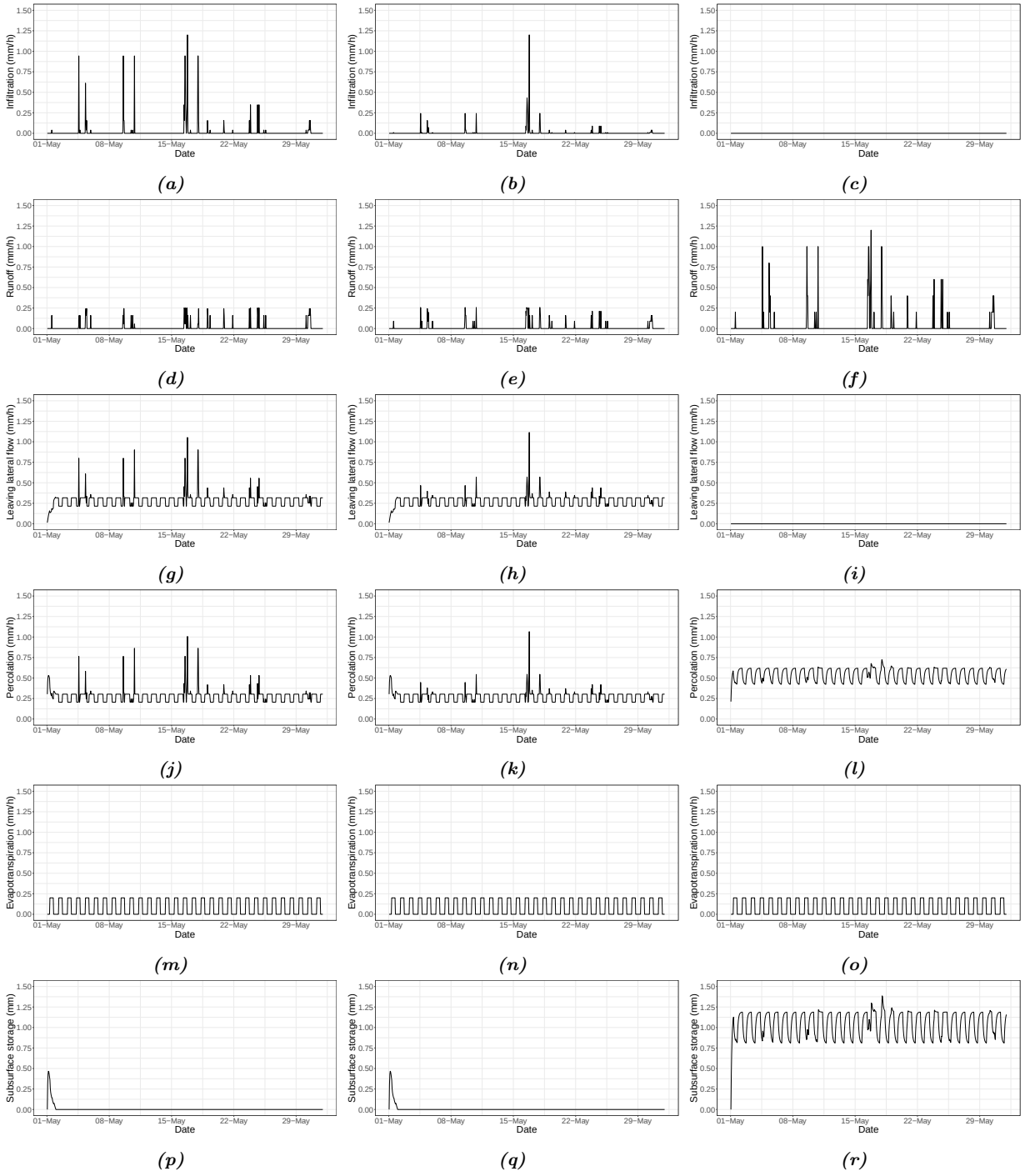

Figure E.6: *Output of Part II of the model for the growing season. The simulation was done for May 2022.* ***(a)*** *LPD: infiltration.* ***(b)*** *LPD+: infiltration.* ***(c)*** *Bare: infiltration.* ***(d)*** *LPD: runoff.* ***(e)*** *LPD+: runoff.* ***(f)*** *Bare: runoff.* ***(g)*** *LPD: lateral flow.* ***(h)*** *LPD+: lateral flow.* ***(i)*** *Bare: lateral flow.* ***(j)*** *LPD: percolation.* ***(k)*** *LPD+: percolation.* ***(l)*** *Bare: percolation.* ***(m)*** *LPD: evapotranspiration.* ***(n)*** *LPD+: evapotranspiration.* ***(o)*** *Bare: evapotranspiration.* ***(p)*** *LPD: evapotranspiration.* ***(q)*** *LPD+: evapotranspiration.* ***(r)*** *Bare: evapotranspiration.* ***(s)*** *LPD: subsurface storage.* ***(t)*** *LPD+: subsurface storage.* ***(u)*** *Bare: subsurface storage.*